

The Role of the Central Nervous System in the Integration of Proprioceptive Information

BY

Joseph S. Soltys

Submitted to the graduate degree program in Mechanical Engineering and the Graduate Faculty of the University of Kansas in partial fulfillment of the requirements for the degree of Doctor of Philosophy.

Chairperson: Sara E. Wilson

Cary Savage

Carl W. Luchies

Sarah L. Kieweg

John Keighley

Date Defended: September 15, 2011

The Dissertation Committee for Joseph S. Soltys certifies that this is the approved version of the following dissertation:

The Role of the Central Nervous System in the Integration of Proprioceptive Information

Chairperson: Sara E. Wilson

Date approved:

Abstract

The proprioceptive system provides feedback on human performance that makes it possible to learn and perform novel tasks. Proprioception predominately arises in the peripheral nervous system at the muscle spindle organ. Mechanical stimulus such as vibration has been implicated in altering muscle spindle afferent signals used as feedback. Researchers have utilized this understanding to document gross performance changes resulting from a muscle spindle disruption paradigm. Findings of this work have demonstrated that the altered proprioceptive feedback alters performance both during and after vibration exposure. This has also led many to postulate that altered proprioceptive feedback due to environmental working conditions may be responsible for many incidences of musculoskeletal injury, including low back pain.

In order to more fully understand how proprioceptive feedback is integrated into a motor response it was required to investigate activity within the central nervous system, itself the target of the spindle afferent, both before and after receiving a modulate afferent. We developed a protocol based on measures of average velocity to test for this activity. Our investigation began we examining whether or not average velocity, in the form of seated sway velocity, would be sensitive to applied vibration. We found that while vibration was applied; mean sway speed increased significantly above pre vibration levels, regardless of feedback and task difficulty. A computer based pursuit task was then implemented in order to investigate performance relative to timing of vibration exposure. Our results revealed a significant decrease in pursuit velocity during vibration from pre-vibration velocity. Additionally, subjects demonstrated an equal magnitude but opposite increase in pursuit speed after vibration was removed. This protocol was then replicated in a functional-MRI to compare the gross motor pursuit task performance with the corresponding BOLD imaging data. We observed a similar decrease/increase pattern of joystick pursuit velocity. The corresponding cortical activity revealed patterns of inhibition consistent with cognitive inhibition. The current findings support proprioception as a central inhibitory control mechanism that shifts cortical networks dependent on available sensory stimulus.

Acknowledgements

I have so many people to thank for making this work possible. Without each of their contributions it would not have been possible I would like to extend my gratitude to my advisor Dr. Sara Wilson for her guidance, insight, and giving me the freedom in the pursuit of this project. She has also rounded out my graduate education with opportunities as a reviewer, writing (and being awarded) grants and gaining experience on a variety of other projects. I would also like to thank my committee members, Dr. Carl Luchies, Dr. Sarah Kieweg, Dr. Cary Savage, and Dr. John Keighley for all of their support. To my friends at Hoglund Brain Imaging Center, especially Rebecca Lepping, thank you for being my invaluable guides on my journey through fMRI.

During my time as a graduate student I took great comfort knowing that there were several good friends to share both the joys of successes (however small) and the frustration of setbacks (however large). I would like to thank all of my labmates and fellow graduate students, especially Tim Craig, Farhana Lamis, and Dr. Robert Berendt for their friendship and understanding through the whole journey.

I would also like to thank the Madison and Lila Self Graduate Fellowship. This is a truly wonderful program that has given me a better understanding of myself as both a professional and individual. I am sincerely grateful for being included in such select group of people. Thank you Patty, Cathy, Sharon, and Jimmy.

And finally, I would like to thank my family. To Tina, my wife, thank you for your love and patience. I am a better man having you in my life. To my daughter Lila, you have inspired me more than I ever thought possible, I love you very much. Mom and Dad, thank you.

Table of Contents

Chapter 1 - Introduction	1
Background	1
The Anatomy and Physiology of Proprioception	3
<i>The Proprioceptive Feedback Loop</i>	3
<i>The Muscle Spindle Organ</i>	5
<i>Afferent Pathway</i>	7
<i>The Cerebral Cortex</i>	8
<i>Cortico-Cortico Transmission</i>	9
<i>Efferent Pathway</i>	10
<i>Other Brain Structures involved in processing proprioception</i>	11
The Effects of Vibration on Proprioception	11
<i>Effects of Vibration on the Muscle Spindle Organ</i>	12
<i>The Effects of Vibration on Afferent Response</i>	13
<i>Muscle Conditioning</i>	13
<i>Muscle Excitability</i>	14
Measures of Proprioceptive Performance	15
<i>Examining the Role of Proprioception in Motor Control</i>	16
The Use of Brain Imaging to Examine The CNS.....	18
The Current Gap.....	21
Specific Aims and Objectives	22
Significance	24
References	29
 Chapter 2 - Seated Sway is Sensitive to Local Vibration	 35
Abstract	35
Introduction	36
<i>Low Back Pain</i>	36
<i>Anatomy Of The Spine</i>	36
<i>Lumbar Spine Control</i>	38
<i>Measures of Sway</i>	39
<i>Mean Sway Speed</i>	40
Methods.....	41
Results	42
<i>Discussion</i>	44
References	53
 Chapter 3 - The Effects of Vibration on a Joystick Pursuit Task	 55
Abstract	55
Introduction	56
<i>The Case For Velocity Sense</i>	57
<i>Pursuit Tasks</i>	57
<i>Anatomy and Physiology of the Human Arm</i>	58
<i>Purpose</i>	62
<i>Objectives and Hypotheses</i>	62
Methods.....	63
Results	66
Discussion	68
References	85
 Chapter 4 - Vibratory Device Design for Functional MRI	 88
Abstract	88

Introduction	89
<i>Design Evolution</i>	90
Methods	91
Results	92
Discussion	93
References	98
Chapter 5 - Central Integration of Proprioceptive Information	99
Abstract	99
Introduction	101
<i>Sensorimotor Centers of the CNS</i>	102
<i>Objectives and Hypotheses</i>	103
Methods	104
Results	107
<i>Joystick Kinematics</i>	107
<i>pVEL</i>	108
<i>iVEL</i>	108
<i>Peak to Peak</i>	109
<i>Brain Activations</i>	109
<i>Main Effects</i>	110
<i>Interactions</i>	112
Discussion	113
<i>Joystick Data</i>	114
<i>Cortical Activations</i>	115
<i>Summary</i>	119
References	141
Chapter 6 - Summary	144
Review of the Included Studies.....	144
Limitations of the Current Research and Suggestions	146
Conclusions	148
Appendices	149
Appendix A: Common Abbreviations.....	149
Appendix B: Forms	150
<i>Sway Consent Form</i>	150
<i>Joystick Pursuit Consent Form</i>	153
<i>fMRI Pursuit Consent Form</i>	156
Appendix C: Additional Figures	163

Table of Figures

FIGURE 1: THE PROPRIOCEPTIVE FEEDBACK LOOP	26
FIGURE 2: THE MUSCLE SPINDLE ORGAN	27
FIGURE 3: THE SPINDLE AFFERENT INTEGRATION LOOP	28
FIGURE 4: LUMBAR VERTEBRA.....	48
FIGURE 5: EXPERIMENTAL SETUP	49
FIGURE 6: MEAN SWAY SPEED RESULTS	50
FIGURE 7: BALANCE TIME RESULTS	51
FIGURE 8: EXPERIMENTAL TIMELINE.....	74
FIGURE 9: EXPERIMENTAL SETUP	75
FIGURE 10: PURSUIT TASK PROTOCOL	76
FIGURE 11: RESULTS - TIME ON TARGET	77
FIGURE 12: RESULTS - POLYFIT VELOCITY (pVEL)	78
FIGURE 13: RESULTS - INSTANTANEOUS VELOCITY (iVEL)	79
FIGURE 14: RESULTS - PEAK TO PEAK MOVEMENT (PK-PK)	80
FIGURE 15: RESULTS - AVERAGE TIME BETWEEN PEAKS (DT)	81
FIGURE 16: PNEUMATIC VIBRATOR DESIGN EVOLUTION	95
FIGURE 17: COMPARISON OF ROTOR DESIGN - FREQUENCY PERFORMANCE	96
FIGURE 18: PERFORMANCE CURVES (FINAL DESIGN)	97
FIGURE 19: PURSUIT TASK PROTOCOL - fMRI	121
FIGURE 20: EXPERIMENTAL TIMELINE - fMRI	122
FIGURE 21: RESULTS FMRI - POLYFIT VELOCITY (pVEL)	123
FIGURE 22: RESULTS FMRI - INSTANTANEOUS VELOCITY (iVEL).....	124
FIGURE 23: RESULTS FMRI - PEAK TO PEAK MOVEMENT (PK PK)	125
FIGURE 24: JOYSTICK PURSUIT TIME ON TARGET (TOT).....	163
FIGURE 25: JOYSTICK PURSUIT TIME BETWEEN PEAKS (DT)	164

Table of Tables

TABLE 1: SWAY RESULTS ANOVA	52
TABLE 2: FOREARM ANATOMY	73
TABLE 3: JOYSTICK pVEL ANOVA	82
TABLE 4: JOYSTICK iVEL ANOVA	83
TABLE 5: JOYSTICK Pk Pk ANOVA	84
TABLE 6: fMRI PURSUIT pVEL ANOVA	126
TABLE 7: fMRI PURSUIT iVEL ANOVA	127
TABLE 8: fMRI PURSUIT Pk-Pk ANOVA	128
TABLE 9: CONTRAST BL + + vs DV - -	129
TABLE 10: CONTRAST BL + + vs DV - -	130
TABLE 11: CONTRAST BL + + vs PV - -	131
TABLE 12: CONTRAST BL + + vs PV - -	132
TABLE 13: CONTRAST DV + + vs PV - -	133
TABLE 14: CONTRAST DV + + vs PV - -	134
TABLE 15: INTERACTION CONTRAST BL - + vs DV + -	135
TABLE 16: INTERACTION DIRECTION BL - + vs DV + -	136
TABLE 17: INTERACTION CONTRAST BL - + vs PV + -	137
TABLE 18: INTERACTION DIRECTION BL - + vs PV + -	138
TABLE 19: INTERACTION CONTRAST DV - + vs PV + -	139
TABLE 20: INTERACTION DIRECTION DV - + vs PV + -	140
TABLE 21: JOYSTICK PURSUIT ANOVA (DT)	165
TABLE 22: JOYSTICK PURSUIT iVEL - ANOVA POST HOC	166
TABLE 23: JOYSTICK PURSUIT iVEL BONFERRONI	167
TABLE 24: JOYSTICK PURSUIT pVEL - ANOVA POST HOC	168
TABLE 25: JOYSTICK PURSUIT pVEL BONFERRONI	169
TABLE 26: JOYSTICK PURSUIT Pk-Pk - ANOVA POST HOC	170
TABLE 27: JOYSTICK PURSUIT Pk-Pk BONFERRONI	171
TABLE 28: fMRI PURSUIT pVEL - ANOVA POST HOC	172
TABLE 30: fMRI iVEL - ANOVA POST HOC	174
TABLE 32: fMRI Pk-Pk - ANOVA POST HOC	176
TABLE 33: TALAIRACH PEAK COORDINATES BL+ + vs DV - -	177
TABLE 34: TALAIRACH PEAK COORDINATES BL+ + vs PV - -	178
TABLE 35: TALAIRACH PEAK COORDINATES DV+ + vs PV - -	179
TABLE 36: TALAIRACH PEAK COORDINATES BL-+ vs DV +-	180
TABLE 37: TALAIRACH PEAK COORDINATES BL-+ vs PV +-	181
TABLE 38: TALAIRACH PEAK COORDINATES DV-+ vs PV +-	182

Chapter 1 - Introduction

Background

The human body has an excellent sensory system that allows individuals to coordinate body movements and successfully interact with their environment. This system processes information from sensory receptors sensitive to both the external environment (exteroceptors) and the body itself (interoceptors). This document focuses specifically on the performance of the proprioceptive system, which relies on feedback from interoceptors.

The proprioceptive system creates an internalized map of the body, locating limbs and joints in relation to one another in both space and time. This internalized body schema is the result of combined information from several different sensory elements (such as muscle spindle organs, cutaneous sensors, and golgi tendon organs) located throughout the body [1, 2]. The central nervous system (CNS) collects the information from the individual sensors of a limb and then interprets it to create a perception of that limb's position and movement relative to the rest of the body [3]. In biomechanics research, the body's sense of self-location and movement is commonly referred to as proprioception [1]. In a simple example, proprioception allows one to successfully perform tasks like touching one's own nose with one's eyes closed.

When properly functioning, the proprioceptive system allows us to learn new tasks and perform routine tasks both quickly and safely. Persons in a variety of occupations, however, are subject to environmental conditions that can artificially alter proprioceptive feedback. One well-documented condition common to truck drivers, pilots, and machine operators is the exposure to vibration [4-7].

The sensitivity of muscle spindle organs (a primary proprioceptive sensor) to vibratory stimulus has been well documented in the laboratory setting [8-13]. It has been established that vibrations with frequencies within the range of 20-120 Hz create an illusion of limb movement or altered limb-matching position [14,

15]. Increased errors in targeting and postural tasks have also been demonstrated, lasting up to 30 minutes after vibration is removed [8, 16, 17]. These prolonged performance deficits may be attributed, at least in part, to a centrally occurring phenomenon such as neuromotor habituation or adaptation to the vibratory stimulus [18, 19].

Regardless of the source, impaired proprioceptive feedback is not only detrimental to control but may also pose increased risk for injury. While in our simple example, this could create the dangerous opportunity of poking oneself in the eye rather than touching the tip of one's nose, in more complex body systems (like the spine), altered muscle response could result in injury such as low back pain (LBP) [20]. Here, the poor postural control may result in excessive loading of the soft tissues supporting the back [21]. Low back pain alone is a condition affecting up to 80% of the population, has a very high rate of recurrence (80%), and is a leading driver in musculoskeletal disorder spending in the United States [22].

This is not to say that injury prevention alone is the goal for more thoroughly understanding the proprioceptive system. There are many potential opportunities in the fields of therapy and rehabilitation. Vibration has recently has been implemented in the soles of shoes as a means to improve sensorimotor function such as standing balance in different population groups (aged, diabetic neuropathy, stroke) [23, 24].

Additionally, robotic training systems have been developed and used in rehabilitation to measure and improve task performance in such groups [25, 26]. The potential for these and future interventions may be further aided by a better understanding of the proprioceptive feedback loop. While a large portion of our current knowledge has been derived from animal models, this dissertation is restricted to work completed with humans.

In this introduction, we examine:

1. *The anatomy and physiology of proprioception*
2. *What is currently known about the effects of vibration on proprioception both during and after vibration exposure*
3. *Measures to examine the role of proprioception in motor control*
4. *Brain imaging and other techniques to examine the CNS*

The Anatomy and Physiology of Proprioception

The proprioceptive system aids humans in the control of everyday motor tasks. As early as 1888, researchers began describing the ability of the human body to sense the position and movement of its limbs and trunk as kinesthesia [27]. The term proprioception was later introduced by Sherrington to define the body's "sense of self" [28]. Despite arguments that the kinesthetic sense is predominantly behavioral in nature (movement) and proprioception including a cognitive component (movement + perception), the two terms are frequently used interchangeably. Regardless of the terminology used, the body's self-recognition is driven by signaling from sensory elements in the peripheral nervous system (PNS) that are integrated by the central nervous system (CNS) [29]. Exactly how this information is processed to create a coordinated response and ultimately control movement is still hotly debated [30-35]. As such, several different mathematical models/simulations and experimental paradigms have been developed to try to elucidate an understanding. However, before a thorough discussion of these experiments can be undertaken, it would be prudent to review the basic anatomy and physiology of the proprioceptive feedback loop, from transducer to mover.

The Proprioceptive Feedback Loop

The proprioceptive system provides non-visual feedback to the CNS by sensors in the PNS. This information is used to generate a moment-to-moment map of the body schema, locating the relative orientation and location of the head, trunk, and limbs to one another [36, 37]. In a sense, this can be thought of as an internal GPS so that simple tasks, such as closing one's eyes and touching one's own nose with one's finger, can be accomplished with relative ease.

This internal information can be incorporated with visual information allowing a person to interact with their surroundings. In another simple example, the visual system targets a doorknob establishing a goal location based on the current body state detected by the proprioceptive system. The hand moves to the doorknob, turns it, and opens the door. In a sense, proprioception provides information similar to that on the dashboard of a car (compass direction, velocity, RPMs). While useful in describing the general state of the car, this information requires a map showing the actual position so that the task (traveling from A to B) may be successfully completed. In the car example, feedback is routed to the car's computer to generate the appropriate response, but in the human body this feedback must be transmitted to and processed by the CNS before a muscular response can be elicited.

The steps of the proprioceptive feedback loop may be categorized to include signal acquisition at the receptor (spindle organ), signal transmission, signal integration, motor recruitment, and finally the realized movement [Figure 1]. Our current understanding of the contributions of the proprioceptive system arises from a few classes of experiments. Those investigating the response of the peripheral sensor (looking at the ascending, or afferent, leg of the loop), those looking at motor excitability (looking at the descending -efferent- leg of the loop), and those looking at the total response of the loop in terms of task performance (referred to as traditional studies).

This proprioceptive feedback loop can also be described in traditional systems engineering terms in the form of a block diagram. The process variable in our simple example here is the elbow angle θ . Here

the afferent information from the spindle organ is shown as the negative feedback loop and is generated for each position and movement of the elbow joint. This information is then fed to the system controller, in this case the brain, where a control strategy is then formulated and a response is then sent to the final control element (FCE), the motor neurons of the appropriate muscles. This process is then repeated until the task or goal is accomplished.

The Muscle Spindle Organ

In order to provide the proper muscular response to an external or internal stimulus, reliable feedback must be present. Proprioceptive feedback arises from several different peripheral sources in the muscles, joints, and skin that are sensitive to stretch, pressure, force, and vibration [1, 38, 39]. While each of these subsystems has been demonstrated to contribute partially to the overall "sense of self", the muscle spindle organ is currently recognized as the primary contributor to proprioception [13, 40, 41]. A review of the basic anatomy and physiology of the muscle spindle organ (MSO) follows in the text below and can be seen in Figure 2.

The muscle spindle organ is a mechanoreceptor in the PNS. As a mechanoreceptor, the spindles transduce a mechanical stimulus (stretch) into electrochemical signals transmitted to the CNS. The MSO is composed of small muscle fibers (intrafusal) enclosed in a connective tissue capsule. These capsules are connected in parallel to the extrafusal (main) muscle fibers [41]. Both muscle fiber types are capable of generating a force through contraction thanks to alpha (extrafusal) and gamma (intrafusal) neurons. By its parallel orientation, the MSO is well situated to provide information on length changes of the extrafusal muscle fibers, and ultimately both position and velocity of the limb containing the signaling MSOs.

The spindle organ itself is composed of different types of intrafusal muscle fibers (nuclear bag and nuclear chain fibers). The fibers are named due to their relative shapes, the orientation of their nuclei, and diameter. In both types of intrafusal fibers, the contractile mechanisms are only found along the polar

(end) regions. Within the equatorial (central) region are the sensory endings themselves. This polar/equatorial organization of the contractile and sensory elements respectively, allows for the sensitivity of the MSO to be adjusted for any given muscle length, essentially by taking up the slack in the spindle itself via gamma motor innervation [42, 43].

Nuclear bag fibers have a well-defined central "bag" region in which the muscle fiber's nuclei reside in clusters. The bag fibers are further divided into two types based on contraction speed and innervation. These two types of bag fibers are the bag1 and bag2 fibers. Bag1 fibers are innervated by the dynamic gamma neurons and primarily control the spindle's overall dynamic sensitivity. Bag2 fibers are innervated by the static gamma neurons and are primarily concerned with the spindle's static sensitivity [41].

The nuclear chain fiber is long and thin and has its nuclei arranged in a row. The chain fibers are smaller in diameter, shorter, and have a much higher contractile speed than either of the bag fibers. The chain fibers, like the bag2 fibers are innervated by the static gamma neurons (and may share connections with the same neuron). Every muscle spindle organ has both of these fiber types, though based on location within the body each MSO may have some unique combination of multiple bag and chain fibers.

There are two primary sensory afferents that arise in the spindle organs [41]. These afferent neurons are classified by diameter and conduction speed. Type Ia sensory endings are the larger and faster conducting of the afferent nerves. The type Ia endings wrap around the central regions of both the bag and chain fibers. Type II sensory afferents are smaller and slower conducting, and primarily connect to the nuclear chain fibers in a non-spiral branched out nerve ending. Type II endings are thought to be primarily sensitive to the dynamic changes in muscle length (velocity). The muscle spindle provides unique feedback, in terms of pulse train frequency, during both static and dynamic tasks, indicating both position and velocity separately [44].

Exactly how these afferent signals from the different intrafusal fibers are used to generate a feedback signal useful for proprioception and motor control is still unknown and hotly contested [41, 45]. This is complicated by many different observations demonstrating that afferent feedback is generated from both passive (stretched by the extrafusal muscle fibers) and active (fusimotor/gamma activated) muscle spindle organ [46]. While there are several interesting motor control questions that arise in terms of control variables and strategy, that discussion is beyond the scope of the current work.

In order to create a sense of body position and movement (kinesthesia) the muscle spindle afferent must travel from the muscle spindle organ itself to the cortex of the brain through a chain of neurons connecting the sensor to the brain [42]. While there is still much to be discovered in how the muscle spindle afferents are ultimately processed to generate a motor control response, the general pathway these signals take is fairly well understood [Figure 3]. Since the focus of this particular work is the integration of proprioceptive information from both the upper limb and trunk what follows is a more specific discussion of the pathways described in Figure 1. This will provide a general understanding of the regions within the CNS that are expected to be contributors to processing proprioceptive information. The specific locations of interest within the brain itself will be discussed in further detail in chapter five. The following discussion will provide a general understanding of the connections along the greater proprioceptive feedback loop.

Afferent Pathway

The journey of MSO feedback begins as the afferent signals enter the spinal cord. The cell body itself is housed in the dorsal root and projects ipsilaterally to the medulla. Here in the dorsal column nuclei the ascending signal then synapses at either the nucleus gracilis (legs/lower trunk) or nucleus cuneatus (arms/upper trunk), depending on the origin of the feedback, before decussating (crossing over midline) to the opposite side of the brain stem. Both pathways then ascend in the medial lemnisci before continuing to the thalamus via the ventral posterior nucleus. From here the signal is projected to the cerebral cortex.

This route is known as the dorsal column-medial lemniscal system (DCML) and allows extremely fast transmission of information due to its high conduction speed (30-110 m/sec) [42]. With this speed, the DCML is the best-suited spino-cortical pathway to preserve temporal and spatial signal fidelity. Once in the cortex, neuronal connections become exceedingly complex, the discussion to follow is a general description of the pathways for sensorimotor transmission within the cortex of the brain.

The Cerebral Cortex

At first glance the brain appears as a lumpy, wrinkled mass of tissue not too dissimilar in appearance from a de-shelled walnut. If one were to view a cross section of the brain in the coronal (or any other) plane one would observe different layers of tissue and a very complicated geometry along the perimeter. In terms of kinesthesia we are chiefly interested in the locations and activity of the outermost layer (the cortex itself). The cortex is divided into different regions that can be generally identified by examining the topography of the brain.

The brain has two hemispheres (left and right) defined by the sagittal running longitudinal fissure. These hemispheres are further divided into the well-known lobes: Frontal Lobe, Parietal Lobe, Temporal Lobe, and Occipital Lobe. These lobes DO NOT describe functional locations of the brain. Several well-defined major anatomical features primarily define these lobes in humans: lateral fissure, central fissure, etc. The lobes are divided into functional units irrespective of, but defined by, the local gyri and sulci within the lobes. Within this work we will be focusing on the motor and sensory areas associated with proprioceptive feedback.

The majority of the cerebral cortex is made up of neocortex containing six distinct layers described by the types of neurons they contain (stellate or pyramidal) and whether or not the layer is composed mostly of neural cell bodies or processes. Stellate cells are star like in shape with short dendrites and primarily innervate other local cells (laterally within a layer). Pyramidal cells are pyramid shaped with long

dendrites projecting to the surface of the cortex (vertically), to other parts of the cerebral cortex or other CNS structures. The outermost layer is layer I, the deepest layer is layer VI. Incoming afferent signals (from the MSO) first reach the layer IV (internal granular level) neurons of the cortex where the signals are then sent to both superior and inferior cortex levels.

Looking at the brain in the sagittal plane the large central fissure (central sulcus) is visible as a valley that effectively divides the anterior from the posterior brain. The central sulcus separates the motor and somatosensory areas of the cerebral cortex. The somatosensory regions are located posterior while the motor areas are situated anterior the central sulcus.

The cerebral cortex is broken into five types of areas. These are primary and secondary motor areas, primary and secondary sensory areas, and association areas (the majority of the cortex outside of the main reception and motor areas). The motor cortex is divided into the primary and secondary regions. The primary motor cortex consists of the area immediately anterior of the central sulcus including the pre-central gyrus and is ultimately responsible for the signals generated to control muscle contraction (including of the muscle spindles) and body movements.

Like the motor region, the somatosensory region is divided into a primary and secondary cortex. The primary somatosensory cortex is located just posterior the central sulcus (post-central gyrus). The information received here includes signaling from muscle spindles.

Cortico-Cortico Transmission

In general, somatosensory information first arrives at the primary sensory area for a particular sensory system. The signal then projects to the secondary somatosensory cortex, located posterior and inferior the primary region. From the secondary somatosensory region the information is then sent to an association area. These association areas integrate and combine information from several different sources in order to generate a higher order response. In the case of proprioceptive information from the secondary

somatosensory cortex, this information is projected to the posterior parietal association cortex where signals from the visual and auditory systems are also received. From there, the signal then projects to one or many secondary motor area(s). The secondary motor areas finally project to a primary motor area before traveling the efferent pathway to the appropriate motor neurons of the body.

Efferent Pathway

From the appropriate location (pertaining to the body location based on the human motor homunculus) within the primary motor cortex the now integrated response is transmitted to the internal capsule. From the internal capsule, the specific pathway of the response signal splits into one of four descending tracts depending on the region of the body that is acting. For distal limbs, the response travels dorsally, while for proximal muscles the response travels ventrally.

The dorsolateral motor pathways (DLMPs) control the response of distal limbs. The dorsolateral corticospinal tract (DLCST) descends ipsilaterally and decussates (without synapsing) to the interneurons of the contralateral side. The response signal then synapses directly on the motor neurons of the appropriate limbs. The dorsolateral cortico-rubrospinal tract is less direct and descends from the cortex to the red nucleus. In the red nucleus the axons synapse and decussate descending through the medulla and continue to the interneurons before ultimately stimulating the motor neurons generating the muscular response.

The ventromedial motor pathways conduct the response to those muscles located more proximally. The ventromedial corticospinal tracts descend ipsilaterally. Along the spinal cord these VMSPT axons innervates interneuron-motor circuits along both sides of the spine. The ventromedial cortico-brainstem-spinal tracts descend ipsilaterally but before reaching the spine travel through a network of brain stem sensorimotor structures (Tectum, Reticular Formation, and Vestibular Nucleus) before descending along

both sides of the spinal column. Again, each neuron synapses to interneuron-motor circuits on both sides of the spine.

Other Brain Structures involved in processing proprioception

While the cortex is discussed in depth, it should also be noted that additional brain structures contribute to proprioception. These include the cerebellum and basal ganglia. The primary contributions of the cerebellum and basal ganglia are thought to be modulation and coordination of motor activity and learning. Recent studies have demonstrated changes in cerebellar activities during a joystick pursuit task for independent changes in cursor gain, movement extent, and velocity [47, 48]. In general it is thought that the cerebellum is more involved in postural adjustment and balance, while the basal ganglia is involved with distal limbs.

The Effects of Vibration on Proprioception

In the proprioceptive feedback loop, the ultimate goal is to control the joint angle (θ) within a certain tolerance to accomplish a task and avoid injury. We have already alluded to situations where this feedback loop may be disrupted, impairing that control. In particular, industries where workers are regularly exposed to whole body vibrations appear to be at a higher risk for experiencing low back pain injuries possibly due to impaired lumbar control [5-7, 49]. Further, similar proprioceptive impairments have been produced in various forms in laboratory settings [8, 13, 50].

While the gross effects of the disrupted proprioceptive feedback loop have been extensively studied and are well understood, exactly how these kinesthetic illusion errors come about is not completely agreed-upon. Before we delve into these specifics involving the effects of vibration on the overall response during a motor task we will first focus on the changes known to occur within the PFL. The possibilities include: changes to the afferent leg, changes in the CNS processing of the afferent information, changes

in the descending leg, or some combination of these changes PFL. What follows is a review of the currently understood changes along the proprioceptive control loop due to applied vibration.

Effects of Vibration on the Muscle Spindle Organ

The muscle spindle organ has a demonstrated sensitivity, with unique outputs for, static lengths and changes in length of extrafusal muscle fibers [41]. It has documented by numerous studies that both the static and dynamic signaling of the muscle spindle organs are sensitive to applied vibration [13, 51]. The afferent MSO signaling entrains to the frequency of the applied vibration [50]. This is to say that, a signaling frequency indicating a particular position or velocity, when subjected to an applied external vibration of a lower frequency would indicate a muscle length or velocity that is smaller in magnitude than the true muscle length/slower than the true velocity [44]. The perceived movement resulting from the modulated afferent has been described in literature as a "kinesthetic illusion".

The muscle spindle organ is particularly sensitive to applied vibrations in the range of 20-120 Hz, with a "sweet spot" for inducing a kinesthetic illusion between 60 and 80 Hz [14, 15]. Furthermore, the overall result of this modulated proprioceptive feedback manifests as changes in task performance persisting well beyond the period of vibration [8, 17]. Therefore, the large populations that experience vibrations in the workplace could be at increased incidence for LBP not only during working hours but for a period of time after work as well.

There is some discrepancy, however, as to how long these effects persist. Some have demonstrated the induced errors lasted anywhere from a few minutes to a half-hour post vibration [8, 16, 17]. However, this is somewhat complicated by observations via direct microneurographic recordings that indicated that spindle afferents recover relatively quickly (on the order of seconds) once free of the influence mechanical vibrations [13]. The recovery periods observed during these recordings corresponded similarly to the kinesthetic illusions observed by subjects, meaning that the induced illusion was also

followed by a return illusion [52]. These observations, however, were made after a relatively short duration of vibration, less than 1 minute, and are generally an order of magnitude shorter than those used in the traditional response studies. While these altered afferents may help explain a portion of the altered proprioception observed, the difference in durations suggests there is likely a stronger contributing influence than simply the afferent source information being fed to the controller.

While during vibration changes in performance can be directly attributed to the disrupting vibration frequency itself, what is not known is why there is a persistent change after the external vibration has been removed. Some insight may be gleaned looking back at our proprioceptive feedback loop diagram. Since changes in any portion of the loop may be responsible for lasting changes in the overall output of the system. Along with the changes in the afferent leg of the loop, changes may also occur in the CNS processing of this information, covered in detail in chapter five. Changes may also be found on the descending leg of the loop, which we will examine next.

The Effects of Vibration on Afferent Response

Another possible source of these kinesthetic illusion errors are alterations in the descending leg of the proprioceptive control loop. These can be changes (both intra and extrafusal fibers) in the muscle properties themselves or also the history of stretch-shortening cycles of the muscles themselves (thixotropy).

Muscle Conditioning

While traditional studies investigating proprioception have primarily used an external stimulus such as applied vibration, some researchers noted changes in overall performance based on contraction history of the musculature. This muscle history alters the properties of not only the extrafusal fibers, but also the fibers of the muscle spindle organs themselves [53]. This has led to the practice of preconditioning muscles in some experiments, often expressed as an isometric contraction of different lengths. Cao et al.

found a decrease for longer holds and increase for longer holds in spindle sensitivity to stretch velocity only for lengthening tasks [54]. A similar increase in position sense error has been observed with an external vibration and preconditioning [55]. The source most commonly attributed to these thixotropic changes is the tacking up of the "slack" in the intrafusal fibers created when the extrafusal fibers shorten. Investigating the long-term effects has proven more difficult since the muscles and muscle fibers are constantly changing length throughout daily activities.

Muscle Excitability

What has often been reported is that applied vibration increases the relative amplitude of motor evoked potentials (MEPs) in the antagonist muscle opposite the vibrated muscle [52]. This is essentially the strength of the muscle contraction given a known input stimulus. Typically this is tested by means of transcranial magnetic stimulation (TMS) used as an input to the motor cortex and a measured electromyographic (EMG) response. While the findings on muscle excitability and corticospinal stimulation provide useful insight, it should be noted that the reliability of results from some of the methodologies implemented (TMS and use of the F-wave) are still under debate [56, 57].

Generally an increase in MEP amplitude has been observed in the vibrated muscles corresponding with the frequencies known to alter muscle spindle afferents, with a maximum excitability around 75 Hz [58, 59]. While the agonist muscle excitability appears to return to normal post vibration, lasting increases have been observed in the antagonist [60]. The opposite has also been observed, with the relative MEP increasing temporarily during vibration before temporarily decreasing post vibration, corresponding to self-reported kinesthetic illusions of flexion and return making these results inconclusive [52].

The third possible source of kinesthetic illusions/proprioceptive errors is the proprioceptive feedback loop processing centers of the CNS. Evidence for CNS driven changes in motor task performance is found in a series of experiments using advanced imaging in conjunction with mechanical vibration and a cortical

stimulation technique known as transcranial magnetic stimulation (TMS). In both types of study, researchers have repeatedly reported subjects perceiving movement of limbs up to and beyond the physiological limits, even though no movement is present. These studies are covered in further detail in chapter five. While none of the previously mentioned studies directly investigated active tasks, the implication of perceived motion when none exists presents a potential source of kinesthetic error that must be investigated further.

Measures of Proprioceptive Performance

We have previously described the necessity of the proprioceptive feedback loop for the control and learning of everyday activities. We have also noted certain pathologies and environmental conditions may alter proprioceptive feedback. In the previous sections, the general anatomy and physiology of the muscle spindle organ as well as the effects of vibration on the afferent and efferent legs within the PFL have been covered. We will now turn our attention to the overall assessment strategies of proprioceptive performance.

Performance-based tasks have been widely used to probe the capabilities of the human proprioceptive system [8, 52, 61, 62]. Many of these research studies have made use of locally applied vibration in the range of 20-120 Hz to disrupt the output of the MSO. The key findings of such experimental work have documented the conditions under which kinesthetic illusions are created and how they affect overall performance [52, 63, 64].

The following review is a brief summary of the techniques and experimental paradigms most likely to be encountered in the literature in assessing proprioception and the effects of vibration. This is in no way a comprehensive survey of all paradigms used, but a simple survey of the techniques a reader is most likely to encounter in current literature.

Examining the Role of Proprioception in Motor Control

Experiments investigating proprioceptive performance are typically a movement task involving a single joint with the goal of reproducing a particular motion or angle. Common protocols make use of the possible combinations of actively or passively moving a single limb to match either the contralateral limb (matching and targeting tasks) or reproduce the previous state of the ipsilateral limb (reposition test). Since visual information can strongly influence performance, the tested limb is often not visible to the subject. The movement parameter may be, but is not necessarily limited to, a kinematic variable (position or velocity), an activation variable (muscle EMG), or a posture-based sway-measure. Therefore, these traditional task-based measures are indirect measures of proprioceptive performance. In practice, experiments often employ multiple measures to more fully test their hypotheses [11, 44]. Care must be taken when interpreting results, however, as conclusions must take into account the different experimental conditions the research was conducted under.

Since vibration has been demonstrated to alter the afferent signaling of the MSO, It has become the perturbation of choice when conducting research on proprioceptive feedback. As in the case of the actual task protocol, the perturbing vibration may be applied to the limb being tested or the contralateral limb (the reference signal). Furthermore the vibration frequency may be anywhere within the MSO is sensitive to as proprioceptive errors are most strongly induced within this range [15].

In the classic version of the angle-matching test, subjects were instructed to match active elbow extension angles of one arm while vibration was applied to the biceps of the other arm. Rogers et al., observed larger than control extension angles of the vibrated arm due to faster extension movements [16]. This basic test and results have been repeated in similar fashion many times [12, 39, 55, 65, 66]. These findings consistently report proprioceptive errors are primarily generated during lengthening of the vibrated muscle. With this form of testing it was also demonstrated, using combinations of biceps/triceps

vibration locations, that proprioceptive error was only generated, and directly related to the magnitude of, the imbalance in afferent signaling frequencies of the agonist/antagonist pair [67].

A popular variant of the angle-matching test is the targeting task. The main difference being that the targeting task primarily utilizes a predefined endpoint [11, 68]. This test often includes a training period before assessment and may be tested with the same limb (ipsilateral) or the opposite side limb (contralateral). These targeting tasks have often reinforced the findings that kinesthetic illusions are only fostered in the lengthening direction. Sittig et al. used such a paradigm to demonstrate the independence of position and velocity as feedback for slow and fast movements respectively [44]. Cordo et al. however reported that the actual direction of error depends on when exposure to vibration occurs. Subjects, in this study, were instructed to release a mechanical grip at a predetermined elbow angle while the biceps was subjected to vibration. Subjects undershot a targeted release angle while vibration was applied, but overshot if vibration was removed after the start of movement [11]. This implied that while the spindle afferent are sensitive during muscle lengthening, there is also a corrective 'return' error post vibration.

When a single limb or the trunk is assessed, the task becomes a repositioning task. This type of task consists of training the limb to a particular joint angle and reproducing it from memory [8, 9, 20, 69]. In general, the position matching tasks with the smallest absolute error, under normal conditions, are those that implement repositioning of the ipsilateral limb [66]. When vibration has been used as a stimulus, increased reposition errors as well as increased delays in muscle activations have been observed both during and post vibration [8, 20].

The majority of findings thus far have focused on position sense, even though it is well accepted that muscle spindle organs provide position and velocity information [44]. Intuitively, there should be a velocity-based analog for every position based task available and the reported results in velocity task performance have generally corresponded well to the observed changes in position sense. Illusions of

vibration have been observed to occur in the direction of muscle lengthening and result in velocities in the direction of the Ia afferent imbalance [28, 70]. Detection threshold of velocity was found related to the velocity of the movement with muscles controlling more distal movements being sensitive to movement over a much larger angular range [3, 71, 72]. Velocity based studies have not however documented many post vibration effects.

Perhaps some of the most intriguing findings have come from the tests of perceived motion. In these cases, subjects primarily report the relative magnitude or detection of motion of their limb verbally. While errors observed in the previous protocols have been reported within the limits of the activity itself, kinesthetic illusions may induce perceived movements beyond that which is physiologically possible [64, 73]. It has also been demonstrated that an induced kinesthetic illusion may also be transferrable to other parts of the body as well [74]. In the classic, 'Pinocchio' example, an induced illusion of elbow extension while one is touching their nose results in the perception that the nose itself is lengthening [75]. These results strongly encourage the idea that central mechanisms are likely the source of proprioceptive errors, both during and post vibration.

We conclude with the statement that much additional work needs to be undertaken in terms of velocity as a control variable. A better characterization can likely be found in a pursuit task paradigm as a variant of the targeting task. While there is a great deal of information regarding the effects of active muscle vibration, there is less information regarding the post vibration effects, so a protocol testing both during and post effects would be beneficial. Such a task could be performed to increase our understanding of proprioception as traditional studies, but also be coupled with advanced imaging techniques to associate changes in performance with changes in neural correlates.

The Use of Brain Imaging to Examine The CNS

Several imaging modalities have developed relatively recently that provide a more detailed peek into the functioning human brain. While not direct measures of the electrical activity in the brain, there is a large body of work indicating that metabolic correlates such as BOLD are reasonable estimates of direct activity, which for many reasons is not readily practical as of this writing. These modalities include: magnetoencephalography (MEG), positron emission tomography (PET), Electroencephalography (EEG), Functional Magnetic Resonance Imaging (fMRI), Single Unit and Patch Clamp recording. Tradeoffs between each of these techniques are generally made between spatial and temporal resolution with additional considerations including ease of use, safety, and what is necessary to answer the research question. Of these technologies, fMRI has rapidly become one of the most widely implemented brain imaging techniques. This popularity is due to the balance of good spatial (~2 mm) and temporal resolution (~1 sec), the flexibility in research applications it can address, and the relative simplicity of data collection.

The basic premise of an MRI scan is based on the precession of hydrogen atom nuclei about a magnetic field. Hydrogen is chosen because of its abundance in the body. The MRI system is composed of a very large magnetic and powerful magnetic that creates a stable magnetic field to induce general molecular precession in the body. Three smaller magnets within the MRI machine are used to change the focal point of the machine to a different point in the body. A known radio frequency (RF) signal is then transmitted into the bore of the machine and whatever is in it (the human body). The RF energy causes the non-aligned nuclei to resonate at a known frequency, and this response is then measured and fed into a computer to produce an image.

Functional Magnetic Resonance Imaging (fMRI) measures the change in metabolic correlates serving the neurons of the brain. It does not measure the electrical activity of those neurons. Often blood flow into specific regions is used to measure the blood-oxygenation-level-dependence (BOLD). The BOLD signal is essentially the ratio of oxyhemoglobin to deoxyhemoglobin at a particular location, with active neurons

in the brain requiring and using more oxygenated hemoglobin to function. These neural correlates function on a temporal level much slower than actual electrical conduction in the brain. Therefore depending on the cognitive or behavioral task that is being investigated, this response can vary on the order of several seconds.

The hemodynamic response of sensorimotor tasks has been reported to have a latency anywhere between 1.5-2.25 seconds from the start of the movement, ramping up quickly, and peaking within 6 seconds post start [76, 77]. The latencies are not necessarily consistent and may vary from region to region, with visual centers becoming active before supplemental motor area and primary motor regions becoming active last [78].

Functional somatosensory and motor units have been identified and located in humans using fMRI, PET, and others [47, 79, 80]. This has provided valuable insight of active brain centers during performance of simple motor and cognitive tasks. A few researchers have investigated the phenomenon of the altered muscle spindle afferents utilizing these imaging modalities demonstrating that these errors may be due to activity in both motor and somatosensory regions of the brain [81]. This has primarily been undertaken during static tasks. To date it is not evident that any studies have been performed to investigate changes in brain activity while performing a dynamic task with modulated spindle afferents. Nor have there been any investigations into changes in activity or performance after vibration has been removed. It is this gap that the current research has proposed to fill. A review of the current understanding of the use of advanced imaging of proprioception can be found in chapter five.

While the real strength of the MRI technique is the fine detail of anatomical structures available deep within the body provided in the images. The functional aspect allows temporal data to then be mapped to likely centers of activity. Although new technologies and techniques are being developed, current images do not relate image intensity to the tissue's mechanical properties. Some of the smaller MRI models now

being developed and produced are helping to make the technology more mobile and overcoming the once substantial setback of the sheer size of the scanners. Still a relatively young technology in clinical practice, MRI has become a powerful visualization technique and is emerging as a viable option to retrieve more physiological information than originally imagined non-invasively. Some of the drawbacks of an MRI scan include the high cost of owning and operating a scanner; images are collected on still subjects and are not real time. Several patients are also unavailable to receive an MRI scan because of metal fragments in the body or other electromagnetic sensitive technologies, such as pacemakers, that they rely on for healthy functioning. Introducing metal of any sort in an MRI environment can be extremely dangerous simply because of the strength of the magnetic fields involved. A small fragment of ferrous material can easily become a dangerous projectile.

The Current Gap

At this point it would be beneficial to briefly review the findings covered thus far. It has been accepted for a long time that feedback from the peripheral nervous system has played an important part in the human body's "sense of self". This proprioceptive feedback arises primarily from the muscle spindle organ afferents, which are sensitive to both muscle length and changes in muscle length. It has also been demonstrated that applied vibration alters the muscle spindle afferent, which in turn alters overall task performance in terms of position and/or velocity. These changes in task performance may in part be attributable to both changes in afferent and efferent legs of the proprioceptive feedback loop in terms of afferent frequency and muscle excitability respectively. These changes in the ascending and descending legs of the PFL may be able to partially describe performance changes during the presence of vibration. However, due to the short term nature of these changes they are unlikely to be wholly responsible for longer term changes in task performance often observed after prolonged exposure to vibration. This suggests that these persistent changes in task performance may be due to some centrally occurring phenomenon.

Some work has been done to identify primary and secondary motor and somatosensory locations within the brain active during vibration induced kinesthetic illusions. There are none that investigate the persistent changes in task performance. In summary, much of the current research focuses on changes within the PFL during active exposure to vibration, but does not directly consider post vibration performance and recovery. While the majority of task performance and likely CNS changes have been defined in terms of positional performance, velocity also needs to be considered as a target variable. It is the goal of this collective work to lay the groundwork to better understanding of these changes in human performance.

Specific Aims and Objectives

The overall goal of this research was to identify if centrally occurring changes are likely responsible for persistent proprioceptive errors post vibration. More specifically, we aimed to identify regions of the central nervous system that process and integrate velocity-based proprioceptive information during an active motor task. This was performed in a step-by-step fashion of progressively detailed studies building a reference framework for velocity based performance tasks. Together these objectives will help determine whether changes in proprioceptive ability arise in the central nervous system or are driven by peripheral changes previously discussed.

The specific aim of the first study (chapter two) was to determine whether a velocity-based measure of sway could be used to investigate proprioceptive control of the low back and the effects of local muscle vibration. The goal of the sway study was to establish a less variable performance based measure than traditional position-error tasks; this new measure could then be tested in similar tasks for other joints, such as the pursuit task described in chapters three and five.

The study in chapter three had multiple specific aims. The primary objective was to determine if there was a difference in pursuit-task velocity replication both during and post local vibration to the dominant

hand's supinating musculature. A second objective was to determine if 20 minutes of recovery time after vibration was sufficient to return to pre-stimulus levels. In terms of task performance we posed the question, "Is proprioceptive control of velocity sensitive to both the during and post vibration effects of vibration?" The merits of this chapter not only extend our current understanding of velocity based proprioceptive tasks, but it also verifies the likely success of the imaging work described in the chapter five study.

The specific aim of the fourth chapter was to discuss the design process of a device to provide a reliable and controllable stimulus in a strong magnetic environment. We particularly focus on implementing a design process using rapid prototyping technology. A compatible vibration device would allow the modification of the proprioceptive inputs in an MRI environment with minimal interruptions of the protocol, allowing all subsequent measures to be related to a single structural scan. Additionally, proper design would not leave artifacts in the resulting scanned images. This is a discussion of common design considerations for imaging studies as well as the evolution of the currently designed functional prototype.

The collection of studies culminates in chapter five with the specific aim to relate the performance-based measures developed through the preceding work with the neurological information obtainable via fMRI. This was primarily an attempt to answer the question, "What cortical regions are active during a normal pursuit task and what changes in activity are observed during and post vibratory stimulus?" A secondary objective was to determine if there was a likely association of task performance and changes in activity of sensory and/or perceptual area(s) of the brain. Making the link between brain activity and motor performance would allow us to determine whether or not central habituation or another phenomenon may be responsible for the persistence of performance-based errors often associated with prolonged vibration exposure. This link would in turn allow for the development of appropriate guidelines or interventions to limit potential injuries and also aid in rehabilitation for pathologies related to compromised motor control.

Chapter six reviews the key findings from each of the chapters and discusses both the limitations and the future logical directions for this research. The results of this work provide a common basis for interpreting and comparing current and future results in the area of human motion control.

Significance

Research in the control and movement of posture in humans has been an important tool in advancing fields ranging from: physical therapy and rehabilitation to ergonomics and injury prevention to prostheses development and the enhancement of human performance [23, 25, 82-86]. Areas of research focusing particularly on the perception of limb position and movement (kinesthesia) have used task performance as an indirect measure of this ability [9, 87]. Often, these studies have taken advantage of the illusory effects elicited by locally applied vibrations on the afferent signals of the muscle spindles [8, 13, 15, 55, 70]. Though this has led to useful results, the high variability often observed in these measures has made comparison and interpretation of findings difficult. Some kinesthetic studies have been conducted using a more direct measure of brain activity, fMRI imaging [74, 80, 88]. These studies though, have been mainly limited to static tasks [79, 88]. While the effects of applied local vibration have been well documented on kinesthesia during motor tasks and in brain imaging studies, there are so far no known studies combining the two approaches.

Existing measures of proprioceptive performance, such as the ability to replicate joint angles or joint angle velocities are indirect and influenced by changes in all stages of the proprioceptive feedback loop though perception is a higher order response [60, 88, 89]. Therefore it would be useful to correlate these changes in output with changes in the processing of this proprioceptive feedback. A measure based on data related to the physiological phenomenon related to brain activity could better illuminate the strategies used for feedback and the control of motion.

This increased understanding would then allow for a more accurate and appropriate identification of factors contributing to impaired neuromuscular function. Additionally, appropriate countermeasures could be investigated to help return the neuromuscular system to the non-impaired state. This work provides a useful framework for clarifying the role of the central nervous system in contributing to the body's sense of kinesthesia.

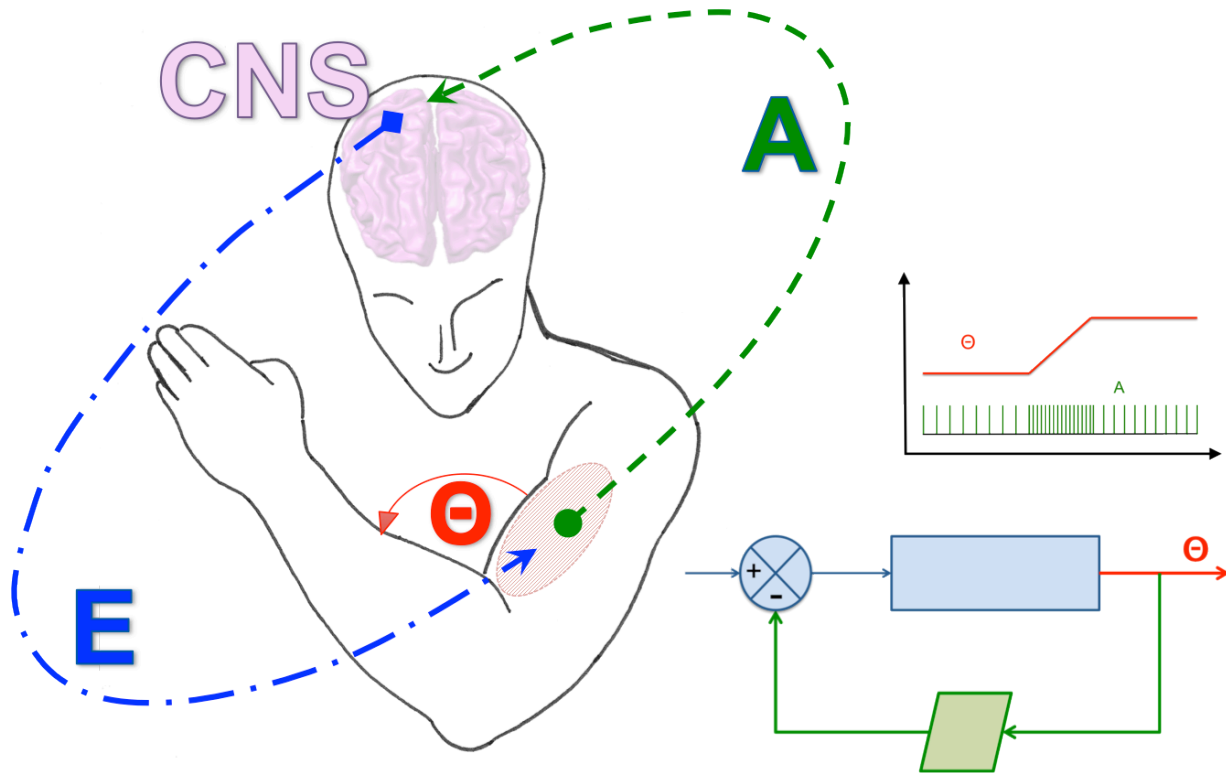


Figure 1: The Proprioceptive Feedback Loop

The above figures depict the complete cycle of proprioceptive feedback resulting in a motor response. The signal is initially generated in a peripheral muscle receptor (muscle spindle organ) and travels to the central sensory centers of the brain via the Ia afferent (A). The incoming signal is then integrated with information from other sensory locations (visual, vestibular, etc.) to formulate an appropriate response as the signal travels from the sensory centers of the CNS to the motor centers. The calculated response is then transmitted to the motor nucleus of the appropriate muscle via the efferent pathway (E) which results in a new joint angle (theta). The top inset demonstrates how the muscle afferent signal is sensitive to not only changes in joint angle (theta) corresponding to different muscle lengths, but also has a unique signaling properties for the transient state. The lower inset shows a simplified representation of the proprioceptive feedback loop in terms of a standard block diagram.

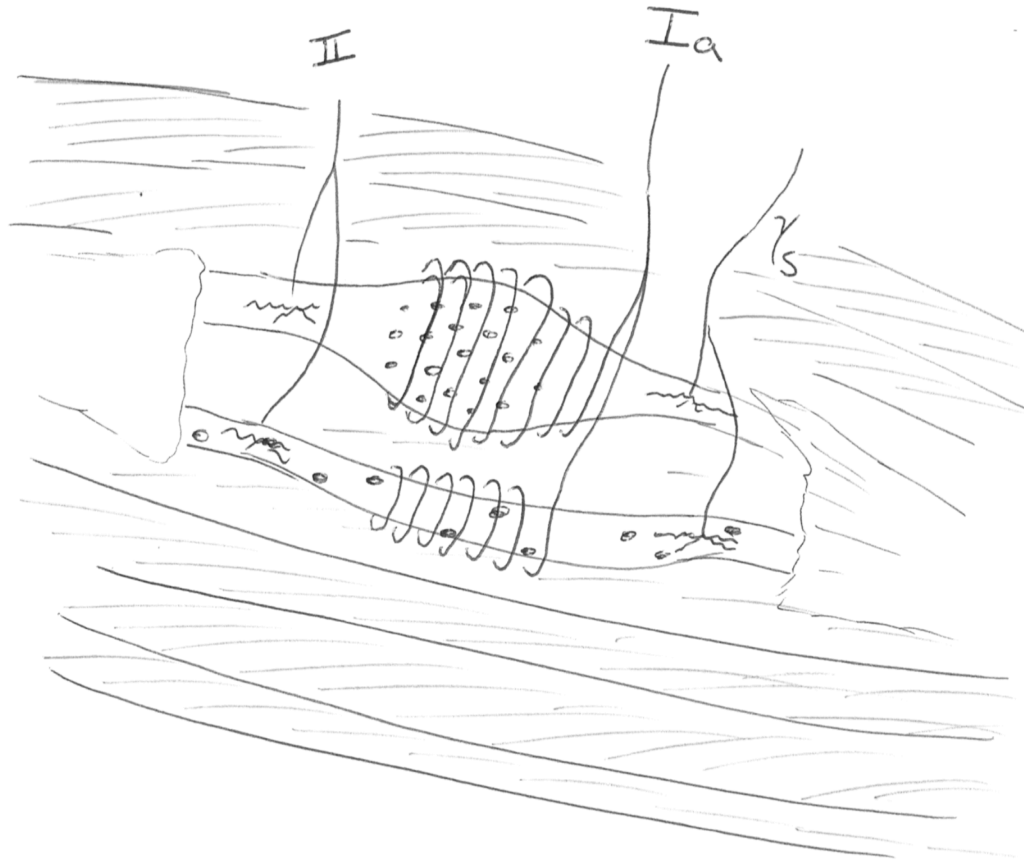


Figure 2: The Muscle Spindle Organ

Above is the traditional depiction of the muscle spindle organ (MSO). The spindle organ itself is located parallel to the extrafusal (skeletal) muscle fibers. Afferent signals are generated primarily from the Ia fiber originating on the central regions of both bag (top) and chain (bottom) fibers. A second smaller afferent (type II) can be observed to arise from a granular nerve ending along the polar regions of both the chain and bag2 (shown) fibers. Each type of intrafusal fiber also receives contractile innervation via a gamma motor neuron. Not depicted is a bag1 (dynamic sensitive) bag fiber (it would not have a type II afferent).

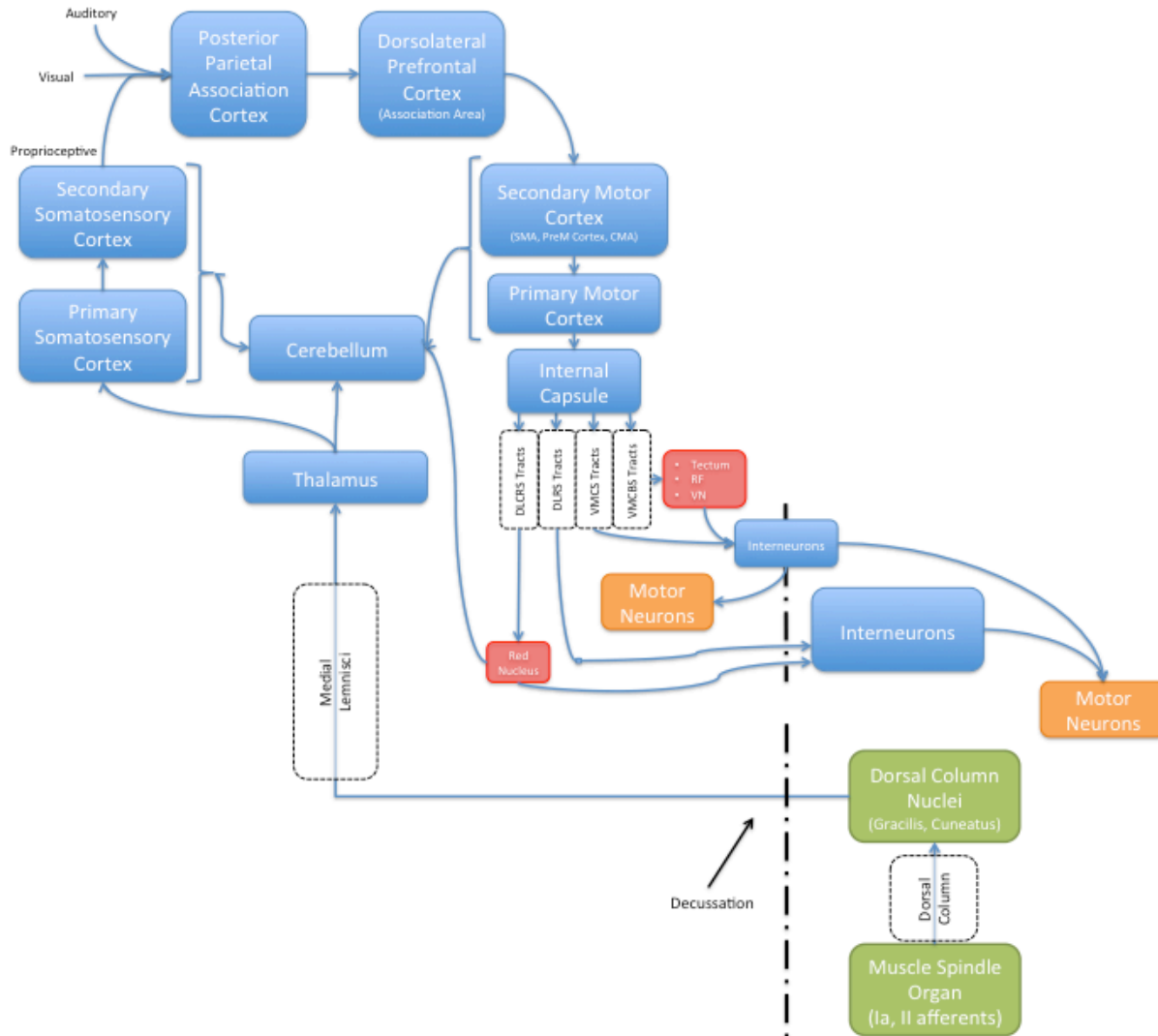


Figure 3: The Spindle Afferent Integration Loop

This is a general depiction of the transmission of proprioceptive feedback originating from a muscle spindle organ. The dashed line represents the body midline. Note that information flows through the thalamus and through the somatosensory cortex before being combined with auditory and visual feedback in association areas before becoming a motor response. Subcortical structures such as the cerebellum receive inputs from the sensory, motor, and red nucleus. Also note that complex sorting of the efferent signal from the primary motor cortex (M1). Ventromedial tracts projects to interneurons along the spinal cord to control proximal muscles along both sides of the spine, while Dorsolateral tracts project to proximal muscles of the limbs to one side of the spine.

References

- [1] D. F. Collins, K. M. Refshauge, G. Todd, S. C. Gandevia., Cutaneous receptors contribute to kinesthesia at the index finger, elbow, and knee. *Journal of Neurophysiology*, 94: 1699-706, 2005.
- [2] U. Windhorst. Muscle proprioceptive feedback and spinal networks. *Brain Res Bull*, 73: 155-202, 2007.
- [3] G. K. Kerr, C. J. Worringham., Velocity perception and proprioception *Sensorimotor Control of Movement and Posture*, 508: 79-86, 2002.
- [4] R. P. Blood, J. D. Ploger, P. W. Johnson., Whole body vibration exposures in forklift operators: comparison of a mechanical and air suspension seat. *Ergonomics*, 53: 1385-94, 2010.
- [5] T. Waters, A. Genaidy, H. Barriera Viruet, M. Makola., The impact of operating heavy equipment vehicles on lower back disorders. *Ergonomics*, 51: 602-36, 2008.
- [6] F. Gerr, L. Mani., Work-related low back pain. *Primary care*, 27:865, 2000.
- [7] M. H. Pope, T. H. Hansson., Vibration of the spine and low back pain *Clinical orthopaedics and related research*, 279:49, 1992.
- [8] M. Arashanapalli, S. E. Wilson., Paraspinal muscle vibration alters dynamic motion of the trunk. *J Biomech Eng*, 130:021001, 2008.
- [9] P. M. Bernier, R. Chua, J. T. Inglis, I. M. Franks., Sensorimotor adaptation in response to proprioceptive bias. *Exp Brain Res*, 177: 147-56, 2007.
- [10] S. Brumagne, R. Lysens, S. Swinnen, S. Verschueren., Effect of paraspinal muscle vibration on position sense of the lumbosacral spine *SPINE*, 24: 1328-31, 1999.
- [11] P. Cordo, V. S. Gurfinkel, L. Bevan, G. K. Kerr., Proprioceptive consequences of tendon vibration during movement *Journal of Neurophysiology*, 74: 1675-88, 1995.
- [12] G. M. Goodwin, D. I. McCloskey, P. B. Matthews., The contribution of muscle afferents to kinaesthesia shown by vibration induced illusions of movement and by the effects of paralysing joint afferents. *Brain*, 95: 705-48, 1972.
- [13] E. Ribot-Ciscar, C. Rossi-Durand, J. P. Roll., Muscle spindle activity following muscle tendon vibration in man. *Neurosci Lett*, 258: 147-50, 1998.
- [14] J. B. Fallon, V. G. Macefield., Vibration sensitivity of human muscle spindles and Golgi tendon organs. *Muscle Nerve*, 36: 21-9, 2007.
- [15] J. P. Roll, J. P. Vedel., Kinesthetic role of muscle afferents in man, studied by tendon vibration and microneurography *Experimental Brain Research*, 47: 177-90, 1982.
- [16] D. K. Rogers, A. P. Bendrups, M. M. D. Lewis., Disturbed proprioception following a period of muscle vibration in humans *Neuroscience letters*, 57: 147-52, 1985.
- [17] M. M. Wierzbicka, J. C. Gilhodes, J. P. Roll., Vibration-induced postural post effects. *J Neurophysiol*, 79: 143-50, 1998.

- [18] K. Rosenkranz, A. Pesenti, W. Paulus, F. Tergau., Focal reduction of intracortical inhibition in the motor cortex by selective proprioceptive stimulation *Experimental Brain Research*, 149: 9-16, 2003.
- [19] K. Rosenkranz, J. C. Rothwell., Differential effect of muscle vibration on intracortical inhibitory circuits in humans. *Journal of Physiology*, 551: 649-60, 2003.
- [20] L. Li, F. Lamis, S. E. Wilson., Whole-body vibration alters proprioception in the trunk *International Journal of Industrial Ergonomics*, 38: 792-800, 2008.
- [21] M. M. Panjabi., The stabilizing system of the spine. Part II. Neutral zone and instability hypothesis. *J Spinal Disord*, 5: 390-6; discussion 397, 1992.
- [22] S. Pai, L. J. Sundaram., Low back pain: an economic assessment in the United States. *The Orthopedic clinics of North America*, 35:1, 2004.
- [23] J. M. Hijmans, J. H. Geertzen, W. Zijlstra, *et al.*, Effects of vibrating insoles on standing balance in diabetic neuropathy. *J Rehabil Res Dev*, 45: 1441-9, 2008.
- [24] W. Liu, L. A. Lipsitz, M. Montero-Odasso, *et al.*, Noise-enhanced vibrotactile sensitivity in older adults, patients with stroke, and patients with diabetic neuropathy *Archives of physical medicine and rehabilitation*, 83: 171-6, 2002.
- [25] H. I. Krebs, J. J. Palazzolo, L. Dipietro, *et al.*, Rehabilitation robotics: Performance-based progressive robot-assisted therapy *Autonomous Robots*, 15: 7-20, 2003.
- [26] E. Vergaro, M. Casadio, V. Squeri, *et al.*, Self-adaptive robot training of stroke survivors for continuous tracking movements. *J Neuroeng Rehabil*, 7:13, 2010.
- [27] U. Proske, S. C. Gandevia., The kinaesthetic senses. *J Physiol*, 587: 4139-46, 2009.
- [28] D. J. Goble, S. H. Brown., Dynamic proprioceptive target matching behavior in the upper limb: effects of speed, task difficulty and arm/hemisphere asymmetries. *Behav Brain Res*, 200: 7-14, 2009.
- [29] A. G. Feldman, M. L. Latash., Afferent and efferent components of joint position sense; interpretation of kinaesthetic illusion. *Biol Cybern*, 42: 205-14, 1982.
- [30] R. C. M. Daniel M. Wolpert, M. Kawato., Internal models in the cerebellum *Trends in Cognitive Sciences*, 2: 338-47, 1998.
- [31] A. G. Feldman., Once more on the equilibrium-point hypothesis (lambda model) for motor control. *J Mot Behav*, 18: 17-54, 1986.
- [32] A. G. Feldman., Fundamentals of motor control, kinesthesia and spinal neurons: in search of a theory *Behavioral and brain sciences*, 15: 735-7, 1992.
- [33] D. M. W. Z. Ghahramani, Computational principles of movement neuroscience *Nature Neuroscience Supplement*, 3: 2000.
- [34] M. L. Latash., Motor Control: In Search of Physics of the Living Systems *Journal of Human Kinetics*, 24: 7-18, 2010.

- [35] M. F. Levin, Y. Lamarre, A. G. Feldman., Control variables and proprioceptive feedback in fast single-joint movement. *Can J Physiol Pharmacol*, 73: 316-30, 1995.
- [36] A. Maravita, C. Spence, J. Driver., Multisensory integration and the body schema: close to hand and within reach. *Curr Biol*, 13: R531-9, 2003.
- [37] J. T. Shenton, J. Schwoebel, H. B. Coslett., Mental motor imagery and the body schema: evidence for proprioceptive dominance. *Neurosci Lett*, 370: 19-24, 2004.
- [38] C. Blanchard, R. Roll, J. P. Roll, A. Kavounoudias., Combined contribution of tactile and proprioceptive feedback to hand movement perception. *Brain Res*, 1382: 219-29, 2011.
- [39] P. J. Cordo, J. L. Horn, D. Künster, *et al.*, Contributions of skin and muscle afferent input to movement sense in the human hand. *J Neurophysiol*, 105: 1879-88, 2011.
- [40] P. B. Matthews, R. B. Stein., The sensitivity of muscle spindle afferents to small sinusoidal changes of length. *J Physiol*, 200: 723-43, 1969.
- [41] U. Proske. The mammalian muscle spindle *News in Physiological Sciences*, 12: 37-42, 1997.
42. A. C. Guyton, J. E. Hall, *Textbook of medical physiology* (Elsevier Saunders, Philadelphia, 2006).
- [43] E. Ribot-Ciscar, V. Hospod, J. P. Roll, J. M. Aimonetti., Fusimotor drive may adjust muscle spindle feedback to task requirements in humans. *J Neurophysiol*, 101: 633-40, 2009.
- [44] A. C. Sittig, J. J. Denier van der Gon, C. C. Gielen., Separate control of arm position and velocity demonstrated by vibration of muscle tendon in man. *Exp Brain Res*, 60: 445-53, 1985.
- [45] P. E. Crago. Structural Model of the Muscle Spindle *Annals of Biomedical Engineering*, 30: 68-83, 2002.
- [46] M. Hulliger, P. B. Matthews, J. Noth., Static and dynamic fusimotor action on the response of Ia fibres to low frequency sinusoidal stretching of widely ranging amplitude. *J Physiol*, 267: 811-38, 1977.
- [47] R. S. Turner, S. T. Grafton, J. R. Votaw, *et al.*, Motor subcircuits mediating the control of movement velocity: a PET study. *J Neurophysiol*, 80: 2162-76, 1998.
- [48] R. S. Turner, M. Desmurget, J. Grethe, *et al.*, Motor subcircuits mediating the control of movement extent and speed. *J Neurophysiol*, 90: 3958-66, 2003.
- [49] N. P. Reeves, J. Cholewicki, K. S. Narendra., Effects of reflex delays on postural control during unstable seated balance. *J Biomech*, 42: 164-70, 2009.
- [50] S. C. Regueme, J. Barthélemy, G. M. Gauthier, C. Nicol., Changes in illusory ankle movements induced by tendon vibrations during the delayed recovery phase of stretch-shortening cycle fatigue: an indirect study of muscle spindle sensitivity modifications. *Brain Res*, 1185: 129-35, 2007.
- [51] M. Montant, P. Romaguère, J. P. Roll., A new vibrator to stimulate muscle proprioceptors in fMRI. *Hum Brain Mapp*, 30: 990-7, 2009.
- [52] T. Kito, T. Hashimoto, T. Yoneda, *et al.*, Sensory processing during kinesthetic aftereffect following illusory hand movement elicited by tendon vibration. *Brain Res*, 1114: 75-84, 2006.

- [53] J. E. Gregory, A. K. Wise, S. A. Wood, *et al.*, Muscle history, fusimotor activity and the human stretch reflex. *J Physiol*, 513 (Pt 3): 927-34, 1998.
- [54] D. Y. Cao, J. G. Pickar., Lengthening but not shortening history of paraspinal muscle spindles in the low back alters their dynamic sensitivity. *J Neurophysiol*, 105: 434-41, 2011.
- [55] Y. Ishihara, M. Izumizaki, T. Atsumi, I. Homma., Aftereffects of mechanical vibration and muscle contraction on limb position-sense. *Muscle Nerve*, 30: 486-92, 2004.
- [56] J. Z. Lin, M. K. Floeter., Do F-wave measurements detect changes in motor neuron excitability? *Muscle Nerve*, 30: 289-94, 2004.
- [57] M. G. Espiritu, C. S. Y. Lin, D. Burke., Motoneuron excitability and the F wave *Muscle & Nerve*, 27: 720-7, 2003.
- [58] M. Steyvers, O. Levin, S. M. Verschueren, S. P. Swinnen., Frequency-dependent effects of muscle tendon vibration on corticospinal excitability: a TMS study. *Exp Brain Res*, 151: 9-14, 2003.
- [59] M. Steyvers, O. Levin, M. Van Baelen, S. P. Swinnen., Corticospinal excitability changes following prolonged muscle tendon vibration. *Neuroreport*, 14: 1901-5, 2003.
- [60] A. Forner-Cordero, M. Steyvers, O. Levin, *et al.*, Changes in corticomotor excitability following prolonged muscle tendon vibration. *Behav Brain Res*, 190: 41-9, 2008.
- [61] M. Bergenheim, E. Ribot-Ciscar, J. P. Roll., Proprioceptive population coding of two-dimensional limb movements in humans: I. Muscle spindle feedback during spatially oriented movements *Experimental Brain Research*, 134: 301-10, 2000.
- [62] S. M. Verschueren, S. P. Swinnen, P. J. Cordo, N. V. Dounskaia., Proprioceptive control of multijoint movement: unimanual circle drawing. *Exp Brain Res*, 127: 171-81, 1999.
- [63] F. Albert, M. Bergenheim, E. Ribot-Ciscar, J. P. Roll., The Ia afferent feedback of a given movement evokes the illusion of the same movement when returned to the subject via muscle tendon vibration. *Exp Brain Res*, 172: 163-74, 2006.
- [64] E. Naito, H. H. Ehrsson., Kinesthetic illusion of wrist movement activates motor-related areas. *Neuroreport*, 12: 3805-9, 2001.
- [65] D. J. Goble, C. A. Lewis, E. A. Hurvitz, S. H. Brown., Development of upper limb proprioceptive accuracy in children and adolescents. *Hum Mov Sci*, 24: 155-70, 2005.
- [66] D. J. Goble. Proprioceptive acuity assessment via joint position matching: from basic science to general practice. *Phys Ther*, 90: 1176-84, 2010.
- [67] J. C. Gilhodes, J. P. Roll, M. F. Tardysgervet., Perceptual and motor effects of agonist-antagonist muscle vibration in man *Experimental Brain Research*, 61: 395-402, 1986.
- [68] S. M. Verschueren, P. J. Cordo, S. P. Swinnen., Representation of wrist joint kinematics by the ensemble of muscle spindles from synergistic muscles. *J Neurophysiol*, 79: 2265-76, 1998.
- [69] G. Baud-Bovy, P. Viviani., Amplitude and direction errors in kinesthetic pointing. *Exp Brain Res*, 157: 197-214, 2004.

- [70] J. S. Soltys, S. E. Wilson., Directional sensitivity of velocity sense in the lumbar spine. *J Appl Biomech*, 24: 244-51, 2008.
- [71] L. A. Hall, D. I. McCloskey., Detections of movements imposed on finger, elbow, and shoulder joints *Journal of Physiology*, 519-33, 1983.
- [72] D. L. Sturnieks, J. R. Wright, R. C. Fitzpatrick., Detection of simultaneous movement at two human arm joints. *J Physiol*, 585: 833-42, 2007.
- [73] B. Craske. Perception of impossible limb positions induced by tendon vibration. *Science*, 196: 71-3, 1977.
- [74] E. Naito, P. E. Roland, H. H. Ehrsson., I feel my hand moving: a new role of the primary motor cortex in somatic perception of limb movement. *Neuron*, 36: 979-88, 2002.
- [75] J. R. Lackner. Some proprioceptive influences on the perceptual representation of body shape and orientation. *Brain*, 111 (Pt 2): 281-97, 1988.
- [76] S. Boden, H. Obrig, C. Köhncke, *et al.*, The oxygenation response to functional stimulation: is there a physiological meaning to the lag between parameters? *Neuroimage*, 36: 100-7, 2007.
- [77] T. J. Huppert, R. D. Hoge, S. G. Diamond, *et al.*, A temporal comparison of BOLD, ASL, and NIRS hemodynamic responses to motor stimuli in adult humans. *Neuroimage*, 29: 368-82, 2006.
- [78] M. A. Mohamed, D. M. Yousem, A. Tekes, *et al.*, Timing of cortical activation: a latency-resolved event-related functional MR imaging study. *AJNR Am J Neuroradiol*, 24: 1967-74, 2003.
- [79] E. Naito, P. E. Roland, C. Grefkes, *et al.*, Dominance of the right hemisphere and role of area 2 in human kinesthesia. *J Neurophysiol*, 93: 1020-34, 2005.
- [80] P. Romaiguère, J. L. Anton, M. Roth, *et al.*, Motor and parietal cortical areas both underlie kinaesthesia. *Brain Res Cogn Brain Res*, 16: 74-82, 2003.
- [81] E. Naito, T. Nakashima, T. Kito, *et al.*, Human limb-specific and non-limb-specific brain representations during kinesthetic illusory movements of the upper and lower extremities. *Eur J Neurosci*, 25: 3476-87, 2007.
- [82] D. S. Andreasen, A. A. Aviles, S. K. Allen, *et al.*, Exoskeleton for forearm pronation and supination rehabilitation. *Conf Proc IEEE Eng Med Biol Soc*, 4: 2714-7, 2004.
- [83] V. Dietz. Proprioception and locomotor disorders. *Nat Rev Neurosci*, 3: 781-90, 2002.
- [84] N. W. Mok, S. G. Brauer, P. W. Hodges., Postural recovery following voluntary arm movement is impaired in people with chronic low back pain. *Gait Posture*, 34: 97-102, 2011.
- [85] N. W. Mok, S. G. Brauer, P. W. Hodges., Changes in lumbar movement in people with low back pain are related to compromised balance. *Spine (Phila Pa 1976)*, 36: E45-52, 2011.
- [86] C. Rickards, F. W. Cody., Proprioceptive control of wrist movements in Parkinson's disease. Reduced muscle vibration-induced errors. *Brain*, 120 (Pt 6): 977-90, 1997.
- [87] S. Gilman. Joint position sense and vibration sense: anatomical organisation and assessment *Journal of Neurology, Neurosurgery & Psychiatry*, 73:473, 2002.

- [88] E. Naito. Sensing limb movements in the motor cortex: how humans sense limb movement. *Neuroscientist*, 10: 73-82, 2004.
- [89] S. Radovanovic, A. Korotkov, M. Ljubisavljevic, *et al.*, Comparison of brain activity during different types of proprioceptive inputs: a positron emission tomography study. *Exp Brain Res*, 143: 276-85, 2002.

Chapter 2 - Seated Sway is Sensitive to Local Vibration

Abstract

Low back pain is a major contributor to the rising cost of health care and lost productivity in industrialized nations worldwide. Occupations exposing workers to whole body vibrations suggest increased rates of developing low back pain. A possible explanation for this link is that occupational vibrations may impair spinal motor control. Seated sway protocols have been used to examine postural control during simple balancing tasks. The majority of these seated sway studies have used movement extent or area defined by center of pressure excursions. The muscle spindle organ is the mechanoreceptor most responsible for proprioceptive feedback. The muscle spindle organ provides both position and velocity feedback via vibration sensitive afferent signaling. The current research tested whether or not a seated sway protocol using a velocity based metric, rather than traditional position/extent based measures, could be used to test proprioceptive performance. Twelve young and healthy subjects were instructed to sit on a wobble chair atop a Bertec forceplate for trials of up to 20 seconds sampled at 100 Hz. During one half of the trials a stabilizing ring supported the wobble chair. Conditions were block randomized between stable and unstable sitting, eyes open/closed, and vibration on/off. Mean sway speed (MSS) was calculated as the average sample-to-sample change in COP position per trial duration. Mean sway speed was found to increase significantly while vibration was being applied both during stable and unstable sitting. MSS was also found to increase with loss of visual information, but only during unstable balancing trials. A seated sway protocol, with either stable or unstable sitting can successfully be employed to test lumbar control of the lumbar spine.

Introduction

Low Back Pain

Low back pain (LBP) affects large populations of working adults worldwide and is second only to respiratory conditions, such as the common cold, for symptom related physician visits [1]. Upwards of 90% of individuals will experience an episode of LBP at some point in their lives [2, 3]. Of those who experience an initial bout of LBP, there is a recurrence rate upwards of 80% [3]. In the United States alone, LBP is one of the most costly forms of musculoskeletal disorders with losses, associated with lost productivity and health care expenses. This is complicated by the fact that the vast majority (upwards of 70%) of LBP occurrences are of unknown etiology [1]. For many, recovery from LBP is relatively quick, within a matter of days/weeks, however, about 10% end up with a chronic LBP that lasts much longer and accounts for the majority (65-85%) of healthcare spending in this category [2, 3]. In order to control the enormity of the LBP problem it is imperative then, to create a better understanding of the anatomy involved and possible mechanisms for injury. The focus for the remainder of this introduction will review the anatomy and physiology of the lumbar spine, and the possible contributions of impaired proprioceptive control of the lumbar spine to low back injury.

Anatomy Of The Spine

The spine is an alternating series of vertically stacked bones (vertebrae) and disks interconnected by muscles, tendons, and ligaments. On its own, the spinal column has an intrinsic stiffness due to the passive support of these tissues, supporting only a load of approximately 90 N before buckling [4]. The spinal column itself is divided into three sections: the cervical (neck), thoracic (mid-body/rib cage), and the lumbar (low back).

Every vertebra has a large "D-shaped" body with two protrusions (pedicles) on each side of the posterior (flat side) midline [Figure 5]. The pedicles support several processes that form joints along the dorsal

spinal column. The spinous process is the largest of these and is the only process not forming a joint. The spinous process extends away from the vertebral body along the midline and forms the familiar and easily palpable bumps along the back when one bends forward.

The rest of the processes are all mirrored across the vertebral sagittal midline. The transverse processes extend laterally providing a large moment arm for the muscles and tendons connecting them. The superior articular process extends at an angle between the projections of the spinous and transverse processes. For each vertebral level within the spinal column, the superior articular process of the inferior vertebrae meets the inferior articular process of the superior vertebrae forming the facet joints. At the lowermost level of the lumbar spine (L5) the inferior articular process forms a facet joint with the sacrum. Between each vertebral level is an intervertebral disc composed of the nucleus pulposus and anulus fibrosus.

As noted previously, the processes provide a location for the attachment of ligaments and tendons. Depending on the muscle considered, the processes also create a moment arm over which the muscle may create movement of any particular vertebral level independent of adjacent levels. The movement between levels is primarily the result of the deep muscles of the lumbar spine. Of the deep muscles there are two in general that are of interest to our discussion. The lateral intertransversarii connect the transverse processes between lumbar levels. The intertransversarii are further broken into two groups depending on their exact origins and insertions (laterales and mediales), but for simplification we will use the more general lateral intertransversarii as they all generally contribute to extension and lateral flexion. The other deep muscle of the lumbar spine is the multifidus muscle. The multifidi originate at the sacrum and/or the lateral processes of each vertebra and insert onto the spinous process several segments superior. This allows the multifidus to generate forces contributing to lumbar spine extension.

The spinal column has three distinct curvatures for each of the three sections (cervical, thoracic, lumbar) in the sagittal plane. The thoracic spine exhibits a curvature that is concave anterior (kyphosis). The

cervical and lumbar spines each exhibit a unique level of curvature that is concave posterior (lordosis). In the coronal plane of a healthy spinal column segments are in line, with deviations indicated as scoliosis. In general, the inferior vertebral bodies increase in size in order to support each the additional weight above.

Lumbar Spine Control

The five segments of the lumbar spine support the mass of the entire upper body. In order to ensure the overall stability of the upper body, it is necessary to properly control the lumbar base. For simplicity, human balance tasks are often modeled as an inverted pendulum controlling a single angle even though control is exerted on each level [5, 6]. In order to remain upright, it is therefore necessary to continually monitor the movement of the lumbar spine and provide feedback to the central nervous system (CNS) so that appropriate motor recruitment strategies can be implemented.

There is evidence suggesting exposure to vibration in the workplace, such as with pilots, fork-lift operators, truck drivers and other heavy equipment operators (HEVs), is a factor that may more than double the risk of developing low back pain [2, 7-9]. While the exact causes for the relationship are unknown, there is a theory, supported by a large and growing body of literature, that low back pain may be ultimately linked with impaired sensory motor control [10]. Further strengthening this case is the observation that individuals with chronic LBP have demonstrated proprioceptive deficits [11].

The proprioceptive system aids humans in the control of everyday motor tasks, including balance. It provides a level of non-visual CNS generated feedback from sensors in the peripheral nervous system (PNS). Of the possible peripheral sensors, the muscle spindle organ (MSO) is generally accepted as having the greatest contribution to the body's "sense of self". If there is an error in the proprioceptive feedback loop then it is possible that the soft tissues of the low back may experience damage due to excessive strains placed on the tissues leading to cases of LBP.

It is well accepted and backed by numerous studies that both the static and dynamic signaling of the muscle spindle organs are sensitive to applied vibration [12, 13]. The afferent MSO signaling has been demonstrated to modulate towards the frequency of the applied vibration [14]. The muscle spindle organ is particularly sensitive to applied vibrations in the range of 20-120 Hz, with a "sweet spot" for inducing a kinesthetic illusion between 60 and 80 Hz [15]. Furthermore, this modulated proprioceptive feedback has been demonstrated to persist beyond the period of vibration [16, 17]. Therefore the large populations that experience vibrations in the workplace could be at increased incidence for LBP not only during working hours but for a period of time after work as well.

Measures of Sway

Traditionally balance based tasks have been used to assess many parameters affecting standing postures [18, 19]. Recently, studies have attempted to more closely examine control of the lumbar spine by utilizing seated sway protocols [5, 20-23]. By placing the subjects in a seated position, postural adjustments can no longer be achieved through the joints of the lower extremities, forcing an individual to rely primarily on trunk activity to make corrections. In each of these later cases, center of pressure (COP) movements, calculated from measured ground reaction forces were tracked over time as subjects sat on a chair-like platform atop a standard force plate. Though subjects shifted their COP location within their base of support (BOS) these tests are considered static balance tasks. Commonly static balance tasks report results using variables such as range of movement, area, and velocity of the COP movements [24-26].

Although seated sway protocols have used similar sway parameters, different chair strategies have evolved. In some instances, a stable seat has been used [5, 21, 27]. Other researchers have devised seats that provided some level of instability using solid hemispheres of varying diameter, rocker board/ball, or other pivoting technology attached to the bottom of the seat pan [5, 23, 28, 29]. A few of these studies

did examine both stable and unstable chairs and noted longer COP path lengths during unstable sitting than during stable sitting, apparently corresponding to the increased challenge of the task [5, 28].

While this difference in platform stability can be used to gain various insights on postural control it makes comparisons between studies more difficult as they are likely different tasks. Additionally restrictions on data quality are introduced as data collection itself becomes more difficult as the task difficulty increases. One researcher was limited to trials of relatively short length due, in part, to the difficulty of the balance task [5]. It would be useful then to compare if COP responses similar to those during unstable sitting could be elicited during stable sitting by increasing task difficulty.

One possible technique to increase the difficulty of the balance task would be to alter the proprioceptive feedback of the active musculature using vibration. An altered afferent would result in changes along the proprioceptive feedback loop resulting in measurable changes in the COP parameters. It would be reasonable then, to expect these changes to occur as several small short duration corrections within the base of support monitored by slower acting, unaltered vestibular feedback. These corrections would likely show up as changes in velocity of the COP movement over the trials.

Mean Sway Speed

Measures of sway have been used in several studies as a means of investigating postural control while standing [19, 26, 30-32]. Informative sway data is dependent upon choosing an appropriate and reliable measure of sway. Mean sway speed (MSS), has been demonstrated to be a very reliable summary statistic, though like other sway measures is sensitive to visual feedback [24, 27]. Sway parameters such as total path length and sway area have been verified to change with applied vibration. What is not well documented however, is whether or not a velocity based sway measure is also sensitive to applied vibration.

The current study investigated the contributions of the muscle spindle organs to the postural control of the lumbar spine. Specifically, the effects of local vibration applied to the paraspinal musculature during seated tasks were observed. Our hypothesis was that mean sway speed (MSS) would increase in the anterior-posterior (AP) and medial-lateral (ML) directions with the application of local vibration. Additionally, we identified whether or not similar vibration responses were elicited in both stable and unstable seating conditions.

Methods

Twelve subjects (6 F & 6 M, 24.7 ± 4.4 years of age) from the general student population consented to participate in this study, approved by the University of Kansas Human Subjects Committee. All subjects completed a medical history questionnaire screening for recent history of low back pain, balance or other complicating conditions.

The experimental setup consisted of a custom-built wobble-chair positioned atop a force plate (Bertec) [Figure 6]. The wobble-chair was composed of a standard wooden seat pan, an 8" radius CNC-cut MDF-laminate hemisphere, and an adjustable polyvinyl chloride (PVC) footrest fastened to the hemisphere. A rubberized removable support ring was fashioned to fit the underside of the ball and used to create the stable and unstable conditions. The footrest was adjusted to support the subject's legs at a 90° angle throughout the collection period. For safety, support platforms were placed on both sides of the subject and a lab attendant stood quietly behind the subject to catch them if they could not recover in time to prevent falling.

A local vibration of 44.5 Hz was applied at the L3 level of the spinal column using an inertial vibration belt, consisting of a 12 volt DC hobby motor with offset mass, worn over the paraspinal musculature. Only the right side musculature was selected for stimulus in an attempt to force a directional bias in the

ML muscle spindle signaling. A force plate and amplifier (Bertec, Columbus OH) were used to record ground reaction forces sampled at 100 Hz and calculate COP values using the Motion Monitor software.

There were eight experimental conditions in all. These consisted of the possible combinations of: 1) stable or unstable seat, 2) eyes-open or eyes-closed, and 3) local vibration off or on. Three repetitions were collected for each trial condition resulting in 24 total trials, block randomized within the stable or unstable conditions, to minimize effects of order. The duration of each trial was limited to 20 seconds to prevent fatiguing.

For the experimental protocol, the subjects were instructed to sit comfortably upright on the chair, breathing normally, with their hands hanging at their sides and focused on a target, placed at eye level, on the wall approximately 8 feet in front of the subject. The trial duration was officially determined as the time from the start of collection until the subject engaged external support to remain balanced or the 20-second period ended, and was denoted as that subject's balance time. Between the unstable trials the subjects were required to support themselves on the hand rests to prevent fatigue. Subjects were instructed to keep their arms at their sides and against their torso and their legs on the PVC rest during collections, until they felt they could no longer keep their balance.

For each trial the mean sway speed (MSS) was calculated in the anterior-posterior (AP) and Medial-Lateral (ML) directions, as well as the resultant overall. MSS was calculated as the average point-by-point change in COP per trial duration. A Huyhn-Feldt, repeated measures ANOVA was performed in SPSS to test for significant differences in the dependent variables with $\alpha = 0.05$. If a main effect was observed for a particular variable a simple contrast was computed as a post hoc analysis to determine significance between levels.

Results

Figure 6 and Figure 6 summarize subject performance for the previously described protocol. Details of the ANOVA analysis are found in Table 1 and in the paragraphs at the end of this section. Mean Sway Speed is illustrated in Figure 6 for both the AP (solid bars) and ML (hashed bars). All possible combinations of test conditions are presented. The data are lateralized such that the stable seating condition is represented on the left side of the plot, unstable seating on the right. A simple inspection suggests a positive relationship between vibration of the spinal musculature and MSS in both seating conditions in each plane of motion. Looking further, differences between the seating conditions also become apparent as seen by the effect of visual feedback. In the unstable seating condition, visual information appears to play a much larger role as MSS increased in both AP and ML directions in the absence of visual feedback. A similar pattern was not observed in the stable seating data.

Reinforcing the importance of visual information during the more challenging of the balance tasks was evident in the dramatic decrease in balance times observed in Figure 7. Subjects had no difficulty with the stable balance task and were able to maintain an average balance time very close to the max trial length (~18 seconds) during the unstable task. However, once visual feedback was removed, balance times dropped to approximately one-third the eyes open values indicating an extreme difficulty remaining upright. This would suggest that the proprioceptive system alone was not enough to recover balance for this type of task. Indeed, balance time data appeared more dependent on eye condition than whether or not vibration is being applied. This further suggests that these two seating systems are two distinct tasks that appear to rely on the balance control systems differently to achieve success.

Examination of the AP data [Table 1] indicated statistical differences due to the following conditions: seat ($p < .001$), eyes ($p < .02$), vibration ($p < .0001$), and the interactions of seat*eyes ($p < .01$) and seat*vibrations ($p < .02$). The mean sway speed increased in each of the main effects: seat (+5 mm/s), eyes (+3 mm/s), and vibration (+7 mm/s). The significant increases observed in both the eye and seat

conditions suggested that the increased sway velocities were responsible, at least in part, for the shorter balance times observed during the unstable seating conditions.

Examination of the ML data indicated statistical differences due to the following conditions: vibration ($p < .001$), and the interactions of seat*eyes ($p < .03$) and seat*vibrations ($p < .01$). In the medial lateral direction the only observed main effect was due to vibration. The application of local vibration resulted in an approximate doubling of mean sway speed from 12 to 24 mm/sec, continuing the observed relationship of task difficulty and sway speed. The overall velocity magnitudes between the AP and ML directions were observed to be approximately similar though ML speeds were slightly higher overall.

Discussion

In our analysis of the data, an overall effect was observed showing higher MSS with the application of vibration. This increase was found for both the AP and ML directions regardless of visual feedback. Additionally, an interaction of seat*vibration revealed a larger increase in MSS during stable seating with vibration than during the unstable trials. Taken together these findings suggest that the logistically simpler stable seat may be utilized for proprioceptive research with a reasonable expectation for success. This is not to say that the stable seating strategy is superior or preferred in all instances, rather the choice is available dependent upon the question being researched.

The inherent differences between the two seating situations make direct comparisons difficult. During stable seating the individual behaves as an inverted pendulum with the COP movement dependent primarily upon movement of the subject's trunk. Seated on the wobble chair however, the individual behaves differently and movement of the COP becomes dependent upon the movement of the subject's torso in conjunction with the counterbalancing movement of the seat [5, 6]. It would make an interesting investigation to compare the kinematics for each seating case to determine to what extent these differences affect the performance of the sway task. It should also be noted that the task difficulty

increases with a decrease in the diameter of the hemisphere, further stressing the importance of choosing an appropriate level of difficulty for the research question to allow comparisons with the results of others. For example, results could be further convoluted if unstable seats of differing diameter were used, since sway velocity has previously been observed to change due to the ball diameter used [5].

The influence of the visual system was found to be more complex than expected. While it was anticipated that MSS would increase in both AP and ML directions when subjects' eyes were closed, it was only significantly faster in the AP direction. The reason for this is not clear though the interaction between eye-condition and seat-type was observed in both AP and ML directions. No subject was able to maintain balance long enough to complete a trial of 20-second duration on the wobble chair without visual feedback, even though they started from a position where they felt in control. This was evidenced by the average trial length on the wobble chair without visual feedback of about 5 seconds compared to the near 18 seconds with visual feedback [Figure 7]. These findings could be partly confounded by contributions of the vestibular system. Subjects in this experiment may have found it easier to keep a level head during the AP task, effectively bypassing the vestibular system, while the head was held in line with the spine during ML movements allowing for vestibular feedback. The likely influence of the vestibular system during this task was thought to be low because the movements and inputs were at a higher frequency than the low frequency (~ 0.5 Hz) the vestibular system is most sensitive to. A kinematics study would help clarify these points. It was also noted that the change in velocity found due to the main effects for seat type and eye condition were not as large as the increase observed due to vibration.

Some of the observed inconsistencies between the two planes of motion may be attributable to the geometry of the spinal column. Overall changes in MSS due to vibration were observed in both AP and ML directions but changes due to seat type and eye condition were observed in the AP direction only [Table 1]. The exact reasoning for why these two directions were not equally affected is not fully clear though it is plausible that it may be partially be due to the differences in the effective moment arms of the

attached musculature giving a control advantage to the ML direction or that a difference in directional sensitivity may exist depending upon spindle density, muscle geometry, or directional sensitivity of functional muscle groups. It may also be due in part to the task; again an investigation of the kinematics of the two tasks would make this clearer.

There are also a few key observations from Figure 7 to be made. First, if one examines the two halves separately one notices a nice, apparently linear increase in MSS as the balance task difficulty increases from the simplest (Eyes Open + No Stimulus) to the most difficult (Eyes Closed + Lumbar Vibration). This same increase was not observed on the Stable side of the graph where the highest speeds were seen with Eyes Open + Lumbar Vibration. It was originally thought that a similar, though smaller, increase to the one observed on the unstable side would also be observed on the stable side. However we found that during the stable trials mean sway speeds were of similar magnitudes but separated along whether vibration was applied or not. This may again further illustrate a change in the relative roles of the visual, proprioceptive, and vestibular systems being dependent upon the task. Without the response of the visual system, the proprioceptive and vestibular systems may have allowed more movement of the COP before a correction was made resulting in fewer quick corrections that may have resulted when visual information was present. This picture is made even more interesting by the fact that higher MSS's due to vibration in the stable condition did not affect the relative success in terms of balance time as much as they did in the unstable trials. So while subjects were on average moving faster, it was likely over a total range of motion well within the angular limits of stability.

These results suggest that the performance of the proprioceptive system can be measured using seated sway and applied local vibrations provided consideration are made for the balance task itself. Mean sway speed was observed to be more sensitive to vibration during stable seating than unstable seating regardless of whether visual feedback existed resulting in higher mean sway velocities in both AP and ML directions. This suggests that it is possible that proprioceptive feedback may have a greater

importance to local trunk stability during generally stable (small deflection angles) situations while visual feedback plays a greater role in global stability when trunk deflections from upright are much greater. While a similar increased sway speed was observed with vibration during the unstable trials, the effect was not as great. Furthermore, the changes in mean sway speed were observable with a relatively simple setup (quiet, upright, stable seating), suggesting it may be a useful test statistic in a clinical setting. We therefore suggest implementing the stable seated strategy when a strong proprioceptive response is desired. Future studies should include investigating populations experiencing LBP to see if they might also experience changes in mean sway speed, and populations from industries with high incidence of LBP to see if MSS may be a good predictor or injury possibility.

In summary increases in mean sway speed were observed for both a static (stable) and active (unstable) balance tasks due to vibration of the paraspinal musculature. The greatest increases in MSS were observed when vibration was applied using a stable sitting configuration. While similar seated sway protocols have been used to attempt to discriminate between populations, it has not been used to investigate the proprioceptive feedback. Our results suggest that it would theoretically be possible to identify populations with pathologies known to alter proprioceptive performance, such as low back pain, using a simple seated paradigm. Additional studies would need to be conducted to support this.

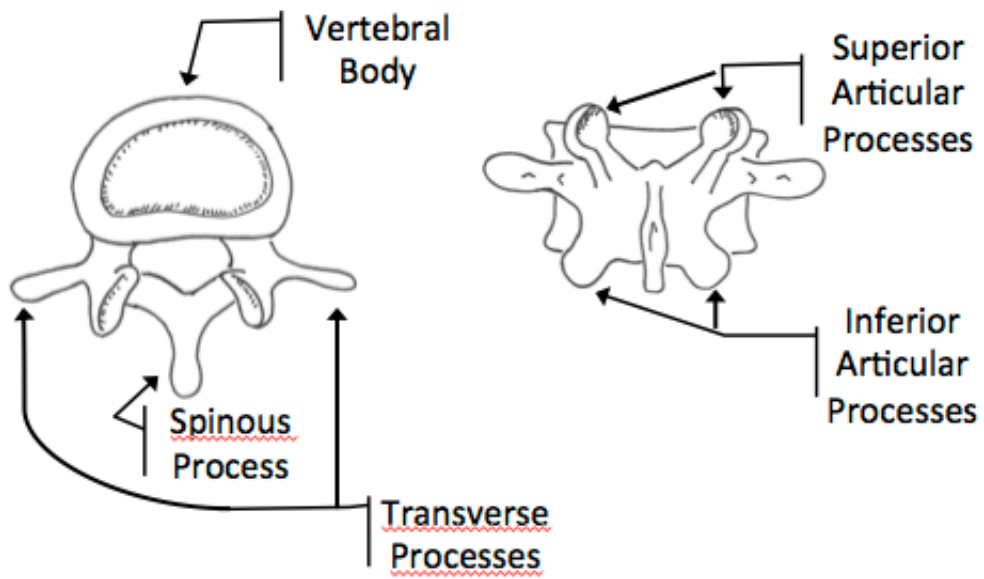


Figure 4: Lumbar Vertebra

A single vertebra is pictured from both the superior (left) and posterior (right) views. Important anatomical landmarks are labeled.

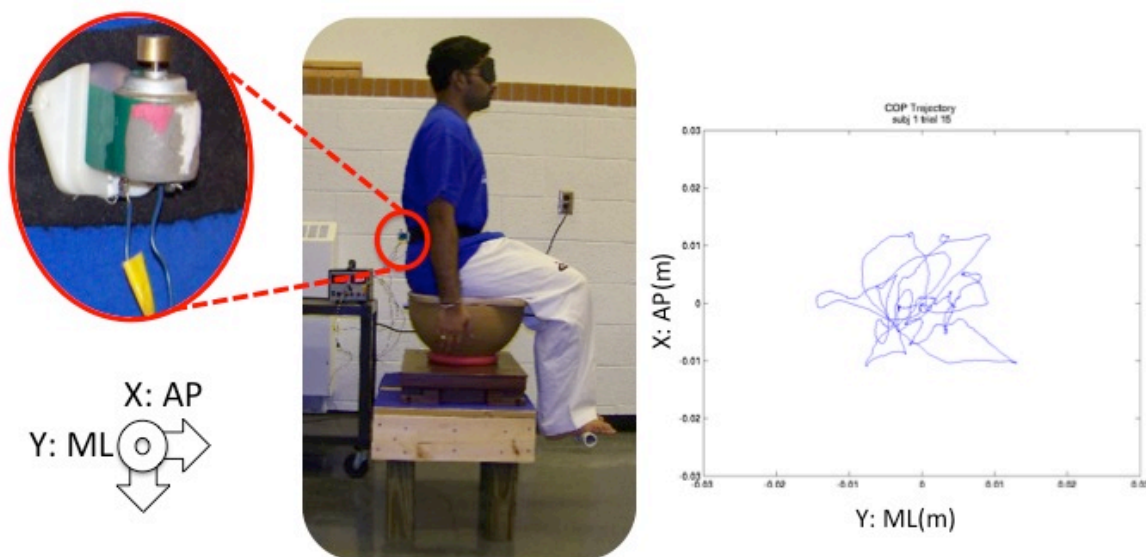


Figure 5: Experimental Setup

A standard DC-motor vibrator (photo insert) was located over the paraspinal musculature. Subjects sat upon an 8" radius MDF hemisphere placed upon a Bertec force plate with feet supported by a PVC footrest. A sand-filled, high-pressure, rubberized tube was fashioned into a ring to create the stable seating condition. Subjects were instructed to sit comfortably upright with hands hanging at their sides. Supports (not pictured) were placed on each side and a lab attendant stood behind subjects as a safety precaution during unstable trials. Ground reaction forces were recorded and used to calculate COP movements for each trial (typical trial blue line).

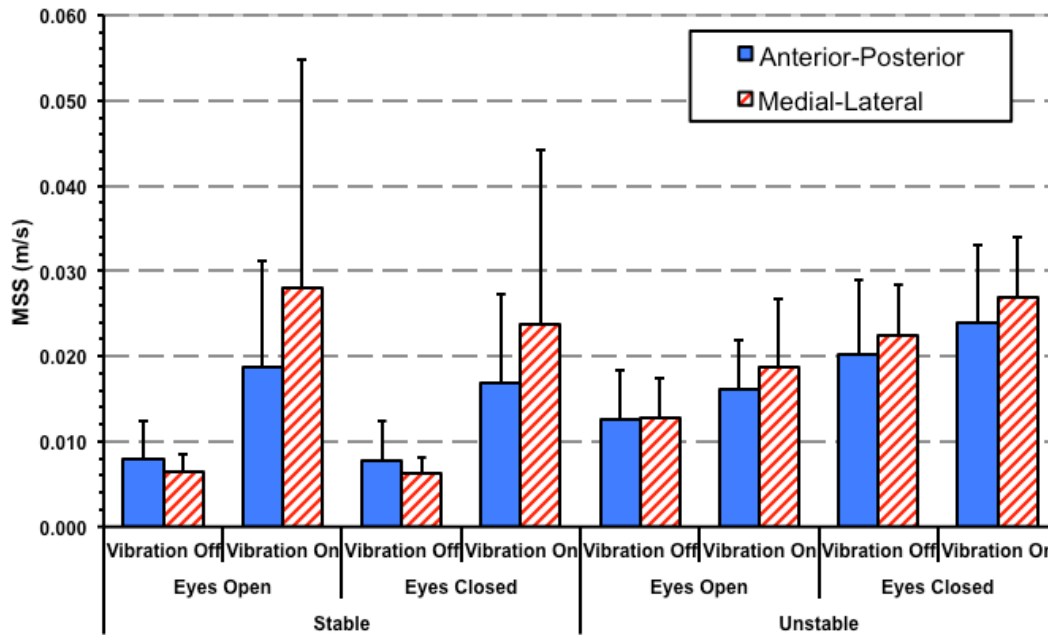


Figure 6: Mean Sway Speed Results

The above figure summarizes the averaged MSS statistic (with standard deviations) across all conditions and all subjects tested. The MSS reported is the average velocity per the entire trial period defined by the balance time. Anterior-Posterior velocities are pictured as solid blue bars, Medial-Lateral velocities are pictured as the red hashed bars. In both seating conditions (left side stable, right side unstable), MSS increased with the addition of vibration.

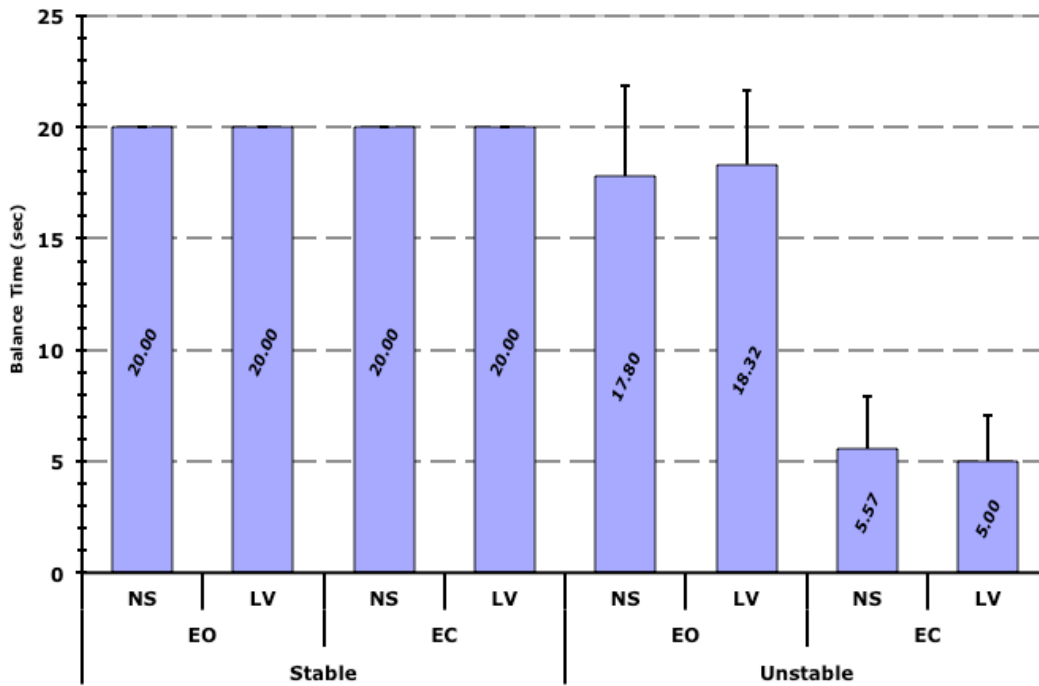


Figure 7: Balance Time Results

Trial lengths were defined by the subjects' ability to remain upright from the start of the trial, up to twenty-seconds in duration. Average length of trials in seconds (with standard deviations) is represented here for all subjects and all conditions. Subject success was inherent during the stable trials and trial durations became much shorter during unstable conditions.

Table 1: Sway Results ANOVA

ML

Effect	DF Num.	DF Den.	F-Value	Pr > F
Seat	1	11	3.49	0.0884
Eyes	1	11	2.28	0.1595
Seat*Eyes	1	11	6.59	0.0262
Vibration	1	11	33.97	0.0001
Seat*Vibration	1	11	11.05	0.0068
Eyes*Vibration	1	11	0.42	0.5309
Seat*Eyes*Vibration	1	11	0.11	0.7509

AP

Effect	DF Num.	DF Den.	F-Value	Pr > F
Seat	1	11	23.42	0.0005
Eyes	1	11	9.19	0.0114
Seat*Eyes	1	11	15.66	0.0022
Vibration	1	11	37.39	<.0001
Seat*Vibration	1	11	8.19	0.0155
Eyes*Vibration	1	11	0.14	0.7169
Seat*Eyes*Vibration	1	11	0.19	0.6724

Results of the Huyhn-Feldt repeated measures ANOVA are summarized above. Bold values indicate statistical significance at the alpha = 0.05 level. Main effects were observed in all conditions in the AP but not the ML direction. Significant interactions were indicated between combinations of Seat, Eyes, and Vibration in both directions.

References

- [1] R. A. Deyo, J. N. Weinstein., Primary care: low back pain *New England Journal of Medicine- Unbound Volume*, 344: 363-71, 2001.
- [2] F. Gerr, L. Mani., Work-related low back pain. *Primary care*, 27:865, 2000.
- [3] S. Pai, L. J. Sundaram., Low back pain: an economic assessment in the United States. *The Orthopedic clinics of North America*, 35:1, 2004.
- [4] J. J. Crisco, M. M. Panjabi, I. Yamamoto, T. R. Oxland., Euler stability of the human ligamentous lumbar spine. Part II: Experiment *Clinical Biomechanics*, 7: 27-32, 1992.
- [5] J. Cholewicki, G. K. Polzhofer, A. Radebold., Postural control of trunk during unstable sitting *Journal of biomechanics*, 33: 1733-7, 2000.
- [6] N. P. Reeves, J. Cholewicki, K. S. Narendra., Effects of reflex delays on postural control during unstable seated balance. *J Biomech*, 42: 164-70, 2009.
- [7] R. P. Blood, J. D. Ploger, P. W. Johnson., Whole body vibration exposures in forklift operators: comparison of a mechanical and air suspension seat. *Ergonomics*, 53: 1385-94, 2010.
- [8] T. Waters, A. Genaidy, H. Barriera Viruet, M. Makola., The impact of operating heavy equipment vehicles on lower back disorders. *Ergonomics*, 51: 602-36, 2008.
- [9] M. H. Pope, T. H. Hansson., Vibration of the spine and low back pain *Clinical orthopaedics and related research*, 279:49, 1992.
- [10] M. M. Panjabi. Clinical spinal instability and low back pain *Journal of electromyography and Kinesiology*, 13: 371-9, 2003.
- [11] B. M. Wand, L. Parkitny, N. E. O'Connell, *et al.*, Cortical changes in chronic low back pain: current state of the art and implications for clinical practice. *Man Ther*, 16: 15-20, 2011.
- [12] M. Montant, P. Romaiguère, J. P. Roll., A new vibrator to stimulate muscle proprioceptors in fMRI. *Hum Brain Mapp*, 30: 990-7, 2009.
- [13] E. Ribot-Ciscar, C. Rossi-Durand, J. P. Roll., Muscle spindle activity following muscle tendon vibration in man. *Neurosci Lett*, 258: 147-50, 1998.
- [14] A. C. Sittig, J. J. Denier van der Gon, C. C. Gielen., Separate control of arm position and velocity demonstrated by vibration of muscle tendon in man. *Exp Brain Res*, 60: 445-53, 1985.
- [15] J. B. Fallon, V. G. Macefield., Vibration sensitivity of human muscle spindles and Golgi tendon organs. *Muscle Nerve*, 36: 21-9, 2007.
- [16] M. M. Wierzbicka, J. C. Gilhodes, J. P. Roll., Vibration-induced postural posteffects. *J Neurophysiol*, 79: 143-50, 1998.
- [17] M. Arashanapalli, S. E. Wilson., Paraspinal muscle vibration alters dynamic motion of the trunk. *J Biomech Eng*, 130:021001, 2008.

- [18] J. H. Allum, C. R. Pfaltz., Visual and vestibular contributions to pitch sway stabilization in the ankle muscles of normals and patients with bilateral peripheral vestibular deficits. *Exp Brain Res*, 58: 82-94, 1985.
- [19] M. Smith, M. W. Coppieters, P. W. Hodges., Effect of experimentally induced low back pain on postural sway with breathing. *Exp Brain Res*, 166: 109-17, 2005.
- [20] S. P. Silfies, J. Cholewicki, N. P. Reeves, H. S. Greene., Lumbar position sense and the risk of low back injuries in college athletes: a prospective cohort study. *BMC Musculoskelet Disord*, 8:129, 2007.
- [21] B. C. Bennett, M. F. Abel, K. P. Granata., Seated postural control in adolescents with idiopathic scoliosis. *Spine (Phila Pa 1976)*, 29: E449-54, 2004.
- [22] H. Forssberg, H. Hirschfeld., Postural adjustments in sitting humans following external perturbations: muscle activity and kinematics *Experimental brain research*, 97: 515-27, 1994.
- [23] R. A. Preuss, S. G. Grenier, S. M. McGill., Postural control of the lumbar spine in unstable sitting. *Arch Phys Med Rehabil*, 86: 2309-15, 2005.
- [24] S. P. Silfies, J. Cholewicki, A. Radebold., The effects of visual input on postural control of the lumbar spine in unstable sitting. *Hum Mov Sci*, 22: 237-52, 2003.
- [25] J. H. van Dieën, L. L. Koppes, J. W. Twisk., Low back pain history and postural sway in unstable sitting. *Spine (Phila Pa 1976)*, 35: 812-7, 2010.
- [26] N. Vuillerme, F. Danion, N. Forestier, V. Nougier., Postural sway under muscle vibration and muscle fatigue in humans. *Neurosci Lett*, 333: 131-5, 2002.
- [27] J. A. Raymakers, M. M. Samson, H. J. Verhaar., The assessment of body sway and the choice of the stability parameter(s). *Gait Posture*, 21: 48-58, 2005.
- [28] P. O'Sullivan, W. Dankaerts, A. Burnett, *et al.*, Lumbopelvic kinematics and trunk muscle activity during sitting on stable and unstable surfaces. *J Orthop Sports Phys Ther*, 36: 19-25, 2006.
- [29] N. P. Reeves, V. Q. Everding, J. Cholewicki, D. C. Morrisette., The effects of trunk stiffness on postural control during unstable seated balance. *Exp Brain Res*, 174: 694-700, 2006.
- [30] J. J. Collins, C. J. De Luca., Random walking during quiet standing *Physical Review Letters*, 73: 764-7, 1994.
- [31] V. M. Zatsiorsky, M. Duarte., Instant equilibrium point and its migration in standing tasks: rambling and trembling components of the stabilogram. *Motor Control*, 3: 28-38, 1999.
- [32] V. M. Zatsiorsky, M. Duarte., Rambling and trembling in quiet standing. *Motor Control*, 4: 185-200, 2000.

Chapter 3 - The Effects of Vibration on a Joystick Pursuit Task

Abstract

Mechanical vibration alters the afferent signals of muscle spindle organs in humans. Changes in afferent signaling have been observed to occur both during and post vibration. Post vibration effects have resulted in position-sensing task errors up to 30 minutes after vibration cessation. There is less information regarding vibration effects on velocity reproduction, especially post-vibration. The current study investigates the effects of mechanical vibration on a computer-based joystick-pursuit-task: during, immediately post, and 20 minutes post-vibration. Eight healthy subjects participated in the current study and were instructed to match the horizontal position of a square joystick-controlled cursor within the diameter of a circular, constant-velocity, target cursor. Visual feedback was presented using a block design alternating between full feedback, target only, and rest conditions respectively. Vibration of approximately 65 Hz was applied over the biceps and supinator muscles of the right arm for 15 minutes duration. The average per-block velocity indicated subjects moved slower relative to baseline while the vibration was being applied and faster immediately post vibration. These findings indicate that a block-design pursuit-task paradigm utilizing velocity based performance measures are sensitive to vibratory manipulation of the proprioceptive system both during and immediately post vibratory stimulus.

Introduction

Applied mechanical vibration has been demonstrated as a reliable tool for modulating muscle spindle afferents. A large body of research exists investigating the link between gross motor performance and vibration modulated spindle afferents [1-3]. Of these investigations the majority focus on task performance during vibration [2, 4-6]. However, it has also been demonstrated that the impaired motor performance may last for periods of up to 30 minutes after the vibration stimulus is removed [3, 7]. Since it is possible that during this period of impaired performance, individuals may be at a higher risk of sustaining injury, it would be useful to further investigate this phenomenon [8-10].

Numerous studies have investigated the effects of vibration on the neuromuscular control of the body during static and dynamic tasks [1-3, 11-13]. While the majority of these performance measures are position-based, few have focused on velocity-based measures even though it has long been understood that the MSO provides both position and velocity information [14-16]. Additionally, while the effects of applied vibration on position tasks are well documented, less is known about the after-effects and recovery from vibration once exposure ends [1, 17, 18]. Even fewer studies have focused on whether similar changes in velocity-based measures are also observed due to vibration [5, 19, 20].

Pursuit tasks present an interesting tool to assess motor performance. A computer-based analogue of the traditional rotary pursuit task would allow for the investigation of several different aspects of performance including movement velocity [21, 22]. While there may be some hesitation to incorporate such a computer based task due to anecdotal evidence suggesting differences in tracking performance between certain cohorts this has been observed not to be the case as long as the pursuing movement of the joystick task directly corresponds with movement of the pursuit cursor [23]. Other traditional markers of performance such as time-on-target (accuracy) and peak-to-peak movements can then easily be calculated from the cursor locations making this a possible assessment tool for clinical locations as well as research labs [24-26].

The Case For Velocity Sense

It has been well accepted for some time that the primary receptor contributing to proprioception is the muscle spindle organ [27-29]. It was also determined early on that the muscle spindle is sensitive to both static and dynamic changes in length [15]. This has given rise to later experiments demonstrating that MSO's provide both position and velocity information [16]. Surprisingly, even though this has been known for some time, the majority of traditional studies in on proprioception have focused almost exclusively on position-based measurements [2, 4, 6].

While much insight has been gained utilizing these position-based tasks, this only provides information on a fraction of the sensory information encoded by the muscle spindles. It is, therefore, important to fill this void in our understanding of proprioceptive feedback and how it contributes to overall motor control. It is promising that a growing body of research makes use of velocity based tasks [14, 19, 20].

Much of the information that is understood about position sense has also been confirmed in velocity sense. Vibration induces change that can affect overall task performance [2]. Kinesthetic illusions are apparent in the direction of muscle lengthening [5, 30]. Unlike position sense, velocity sense is dependent upon both location and timing cues weighted proportionately to the actual movement velocity [14]. Furthermore, the dynamic sensitivity is altered by muscle lengthening history as well as vibration [31]. The interaction of all of these different performance cues, inherent in the derivation of velocity, are likely to have played at least a part in the more widespread use of position based measures.

Pursuit Tasks

Pursuit tasks, in which a human interacts with a computer through an input device attempting to match the position and path of a target cursor, have been widely used in the field of psychology and more recently in biomechanics to assess performance and discern populations with a motor impairment [22, 32]. It is possible this tool could be used to explore the effects of vibration on proprioceptive performance

throughout the proprioceptive control loop. Indeed at least one study has used this paradigm to demonstrate perception of scale during a pursuit task may be attributed to activations in the cerebellum [33].

One of the advantages of implementing such pursuit tasks is that they can be implemented with simple computer peripherals that are readily available such as mice or joysticks [32]. When considering task design, in terms of motor tasks, anecdotal evidence of gender or age bias is unfounded as long as the mapped movement of the pursuit task is not inverted [23]. Although age and gender are not readily discernible these simple task types can discriminate between controls and patients with particular pathologies [32]. Thus, a simple task in which a rightward joystick movement corresponds with a rightward cursor movement may be derived to measure proprioceptive performance with minimal learning and equipment. This combination could then be adapted to the testing environment including medical clinics, work sites, or imaging environments such as an fMRI suite.

Indeed some research has already moved in this direction. Results on cortical activations can be found in chapter six, so here we will focus on the kinematic measurements of task performance. These may be derived simply from the cursor data, provided joints are isolated and restricted to input device movements. What has been established so far is that tracking strategy (step-hold versus smooth) may depend on the type of feedback provided and the implicit instructions to the subjects (e.g., changing attention from location to velocity) [34].

This form of assessment could become valuable in clinical settings as several conditions, including Parkinson's and some forms of dystonia, may present similarly to vibration-modulated proprioception [35-38].

Anatomy and Physiology of the Human Arm

In examining the implementation of a hand/arm pursuit task it is useful to consider the relevant anatomy. The human arm is a complex system of joints, muscles, and bones. The interaction of these components creates a very robust system capable of performing a wide range of tasks. With a possible seven basic degrees of freedom (three at shoulder, two at elbow, and two at the wrist), wide ranges of movements are possible. The primary objective for moving the arm is to position the hand at a particular location in space. Once the desired position is achieved the wrist and fingers allow manipulation of an object. This entails both a location and orientation derived from the degrees of freedom at the shoulder, elbow, and wrist. Hand location can easily be accomplished through the movements of the shoulder (pitch, yaw, and roll) and elbow joint (pitch-flexion/extension), while orientation by the elbow (roll-pronation/supination) and wrist joints (pitch-flexion/extension and yaw).

We often take the ability to perform and learn such grasping and manipulation tasks for granted when we are healthy. Pointing and grasping tasks are much more dependent on hand location and are thus primarily affected by the shoulder complex and elbow flexion/extension. Hand orientation tasks rely on flexion/extension and adduction/abduction of the wrist joint. Additionally, wrist rotation is explicitly linked to forearm pronation/supination by anatomy and physiology. Simple tasks like using a computer joystick as described in the current research studies or turning a doorknob are hand orientation intensive and thus rely on forearm pronation/supination.

What follows is a thorough review of the anatomy and physiology of the structures involved in pronation and supination of the forearm (orientation of the hand). The approach will follow from the proximal connections at the shoulder to the distal connections at the wrist. Starting from the shoulder, the arm is composed of the shoulder joint, the upper arm, the elbow joint, the lower arm (forearm), the wrist joint, and the hand. The subsections will include separately: bones, ligaments, and muscles.

The upper arm orients, locates, and supports the forearm and hand. The single bone in the upper arm is the humerus. Several muscles acting across the shoulder's ball-and-socket (glenohumeral) joint abduct/adduct, flex/extend, and rotate the humerus internally and externally. The ball is the humerus' medial-anterior head and the shallow socket is the glenoid fossa of the lateral scapula (shoulder blade). The shoulder joint is highly flexible (it is actually made of several joints of limited motion) and very unstable. At its distal end, the humerus meets the forearm's two bones, the radius and ulna, forming the hinged elbow-joint. The elbow joint itself, responsible for flexion and extension, is made of two joints. One joint, the humeroulnar joint, encompasses the trochlear notch of the ulna and the humerus' trochlea. The radial head and humeral capitulum form the other elbow joint, the humeroradial joint. The biceps brachii and brachialis produce the flexion force, while the triceps brachii and anconeus produce arm-straightening (extension) forces.

The relative motions of both the radius orient the hand and ulna about the forearm's own long axis [39, 40]. Two joints, one at each end of the forearm allow for this rotation. Just distal the elbow is the proximal radioulnar joint. This joint is a pivot created by the interaction of the radius' head and the radial notch on the ulna. The annular ligament holds the radial head against the notch, stabilizing the joint while allowing rotation. At the forearm's distal end are two more joints, the distal radioulnar joint and the wrist. The distal radioulnar joint is the second joint active in forearm rotation. Here, the ulnar notch moves about the ulnar head's rounded surface. The proximal and distal forearm joints' combined motion rotates the forearm itself, moving the hand between the palm-up (supination) and palm-down (pronation) directions while preserving wrist and elbow parallelism [39]. Once the necessary rotation is met, the wrist can then position the hand so that objects can be manipulated and grasped as needed.

It is important to note that this palm-up to palm-down pronation/supination movement can also be accomplished, at least in part, by the internal and external rotation of the humerus. As an example, hold one arm straight out in front of you with the palm facing down. Flexing the elbow in this position moves

the forearm towards the chest. Now rotate your hand to the palm-up direction. Now, flexing the elbow moves the forearm and hand towards the head. The elbow joint orientation has rotated by approximately 90 degrees. This movement cannot be attributed to the relative motions of the radius and ulna but rather the humerus' own rotation. In order to ensure pronation and supination is attributed to the motions of the forearm bones, elbow joint orientation must be held constant. This can be accomplished by either external fixation or physiologically locking the joint by flexing the elbow and releasing the olecranon of the ulna from the influence of the epicondyles of the distal humerus.

The styloid process forces the wrist to rotate to the same pronation/supination angle as the forearm despite articular cartilage and an articulating disc separating the ulna and wrist. Further proximal are the remaining distal carpal bones or the wrist, the metacarpals of the palm, and the phalanges that form the fingers allowing manipulation of objects in the hand.

Several muscles are needed to control arm and finger movements. The focus of this particular review will be on those muscles influencing forearm movement and in particular, only the musculature exclusively responsible for pronation and supination (not humeral rotation). The origins and insertions, along with function, of these muscles can be seen in Table 2.

Elbow flexion and extension are accomplished by the relative contributions of many different muscles. The biceps brachii and triceps brachii originate on the scapula rather than the humerus. The triceps projects to the olecranon (the elbow's point) on the ulna, with all three heads producing elbow extension force. The biceps brachii projects to the radial tuberosity. Elbow flexion is also created by activation of the brachialis and brachioradialis.

The forearm's primary pronators and supinators originate on the humerus projecting to a point on the forearm or wrist. The pronator teres and pronator quadratus produce rotation towards the palm-down direction. Supination is produced by the action of the supinator muscle. The biceps brachii, due to the

projection on the olecranon produces not only elbow flexion, but also forearm supination at the radioulnar joints.

Purpose

The purpose of this study was to examine the proprioceptive performance of a young healthy cohort using a joystick-based, constant-velocity, pursuit task. Performance was examined for baseline and disturbed feedback using a vibration-based muscle-spindle-organ disruption paradigm. Of particular interest was whether or not the pursuit task could successfully be used to measure changes in task performance due to vibration. Pursuit task performance was evaluated at four time points relative to vibration exposure. These time points included baseline (before vibration exposure), during vibration (a continuous fifteen minute exposure), immediately post-vibration, and after a washout period of 20 minutes from removal of the vibratory stimulus. This information could prove as a necessary foundation for the design of future fMRI studies to examine how modulated proprioceptive information is integrated during a pursuit task.

Objectives and Hypotheses

The primary objective of this study was to determine if there was a difference in pursuit-task velocity replication performance both during and post local vibration to the dominant hand's supinating musculature. A second objective was to determine if 20 minutes of recovery time after vibration was sufficient to return to pre-stimulus levels.

We hypothesized a decrease in movement velocity would be observed during and immediately following application of local vibration when no visual feedback was present. Additionally, we hypothesized that the decrease in velocity would persist for a short period of time before returning to baseline levels within the washout period. A similar pattern was expected in peak-to-peak movements where peak-to-peak amplitude would decrease concurrently with the decrease in velocity. A time-on-target (positional accuracy) measure was not expected to change with the application of or recovery from vibration.

Methods

Eight subjects (4F, 4M, Aged 22.4 ± 2.2), all self-reported as right-handed were recruited from the general population at the University of Kansas and consented to the following Human Subjects Committee approved protocol for this investigation. Each subject was required to complete a short health screening that disqualified individuals who had experienced musculoskeletal conditions including: tendonitis of the elbow, carpal tunnel syndrome, low back pain and/or who were uncomfortable or experienced nausea after prolonged periods of computer use. These individuals were then randomly assigned to one of two groups determining the order in which they experienced the test conditions corresponding to the two timelines indicated in Figure 8.

Testing took place in the Human Motion Control Lab in the department of Mechanical Engineering at the University of Kansas. Subjects lay supine facing a computer screen projected onto the ceiling directly above them. The joystick was supported at a 45° angle and positioned so that the subject's wrist was placed in a neutral position. The elbow was supported at the subject's side and flexed to 45° to meet the joystick, this anatomically locked-out internal and external rotation of the humerus so that the movements of the radioulnar joints provided all wrist rotation. A custom, non-magnetic, pneumatically driven vibration device was placed over the supinator muscle of the forearm [Figure 9]. A second vibration device, (a 12-volt DC motor with offset weight) was located over the biceps of the upper arm. Both devices were previously determined to be capable of generating consistent vibration frequencies within the range of 20-90 Hz (see chapter four for details). For each subject the location of the vibrators was randomly assigned to one of the two previously mentioned locations. A triaxial accelerometer (PCB, Depew NY) was attached to the top of each vibration device with heavy-duty two-sided tape. Random samples of vibration frequency were recorded throughout the vibration portion of the protocol at a sample rate of 1000 Hz.

Prior to data collection, subjects underwent a training procedure to become familiar with the pursuit-task. For the first portion of training (T1), subjects were instructed to perform Task A, (pursuit with feedback, as seen in Figure 10) until the subject could achieve a time-on-target of at least 90% for three consecutive 30-second trials. The subject then performed a modified version of the testing protocol (T2) consisting of consecutive Task A and Task B (pursuit without feedback) blocks of 20 seconds duration until they achieved a time-on-target of at least 60% for both blocks for two consecutive trials. A single 90% time-on-target on T1 followed immediately by a 60% on T2 were required to complete training or else the process was repeated until achieved. The average number of trials to successfully complete training was 12 indicating the relative ease with which this task was acquired. No vibration was applied during training.

After successful completion of the training protocol a baseline level of performance was collected at each level of the pursuit task. The pursuit task levels were: A.) Feedback: Watching a target move about a constant-velocity, straight-line path and trying to match the target motion with a visible joystick controlled cursor, B.) No-Feedback: Watching a target cursor move about a constant-velocity, straight-line path at a given speed and trying to match the target motion with an invisible joystick controlled cursor, and C.) Rest: Watching a target cursor move about a constant-velocity straight-line path at a given speed [Figure 10]. The tasks were presented in the ABC block diagram as seen in Figure 8. Each individual block was 20 seconds in duration and the sequence was repeated three times for each condition. Average performance values for each individual block were then calculated. The feedback program was created in Labview (v8.5) and collected the joystick cursor data at a rate of 50 Hz.

The three unique task conditions were projected onto the ceiling directly above the subject while reclined on a padded chair. During Task A subjects attempted to keep the green square pursuit cursor within the red target cursor circle. During task B subjects continued the target pursuit without visual feedback of the pursuit cursor. During Task C subjects remained still and watched only the target circle movements. The target cursor moved horizontally at a constant speed of 9.6 deg/sec over the middle 60% of the joystick's

range of motion for a total of 24 degrees range of motion. The target circle was extended to provide a window of $\pm 10\%$ or ± 1.2 degrees. The subject-controlled joystick pursuit cursor was represented by a green square and was limited to movement directly on the horizontal axis.

All subjects experienced three baseline measurement collections that were averaged to provide an average baseline. After the baseline measurements, subjects in group #1 were presented with an approximate 65 Hz vibration applied to the supinating musculature of the forearm for a total of 15 minutes duration. This included 65.9 \pm 5.3 Hz to the supinator and 64.4 Hz \pm 2.7 Hz to the biceps. A second series of data collections began at the 6 and 10-minute marks of vibration exposure and were average to provide the average during vibration performance. Immediately following the end of the full 15-minute vibration exposure a third period (post vibration) of data collection occurred. A fourth and final (post washout) collection was obtained at the conclusion of a washout period of 20 minutes post vibration. Those in group 2 saw the washout and vibration orders reversed [Figure 8].

The following measures were calculated. Time-on-target was defined as the portion of the task blocks that the subject kept the joystick-controlled cursor within the tolerance of the target cursor. The peak-to-peak movement amplitude was defined as the total joystick movement between changes in direction of the subject cursor (joystick movement between consecutive max and min pairs). The average velocity was defined using multiple methods. First, it was defined as the slope of the line between consecutive max/min pairs (corresponding to changes in direction) as calculated using a first order pVEL command in Matlab. These pVEL velocity values were then averaged for each pronation and supination movement to provide an average pVEL velocity (pVEL) for each block. The other average velocity calculation was the average instantaneous velocity (iVEL), calculated by the difference in joystick movement between consecutive samples, average per block. The average of these difference values were calculated for each task block. The number of samples between consecutive max/min pairs (DT) was calculated to account for any shift in time that may occur.

A Huyhn-Feldt, repeated measures ANOVA was performed in SPSS to test for significant differences in the dependent variables with $\alpha = 0.05$. If a main effect was observed for a particular variable a simple contrast was computed as a post hoc analysis to determine significance between levels.

Results

There were several interesting results observed in the data collected. In regard to the pursuit task itself, it was important to review the ability of subjects to maintain accuracy while feedback was available. A review of the subjects' ability to maintain time-on-target (TOT) per each task (feedback level) can be viewed in Figure 11. In general subjects were able to remain within the target tolerance approximately 90% of the time when their joystick-controlled cursor was present. During the more difficult Task B, when no feedback was present, subjects were on target approximately 50% of the time compared to approximately 17% of the time when subjects simply remained stationary. No main effect was detected for TOT due to vibration condition ($p = 0.112$) even though there does appear to be reduced ability to maintain TOT during and post vibration.

In terms of testing our hypothesis of change in performance due to vibration, both velocity metrics pVEL velocity (pVEL) and instantaneous velocity (iVEL) indicated statistically significant findings and are described fully in the following sections.

pVEL

The average pVEL velocity data may be viewed in Figure 12. Only feedback conditions A (with feedback) and B (no feedback) were included in the following analysis to avoid the trivial finding of a difference between the active and resting states. The complete statistical results may be found in Table 3: Joystick pVEL ANOVA.

There was a significant difference in the pVEL due to vibration condition ($p=0.000$). As expected, the velocity decreased, about 1.5 deg/sec from baseline, while vibration was actively applied ($p=0.000$). Contrary to our expectations, the post vibration pVEL was found to increase above baseline ($p = 0.037$), by about 1.1 deg/sec. No differences were found between the post washout and baseline velocity ($p > 0.05$).

The interaction between condition and feedback indicated a main effect ($p=0.005$) revealed in the contrast to be due mainly to the during vibration ($p=0.000$) and post vibration ($p=0.037$) conditions. These findings indicate that when relying primarily on the proprioceptive system, the vibration applied resulted in a greater velocity decrease during vibration and a greater increase immediately post vibration when compared to baseline.

PK-PK & DT

In order to determine whether the changes observed in the pVEL statistic were due to a change in total movement distance or changes in the movement time interval (DT), a repeated measures ANOVA was performed for both the peak-to-peak (PK-PK) movement amplitudes [Table 5] and the difference time (DT) measurements.

A main effect due to vibration condition was observed for the PK-PK movements ($p = 0.000$). The post hoc revealed that PK-PK changes were due to differences from baseline observed during vibration ($p = 0.000$). Further, an interaction for vibration condition and feedback was observed ($p = 0.000$) again showing a greater change during vibration without feedback ($p = 0.001$). There were no observed changes in the movement time parameter, DT, due to vibration condition ($p>0.05$) or any other condition. In summary it would appear that the changes observed in the pVEL were primarily attributed to shifts in movement extent rather than changes in duration of the movements.

iVEL

The instantaneous velocity data may be viewed in Figure 13. Only feedback conditions A and B were included in the following analysis to avoid the trivial finding of a difference between the active and resting states. The complete statistical results may be found in Table 4.

A similar pattern as the pVEL was observed for the average instantaneous velocity. Again, a main effect was observed due to vibration condition ($p = 0.000$) with a significant interaction between vibration and feedback ($p = 0.007$). The post hoc revealed a significant slowdown in velocity (~ 1.2 degrees/sec) due to the applied vibration ($p = 0.000$) but not the post vibration condition ($p=0.058$). Again, contrary to expectations the subjects slowed down during vibration and appeared to speed up (~ 0.9 deg/sec) immediately post vibration. The interaction was only found to be significant when during vibration iVEL was compared to baseline ($p = 0.002$). Overall the changes observed with the iVEL were of a slightly lower magnitude than those observed with the pVEL velocity.

Additionally, there was a main effect observed in the iVEL due to repeat within the pursuit task blocks ($p=0.026$) that was not observed in pVEL. Further investigation reveals that this difference does not appear to be representative of task learning. The calculated iVEL was highest on the first iteration followed by a slowdown during the second repeat that is about 0.4 deg/second before increasing iVEL again by about 0.2 deg/sec. While in a traditional learning curve one would expect a curve settling to a particular value, the data suggest that this may simply be due to variability in subject performance due to awareness of the protocol. There is no other data supporting learning during the protocol so this finding may simply be indicative of a Type 1 error.

Discussion

The findings of this experiment supported our primary hypothesis, that muscle vibration would disrupt performance of a velocity based joystick pursuit task. A statistically significant difference in average velocity was observed both during and immediately post vibration when visual feedback of performance was not provided. While a difference in velocity was observed, the directionality of that difference did not completely conform to what was expected. We had originally hypothesized that both during and post vibration velocities would each demonstrate a slowdown in overall subject velocity as the stimulating velocity resulted in a slower than actual efferent signal. While the expected slowdown was observed during vibration, in the block immediately post vibration an increase in velocity was actually observed. As expected average velocities were not statistically different when compared between baseline and after the washout period.

The differences in the two primary measures used pVEL and iVEL are ideological in nature and largely attributable to the end effects of changing rotational direction of the forearm. The pVEL being more influenced by endpoints that have additional pull on the slope of the data fit line. This particular measure is simplistic in its implementation, which could be advantageous in a clinical setting, and it was sensitive to the vibratory stimulus. However, this measure is also sensitive to, but does not provide any information on, changes in performance within a movement. For example, it was often observed that a subject would move slightly ahead or slightly behind the target cursor, resulting in a corrective action (speeding up or slowing down) to bring the cursor back within tolerance. While the data points coinciding with this corrective action were used in the derivation of the fit line, details of this correction are lost.

In terms of detail of information the iVEL, being a point-by-point measure, provided a better trace of the actual performance of the subject. Although in this study the iVEL was averaged over the task block, plotting the point-by-point difference versus time often displays a response that appears to follow what would be expected from the step response of a second-order underdamped system with the target velocity as the system input. While this is not always the case with each movement it is worth noting that such an

analytical approach could result in several additional parameters such as damping ratio, or the time constant, or steady state error, common in engineering controls systems. While not reported here, such an approach is intriguing and would provide a useful investigative tool in proprioceptive performance. This may ultimately prove to be the area where velocity based measures excels over their position based brethren.

The finding that the differences observed in the pVEL velocity were due primarily to changes in movement amplitude was not completely unexpected. As per the design of the experiment, the target cursor was always visible and moving at a constant velocity. This provided the subjects with a timing cue during the no feedback condition (Task B) for when to change direction. According to the data, this seems to be what the subjects did, regardless of the proprioceptive feedback on position, whenever the target cursor changed direction, so did the subjects, as witnessed in no significant changes in the peak-to-peak movement times (DT). This also resulted in significant changes in the peak-to-peak movement amplitude (Pk-Pk). What is not clear is whether or not a similar pattern in the components of pVEL would be observed if the target cursor cue were not available. If the movement were to allow subjects to move to the perceived end of movement, would it coincide with the target end-of-movement? Several different paradigms exist for position based targeting/pointing tasks that could be modified for a velocity task, though the vast majority is for an event-based design as opposed to the block design implemented here. Regardless, this is another area that could provide useful insight for motor performance.

Perhaps the most interesting finding was that immediately after the vibration was removed the average velocity was found to significantly increase. This increase was significantly above both baseline and during vibration velocities for pVEL and significant compared to baseline and very close to significant compared to during vibration for the iVEL velocity. While the during vibration change was expected due to the well documented change in afferent spindle firing during vibration, it is more difficult to explain post vibration.

There is ample evidence gathered from other studies attributing changes in the afferent signal to increased delays in muscle response and changes in muscle excitability [3, 41, 42]. However, observations via direct microneurographic recordings indicate that the spindle afferents recover relatively quickly, on the order of seconds, once removed from the influence of applied vibrations [41, 43]. Similarly, effects on motor excitability were also only observed as similarly temporary in nature [44, 45]. The phenomenon we observed persisted over the entire 3-minute block designed collection period, during which subjects were essentially retrained at the task and able to match baseline performance provided visual feedback was available [Figure 12 & Figure 13]. Taken together these findings would seem to suggest that the persistent errors may be due to a centrally developed phenomenon and not readily explained by studies simply investigating the end motor task performance.

This suggestion, that there was some underlying central source responsible for driving the observed changes in velocity post vibration, is also supported by investigations of perceived movements. An induced "kinesthetic illusion" in a static joint has also been accompanied by a "return illusion" once the stimulus was removed [41]. A similar correction in our observed velocity data could be taking place, although the extent to which the observed velocity changes persist suggests it may be more than a simple return to origin type correction. Induced kinesthetic illusions may also result in perceived movements beyond what is physiologically possible and are also transferrable to other parts of the body [27, 46, 47]. In the classic, 'Pinocchio' example, an induced illusion of elbow extension while one is touching their nose results in the perception that the nose itself is lengthening [48]. Furthermore, recent imaging studies have indicated activations in motor and sensory regions consistent with these perceived movements [46, 49]. These results strongly encourage the idea that central mechanisms are likely the source of proprioceptive errors, both during and post vibration and deserve further investigation.

In summary, both of the average velocity measures used in this investigation proved to be sensitive to the applied vibration. The joystick pursuit task paradigm revealed a significant change from baseline

performance both during and post vibration, before returning to baseline levels of performance after a washout period of magnitude similar to exposure. The methodology above demonstrates that a pursuit task coupled with a MSO disruption paradigm can be implemented to test overall proprioceptive performance. In order to investigate whether central effects are responsible for the observed changes, an advanced imaging modality such as functional magnetic resonance imaging (fMRI) would need to be implemented with a similar paradigm.

Table 2: Forearm Anatomy

Muscle	Origin	Insertion	Action
Biceps Brachii (Short Head)	Coracoid Process of Scapula	Radial Tuberosity	Elbow Flexion & Forearm Supination
Biceps Brachii (Long Head)	Supraglenoid Tubercle	Radial Tuberosity	Elbow Flexion & Forearm Supination
Brachialis	Distal Half of Humerous	Coronoid Process of Ulna & Capsule of Elbow	Elbow Flexion (Acts on Ulna)
Brachioradialis	Lateral supracondylar Distal End of Humerous	Styloid Process of Ulna	Elbow Flexion
Pronator Quadratus	Distal Quarter of Anterior Ulna	Distal Quarter of Anterior Radius	Forearm Pronation
Pronator Teres	Medial Epicondyle of Humerous & Coronoid Process of Ulna	Lateral Radius (Midshaft)	Forearm Pronation
Supinator	Posterior Ulna	Proximal Anterior Shaft of Humerus	Forearm Supination
Triceps Brachii (Lateral Head)	Dorsal Surface of Humerus	Olecranon	Elbow Extension
Triceps Brachii (Medial Head)	Dorsal Surface of Humerus	Olecranon	Elbow Extension

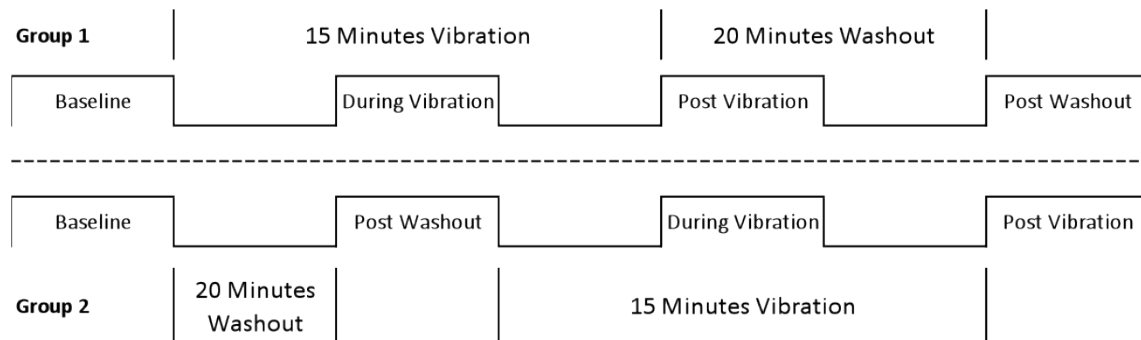


Figure 8: Experimental Timeline

Subjects were randomly assigned to one of two groups determining the order of vibration exposure. An averaged pre-vibration performance level was calculated by averaging three separate runs of the collection protocol. Those in group 1 (top) were then continuously exposed to the vibration condition for 15 minutes. During this stimulus condition an averaged during vibration performance level was calculated by averaging two separate runs of the collection protocol. An immediately post vibration performance level was calculated by a single trial run starting at the end of the vibration period. A final post washout performance level was calculated by a single run of the collection protocol beginning exactly 20 minutes after the cessation of the applied vibration stimulus. Those subjects in group 2 were given the post-washout period evaluation 20 minutes after the baseline performance level was determined before continuing the timeline as before.

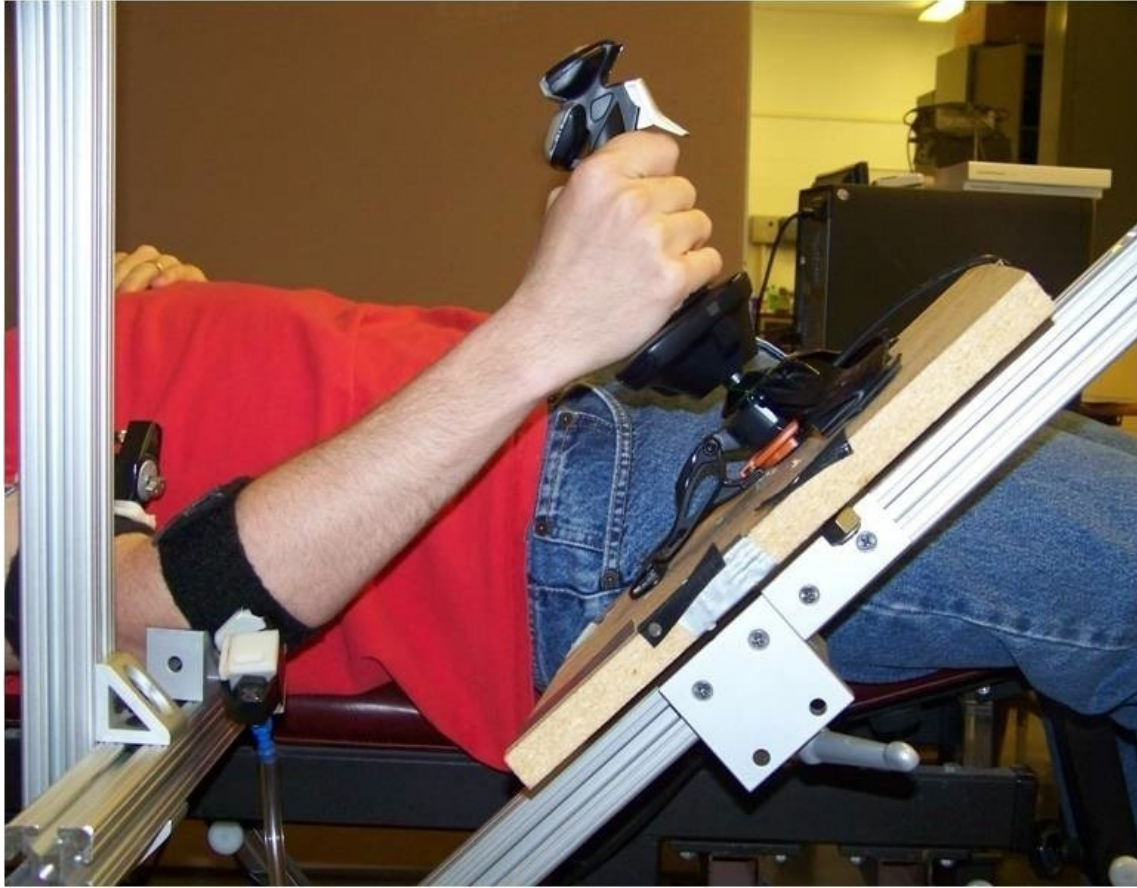


Figure 9: Experimental Setup

Subjects lay supine on a padded bench with their right elbow supported and fixed to a support platform. The joystick was positioned such that the forearm angle was approximately 45 degrees and the wrist was in the neutral position with a comfortable grip. Vibrators were placed over the supinator and biceps muscles. The Feedback protocol was projected directly above subjects on the ceiling while the room lights were dimmed.

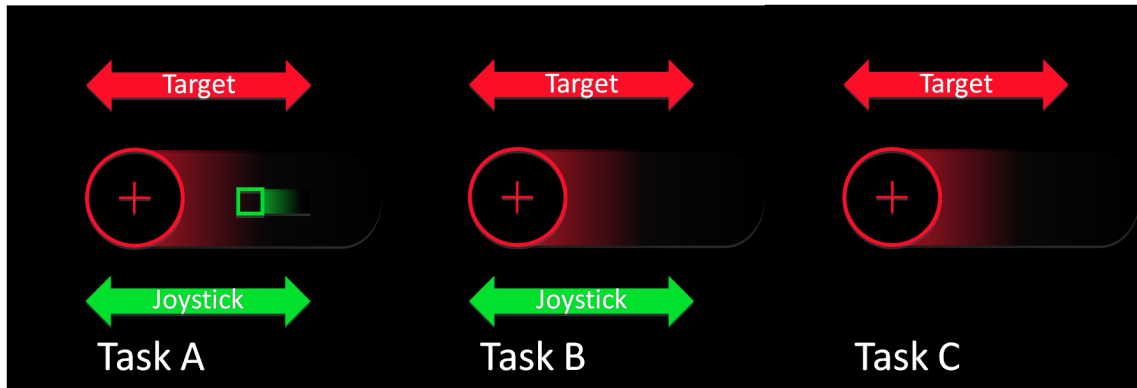


Figure 10: Pursuit Task Protocol

The pursuit task was presented to the subjects in three separate instruction blocks always presented in the same order. During the first block (Task A) subjects manipulated a joystick attempting to keep a square green cursor within the defined radius of a constant velocity target cursor. During the second task block (Task B) subjects continued to use the joystick in attempting to keep the square green cursor within the constant velocity target radius, however the green joystick cursor was now no longer visible. During the final task block (Task C) subjects returned the joystick to the neutral starting position and simply watched the target radius. Task blocks were 20 seconds in duration and the entire protocol was repeated three times per data collection period. Target cursor and joystick cursor movements were limited to the medial-lateral direction only. Subjects were instructed to "Keep the joystick cursor within the target cursor by focusing on the movement velocity of the target cursor." The pursuit task protocol was written using LabVIEW (National Instruments) software and collected joystick cursor position at 50 Hz.

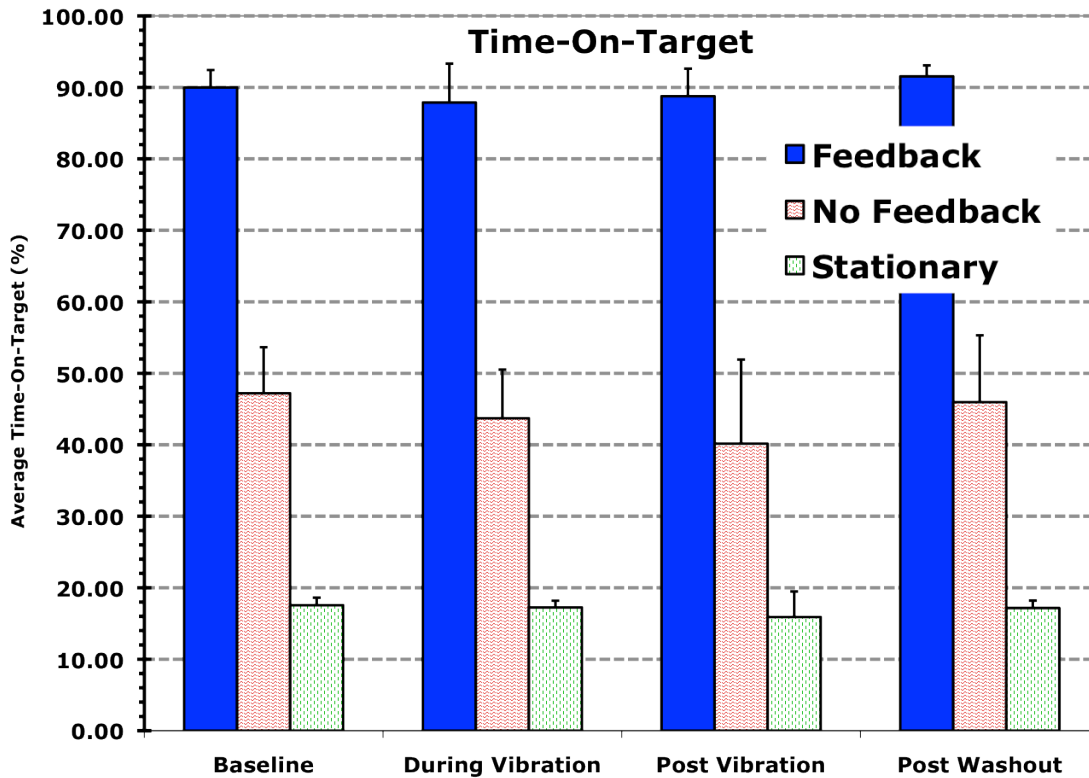


Figure 11: Results - Time on Target

Average percent of the time that the subject cursor was maintained within the tolerance of +/- 10% of the target cursor location with standard deviations. Performance with visual feedback (Task A) is represented by the solid blue columns. Performance without visual feedback (Task B) is represented by the red dash filled columns. The rest condition (Task C) is represented by the green-dot filled bar. Subjects were readily about the 90% mark with visual feedback and approximately at 45% without feedback.

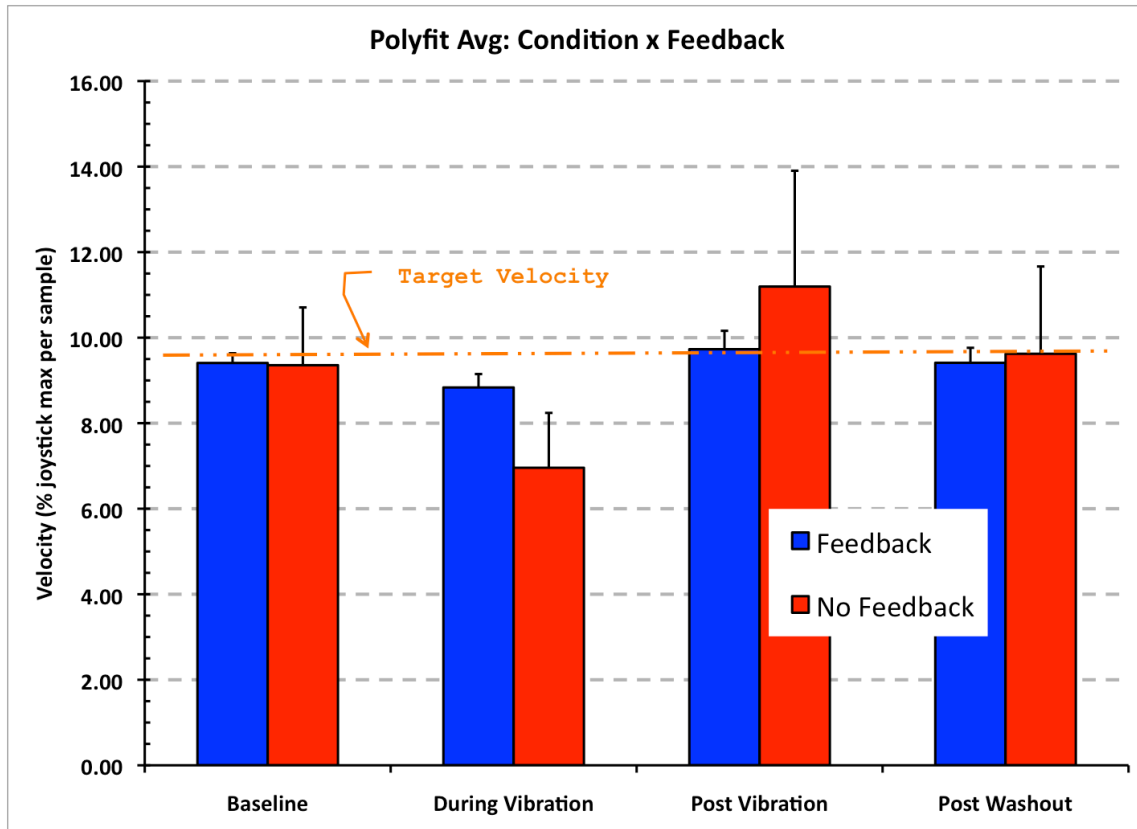


Figure 12: Results - Polyfit Velocity (pVEL)

The slopes of the linear curve fits in degrees per second across feedback and vibration conditions are represented here. The with feedback condition (Task A) is represented by the solid blue columns, the no feedback condition (Task B) is represented by the red hatched column. Target cursor velocity (9.2 deg/sec) is represented by the orange dashed line. Columns are represented with standard deviations. Subjects exhibited a statistically significant decrease in velocity during vibration with an equivalent magnitude increase in velocity immediately post vibration. An interaction was also observed indicating a greater influence of vibration during the no feedback condition (Task B).

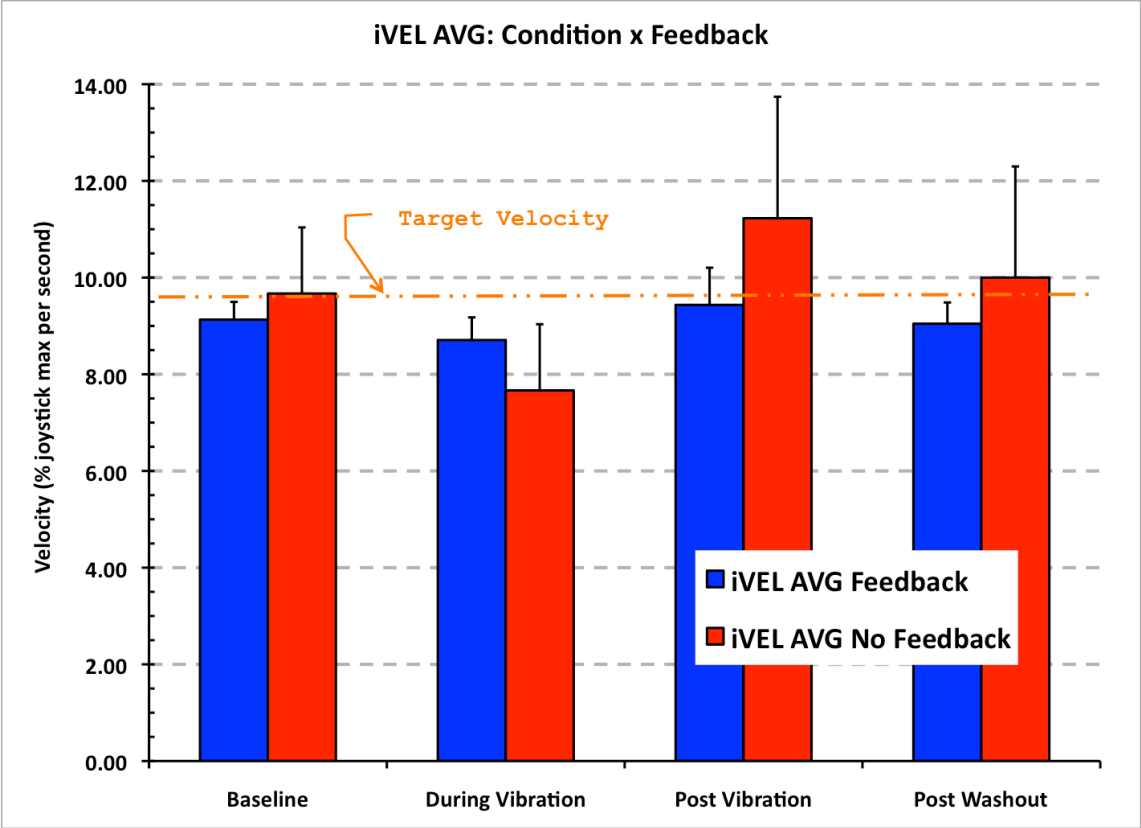


Figure 13: Results - Instantaneous Velocity (iVEL)

The average step-by-step velocities in degrees per second across feedback and vibration conditions are represented here. The with feedback condition (Task A) is represented by the solid blue columns; the no feedback condition (Task B) is represented by the red hatched column. Target cursor velocity (9.2 deg/sec) is represented by the orange dashed line. Columns are represented with standard deviations. Subjects exhibited a statistically significant decrease in velocity during vibration with an equivalent magnitude increase in velocity immediately post vibration. An interaction was also observed indicating a greater influence of vibration during the no feedback condition (Task B).

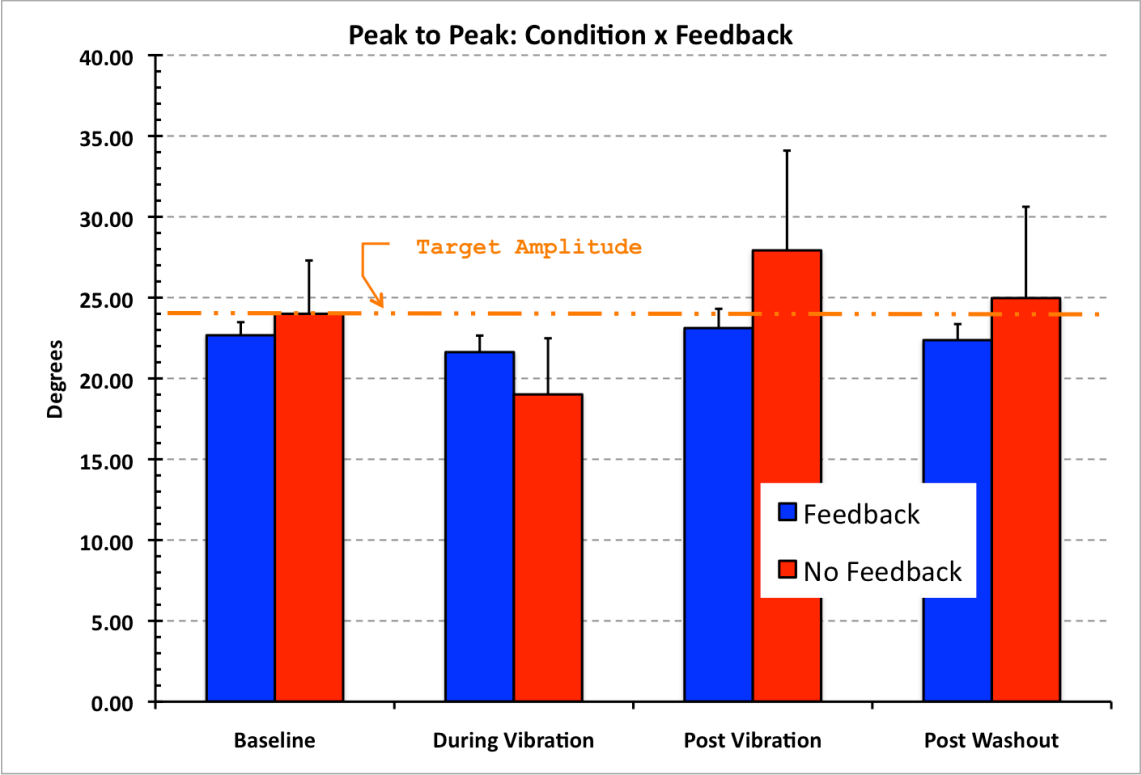


Figure 14: Results - Peak to Peak Movement (Pk-Pk)

The average extent of subject joystick movement (in degrees) for both feedback and vibration conditions are represented here. The with feedback condition (Task A) is represented by the solid blue columns; the no feedback condition (Task B) is represented by the red hatched column. Target cursor movement extent (24 deg) is represented by the orange dashed line. Columns are represented with standard deviations. Subjects exhibited a statistically significant decrease in movement extent during vibration. An interaction was also observed indicating a greater influence of vibration during the no feedback condition (Task B).

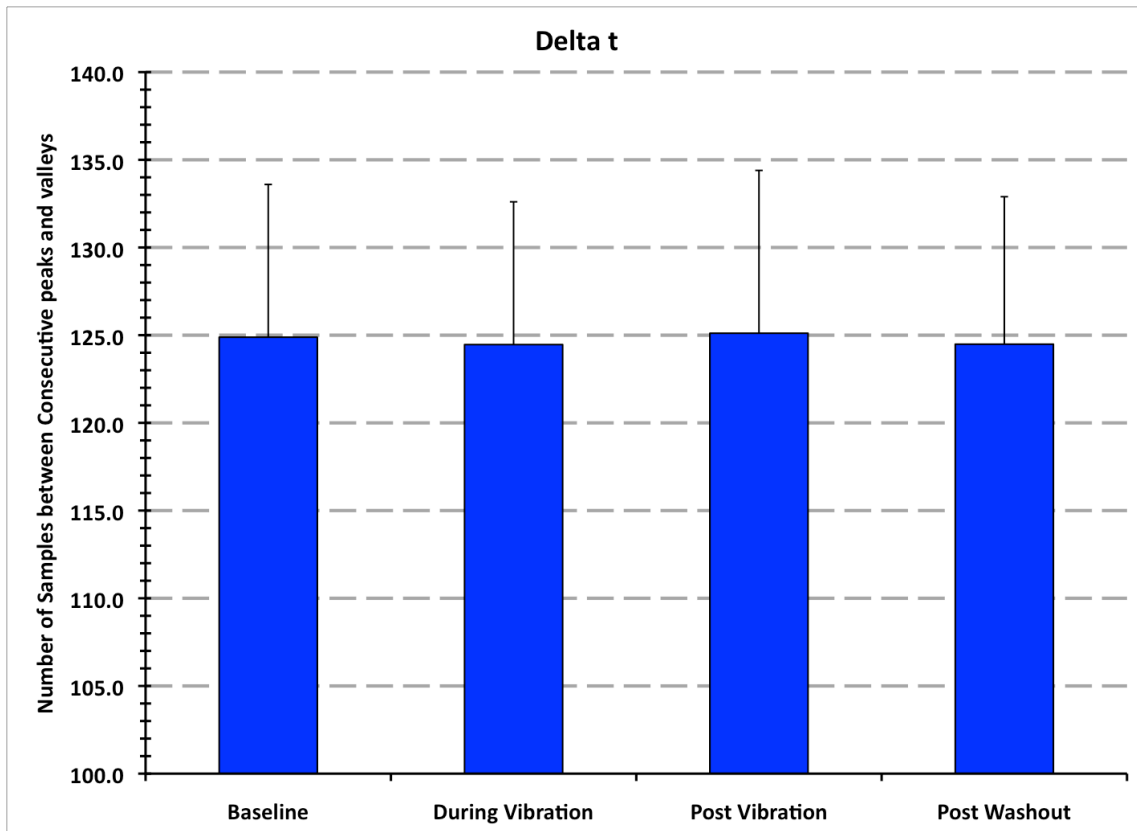


Figure 15: Results - Average Time Between Peaks (DT)

The average time (in samples) for each vibration condition is represented here with standard deviations. There were no statistically significant changes in time for subject peak to peak movements observed due to vibration. This indicates that subjects changed directions approximately at the time the visible target cursor changed directions, regardless if they had reached the target extent.

Table 3: Joystick pVEL ANOVA

Tests of Within-Subjects Effects

Measure:pVEL

Source	df	F	Sig.	Partial Eta Squared	Observed Power ^a
Condition	1.840	26.702	.000	.817	1.000
Repeat	1.867	2.250	.153	.273	.354
Feedback	1.000	.012	.916	.002	.051
Rotation	1.000	.899	.380	.130	.127
Condition * Repeat	6.000	1.408	.238	.190	.477
Condition * Feedback	1.667	10.394	.005	.634	.921
Repeat * Feedback	1.312	2.857	.126	.323	.350
Condition * Repeat * Feedback	6.000	.816	.565	.120	.279

a. Computed using alpha = .05

Table 4: Joystick iVEL ANOVA

Tests of Within-Subjects Effects

Measure: iVEL

Source	df	F	Sig.	Partial Eta Squared	Observed Power ^a
Condition	1.865	20.075	.000	.770	.999
Repeat	2.000	4.991	.026	.454	.701
Feedback	1.000	.775	.413	.114	.116
Condition * Repeat	6.000	1.165	.347	.163	.397
Condition * Feedback	1.686	9.130	.007	.603	.887
Repeat * Feedback	1.449	.489	.571	.075	.101
Condition * Repeat * Feedback	5.036	.867	.515	.126	.267

a. Computed using alpha = .05

Table 5: Joystick Pk Pk ANOVA

Tests of Within-Subjects Effects

Measure:Pk-Pk

Source	df	F	Sig.	Partial Eta Squared	Observed Power ^a
Condition	1.875	20.494	.000	.774	.999
Repeat	1.759	2.253	.156	.273	.342
Feedback	1.000	.899	.380	.130	.127
Rotation	1.000	.153	.710	.025	.063
Condition * Repeat	6.000	.541	.773	.083	.190
Condition * Feedback	1.782	9.985	.004	.625	.925
Repeat * Feedback	1.360	1.004	.374	.143	.155
Condition * Repeat * Feedback	5.696	.192	.974	.031	.091

a. Computed using alpha = .05

References

- [1] M. Arashanapalli, S. E. Wilson., Paraspinal muscle vibration alters dynamic motion of the trunk. *J Biomech Eng*, 130:021001, 2008.
- [2] P. Cordo, V. S. Gurfinkel, L. Bevan, G. K. Kerr., Proprioceptive consequences of tendon vibration during movement *Journal of Neurophysiology*, 74: 1675-88, 1995.
- [3] L. Li, F. Lamis, S. E. Wilson., Whole-body vibration alters proprioception in the trunk *International Journal of Industrial Ergonomics*, 38: 792-800, 2008.
- [4] P. J. Cordo, J. L. Horn, D. Künster, *et al.*, Contributions of skin and muscle afferent input to movement sense in the human hand. *J Neurophysiol*, 105: 1879-88, 2011.
- [5] J. S. Soltys, S. E. Wilson., Directional sensitivity of velocity sense in the lumbar spine. *J Appl Biomech*, 24: 244-51, 2008.
- [6] S. M. Verschueren, P. J. Cordo, S. P. Swinnen., Representation of wrist joint kinematics by the ensemble of muscle spindles from synergistic muscles. *J Neurophysiol*, 79: 2265-76, 1998.
- [7] M. M. Wierzbicka, J. C. Gilhodes, J. P. Roll., Vibration-induced postural posteffects. *J Neurophysiol*, 79: 143-50, 1998.
- [8] R. P. Blood, J. D. Ploger, P. W. Johnson., Whole body vibration exposures in forklift operators: comparison of a mechanical and air suspension seat. *Ergonomics*, 53: 1385-94, 2010.
- [9] F. Gerr, L. Mani., Work-related low back pain. *Primary care*, 27:865, 2000.
- [10] M. H. Pope, T. H. Hansson., Vibration of the spine and low back pain *Clinical orthopaedics and related research*, 279:49, 1992.
- [11] P. M. Bernier, R. Chua, J. T. Inglis, I. M. Franks., Sensorimotor adaptation in response to proprioceptive bias. *Exp Brain Res*, 177: 147-56, 2007.
- [12] J. B. Fallon, V. G. Macefield., Vibration sensitivity of human muscle spindles and Golgi tendon organs. *Muscle Nerve*, 36: 21-9, 2007.
- [13] S. C. Regueme, J. Barthèlemy, G. M. Gauthier, C. Nicol., Changes in illusory ankle movements induced by tendon vibrations during the delayed recovery phase of stretch-shortening cycle fatigue: an indirect study of muscle spindle sensitivity modifications. *Brain Res*, 1185: 129-35, 2007.
- [14] G. K. Kerr, C. J. Worringham., Velocity perception and proprioception *Sensorimotor Control of Movement and Posture*, 508: 79-86, 2002.
- [15] D. I. McCloskey. Differences between the senses of movement and position shown by the effects of loading and vibration of muscles in man *Brain research*, 61: 119-31, 1973.
- [16] A. C. Sittig, J. J. Denier van der Gon, C. C. Gielen., Separate control of arm position and velocity demonstrated by vibration of muscle tendon in man. *Exp Brain Res*, 60: 445-53, 1985.
- [17] C. Duclos, R. Roll, A. Kavounoudias, *et al.*, Vibration-induced post-effects: a means to improve postural asymmetry in lower leg amputees? *Gait Posture*, 26: 595-602, 2007.

- [18] M. J. Gerard, B. J. Martin., Post-effects of long-term hand vibration on visuo-manual performance in a tracking task. *Ergonomics*, 42: 314-26, 1999.
- [19] P. J. Cordo, V. S. Gurfinkel, S. Brumagne, C. Flores-Vieira., Effect of slow, small movement on the vibration-evoked kinesthetic illusion. *Exp Brain Res*, 167: 324-34, 2005.
- [20] S. E. Grill, M. Hallett., Velocity sensitivity of human muscle spindle afferents and slowly adapting type II cutaneous mechanoreceptors. *J Physiol*, 489 (Pt 2): 593-602, 1995.
- [21] R. S. Turner, S. T. Grafton, J. R. Votaw, *et al.*, Motor subcircuits mediating the control of movement velocity: a PET study. *J Neurophysiol*, 80: 2162-76, 1998.
- [22] D. B. Willingham, J. Hollier, J. Joseph., A Macintosh analogue of the rotary pursuit task *Behavior research methods, instruments & computers*, 27: 491-5, 1995.
- [23] J. E. Joseph, D. B. Willingham., Effect of sex and joystick experience on pursuit tracking in adults. *J Mot Behav*, 32: 45-56, 2000.
- [24] S. P. Silfies, J. Cholewicki, A. Radebold., The effects of visual input on postural control of the lumbar spine in unstable sitting. *Hum Mov Sci*, 22: 237-52, 2003.
- [25] J. H. van Dieën, L. L. Koppes, J. W. Twisk., Low back pain history and postural sway in unstable sitting. *Spine (Phila Pa 1976)*, 35: 812-7, 2010.
- [26] N. Vuillerme, F. Danion, N. Forestier, V. Nougier., Postural sway under muscle vibration and muscle fatigue in humans. *Neurosci Lett*, 333: 131-5, 2002.
- [27] B. Craske. Perception of impossible limb positions induced by tendon vibration. *Science*, 196: 71-3, 1977.
- [28] P. B. Matthews, R. B. Stein., The sensitivity of muscle spindle afferents to small sinusoidal changes of length. *J Physiol*, 200: 723-43, 1969.
- [29] D. I. McCloskey. Kinesthetic sensibility *Physiological Reviews*, 58:763, 1978.
- [30] S. Calvin-Figuière, P. Romaguère, J. C. Gilhodes, J. P. Roll., Antagonist motor responses correlate with kinesthetic illusions induced by tendon vibration. *Exp Brain Res*, 124: 342-50, 1999.
- [31] D. Y. Cao, J. G. Pickar., Lengthening but not shortening history of paraspinal muscle spindles in the low back alters their dynamic sensitivity. *J Neurophysiol*, 105: 434-41, 2011.
- [32] D. P. Allen, J. R. Playfer, N. M. Aly, *et al.*, On the use of low-cost computer peripherals for the assessment of motor dysfunction in Parkinson's disease--quantification of bradykinesia using target tracking tasks. *IEEE Trans Neural Syst Rehabil Eng*, 15: 286-94, 2007.
- [33] R. S. Turner, M. Desmurget, J. Grethe, *et al.*, Motor subcircuits mediating the control of movement extent and speed. *J Neurophysiol*, 90: 3958-66, 2003.
- [34] B. J. Martin, J. P. Roll, N. Drenzo., The interaction of hand vibration with oculomanual coordination in pursuit training *Aviation Space and Environmental Medicine*, 62: 145-52, 1991.
- [35] A. Currá, A. Berardelli, R. Agostino, *et al.*, Movement cueing and motor execution in patients with dystonia: a kinematic study. *Mov Disord*, 15: 103-12, 2000.

- [36] J. Prodoehl, D. M. Corcos, S. Leurgans, *et al.*, Changes in the relationship between movement velocity and movement distance in primary focal hand dystonia. *J Mot Behav*, 40: 301-13, 2008.
- [37] S. Siggelkow, A. Kossev, C. Moll, *et al.*, Impaired sensorimotor integration in cervical dystonia: a study using transcranial magnetic stimulation and muscle vibration. *J Clin Neurophysiol*, 19: 232-9, 2002.
- [38] C. Rickards, F. W. Cody., Proprioceptive control of wrist movements in Parkinson's disease. Reduced muscle vibration-induced errors. *Brain*, 120 (Pt 6): 977-90, 1997.
- [39] A. M. Weinberg, I. T. Pietsch, M. B. Helm, *et al.*, A new kinematic model of pro- and supination of the human forearm. *J Biomech*, 33: 487-91, 2000.
- [40] T. Nakamura, Y. Yabe, Y. Horiuchi, N. Yamazaki., In vivo motion analysis of forearm rotation utilizing magnetic resonance imaging. *Clin Biomech (Bristol, Avon)*, 14: 315-20, 1999.
- [41] T. Kito, T. Hashimoto, T. Yoneda, *et al.*, Sensory processing during kinesthetic aftereffect following illusory hand movement elicited by tendon vibration. *Brain Res*, 1114: 75-84, 2006.
- [42] J. P. Roll, J. P. Vedel., Kinesthetic role of muscle afferents in man, studied by tendon vibration and microneurography *Experimental Brain Research*, 47: 177-90, 1982.
- [43] E. Ribot-Ciscar, C. Rossi-Durand, J. P. Roll., Muscle spindle activity following muscle tendon vibration in man. *Neurosci Lett*, 258: 147-50, 1998.
- [44] A. Forner-Cordero, M. Steyvers, O. Levin, *et al.*, Changes in corticomotor excitability following prolonged muscle tendon vibration. *Behav Brain Res*, 190: 41-9, 2008.
- [45] A. Kossev, S. Siggelkow, H. Kapels, *et al.*, Crossed effects of muscle vibration on motor-evoked potentials. *Clin Neurophysiol*, 112: 453-6, 2001.
- [46] E. Naito, H. H. Ehrsson., Kinesthetic illusion of wrist movement activates motor-related areas. *Neuroreport*, 12: 3805-9, 2001.
- [47] E. Naito, P. E. Roland, H. H. Ehrsson., I feel my hand moving: a new role of the primary motor cortex in somatic perception of limb movement. *Neuron*, 36: 979-88, 2002.
- [48] J. R. Lackner. Some proprioceptive influences on the perceptual representation of body shape and orientation. *Brain*, 111 (Pt 2): 281-97, 1988.
- [49] P. Romaiguère, J. L. Anton, M. Roth, *et al.*, Motor and parietal cortical areas both underlie kinaesthesia. *Brain Res Cogn Brain Res*, 16: 74-82, 2003.

Chapter 4 - Vibratory Device Design for Functional MRI

Abstract

In order to test the hypotheses posed at the end of the previous chapter, whether or not during and post vibration proprioceptive changes in pursuit task performance were due in part to changes in the CNS, the design of an appropriate vibratory stimulus was required. The uniqueness of the MRI environment provides specific challenges due to the strong magnetic field and often very limited available space. Traditional materials, such as ferrous metals, may become dangerous projectiles or excessively hot leading subject injury. Additionally, poorly selected materials may distort the image data collected. Finally, the device must operate with a minimal footprint, as the bore must accommodate the combination of both the device and the subject over the functional extent of the task performed. An Ideal device design would have as small a footprint as possible and a magnetic susceptibility not greater than water.

While there are traditional methods by which to achieve these design objectives, including materials and shielding, this adds complexity and cost to the device. The recent expansion and advancements of rapid prototyping offers a unique and low cost solution. Using a three-dimensional printer (Dimension BST 1200) we designed and tested a custom pneumatically driven muscle vibrator. With a footprint slightly larger than 1 square inch and a weight of 28 grams we were able to successfully induce a velocity matching error during a joystick pursuit task protocol, during an active fMRI scan. The total cost of the device was calculated to be approximately \$35 and could be produced in larger quantities by readily available rapid prototyping equipment in a matter of hours. There was some minimal hand finishing and assembly required. This opens up the possibility for improvements in the design of stimulators and testing paradigms for biomechanics research.

Introduction

Functional Magnetic Resonance Imaging (fMRI) promises to grant motor control researchers better opportunities to probe the human proprioceptive system. However, the strength of the magnetic environment of the fMRI does not easily allow for traditional technologies to be used to create the necessary vibratory perturbations. In order to use vibration in conjunction with fMRI, a custom-designed MRI-compatible device was required. While a few different techniques have been found in literature, they tend to lack the blend of simplicity and reliability desired [1-4]. Some have implemented the strategy to use the magnetic fields generated by the scanner itself while many others were pneumatically driven [1, 2, 5, 6]. Commercially available vibrators, modified with proper shielding, are very expensive making them not readily available to many researchers.

Traditionally, proprioception studies have used either an electromagnetic device or inertial device driven by a small direct current (DC) motor to create localized vibrations [7-11]. The presence of the strong magnetic fields in MRI suites makes the use of an electromagnetic device impractical. The device risks either becoming a dangerous projectile or having unreliable performance due to the strength of the magnetic field. While the use of DC motors is impractical, an inertial device with a pneumatic motor provides a realistic option for operation in an MRI device, as long as compatible materials are chosen. Pneumatic devices allow for a wide range of frequencies of operation and can be used to drive pistons or other masses [12-14]. For research paradigms based on muscle spindle disruption, the device would ideally be able to produce vibration consistent frequencies between 10-120 Hz with around 70 Hz the critical value [15].

For the collection of studies presented in this text, several different designs were evaluated. Selection of the final design was based on several factors, but primarily focused on four main design criteria.

These design criteria were:

- 1. The device must be able to generate vibration consistently in the frequency range muscle spindle organs are most susceptible to, with an emphasis on the 60-80 Hz range.*
- 2. The device must be designed from materials allowing preservation of criteria #1 as well as maintaining subject safety and image integrity.*
- 3. The device must maintain criteria #1 in as small a size as possible.*
- 4. The device must be designed and fabricated for the minimal cost possible.*

The following chapter is written to address the design process undertaken per each of the aforementioned design criteria. The primary focus is on the most current iteration of the device and testing is presented in the methods section in accordance with design criteria one. The remaining design criteria are addressed in the following section and include discussion pertaining to the previous designs.

Design Evolution

Initially three different functional designs were considered for evaluation. These included a piston vibrator, vane motor, and a simple rotor with offset weight. Initial proof of concept prototypes were created of the rotor and vane motor designs for testing. The vane motor was inoperable, as the rapid prototyping process used could not maintain the surface finish to provide a functioning prototype. Because of this, the piston vibrator design was also abandoned and design efforts focused on the rotor design. An early prototype was created from simple polyvinyl chloride (PVC) piping, machined nylon spacers, and a brass rod. Thus each subsequent design focused on the rotor with offset ballast in order to generate the needed vibrations [Figure 16].

Every iteration of the pneumatic vibrator was developed using Autodesk Inventor Professional Edition (Autodesk). Standard part files were used to generate the components of the general assembly. These part

files were converted to STL files of high resolution and fabricated on a Dimension BST 1200bs three-dimensional printer (Stratasys Inc.) in duplicate in approximately 3 hours. The designs were dimensioned to be consistent with common components readily available from online or local hardware store vendors to simplify general assembly and lower cost. Final assembly and finishing were performed by hand and consisted of filing holes for the axel and mass and tapping the nozzle inlet and nylon connecting screw holes. All other connections for assembly were press fit design and the device was strapped to the arm with an elastic band.

Methods

Each iteration of the vibrator underwent unique testing for the vibration frequencies to be generated per design criteria #1. The methodology implemented for each iteration was the same, however the testing conditions varied due to air supply (lab air or compressor) and supply tube length used. Performance data provided are for the most recent device design and setup implemented in chapter five.

In accordance with design criteria #2 plastic parts were maximized in the assembly. To simulate the intended environment of the fMRI suite, the two vibrators were connected to the lab air supply utilizing nylon NPT 1/8" barbed connector and 30 feet of 3/8" nylon tubing. The final ten feet of which was split into two 10-foot length sections via a 60-degree "wee-type" nylon connector. The vibrators were located one over the biceps muscle and one over the supinator muscle of the forearm using a 3/4" elastic strap attached to the base plate and tightened with a plastic D-Ring. A triaxial accelerometer (PCB Piezotronic, Depew, NY) was placed on top of the vibrators via two-sided tape.

A data collection program was written with LabVIEW software (National Instruments) to collect vibration trials of ten-seconds duration at 2,000 Hz. During the collection the arm provider randomly simulated the experimental protocol. For a portion of the trials the arm remained stationary and for other portions the subject rotated the forearm. Additionally, the subject was also allowed to isometrically

contract the biceps muscle. This allowed documentation on the possible extent of effects arm stiffness might have on the vibrator performance. Several trials were collected by stepping the input pressure at intervals of 5 or 10 psi prior to the start of the trial. The process by which the input pressures were stepped through was by first increasing pressure after each trial until a frequency over 80 Hz was obtained and then stepping down through the input pressures. At least three trials were performed for each input pressure. The average frequency and amplitude of the vibration for each input pressure trial were then calculated using the LabVIEW vibration analysis toolbox. The vibrators were then swapped to record performance over the other targeted vibration location and the process was repeated.

Results

The previous protocol was repeated for the various iterations of the pneumatic vibrator and the different possible rotor designs. In all cases the vibrator frequency increased with the increasing input pressure in a linear fashion. The final rotor design selected was the "dental drill" styled rotor for its efficiency in generating higher output frequencies with smaller input pressures than the other tested rotor designs [Figure 17]. This was by far the most efficient design, almost 50% more efficient than the next closest "fin" design, given the pressure loss over the entire length of the supply tubing.

Additionally, while there was little variability in device performance due to muscle stiffness or movement, performance did change based on the muscle location [Figure 18]. The slope of the curve for vibrator V2 was much steeper when located on the biceps (1.68 Hz/psi) than when placed on the forearm (1.44 Hz/psi). The slope of the curve for vibrator V1 did not vary quite as much but was still higher when located on the biceps (1.47 Hz/psi) than on the forearm (1.42 Hz/psi). Since the target frequency was in the 70 Hz range the combination of V1 on the biceps and V2 on the supinator with a supply pressure of 50 psi were selected as the best configuration for the MSO disruption paradigm in the following study of chapter five.

Discussion

The goal of this chapter was to create a vibration device that would meet four key criteria. First, the device had to produce consistent vibration over the observed sensitivity window of the muscle spindle organ, with an ability to maintain a 60-80 Hz vibration. This first goal would necessarily have to have some level of optimization in order to operate with as low an input air pressure as possible. The second goal was to choose operable materials for the design that would ensure the design maintained performance within the MRI bore while preserving both the safety of the subject and the integrity of the imaging data. Third, the device had to be designed to reach the previous two performance goals in as small a volume as possible. The fourth and final goal was to design and build the vibration device at minimal cost. In order to achieve these goals, rapid prototyping was implemented.

The final design implemented in the capstone study (chapter five) was successful in meeting each of the defined design criteria. Final testing achieved a consistent 70 Hz vibration at both vibrators with an input pressure of 50 psi over the entire 30 feet of supply line. While not a small volume of air when considering continuous operation for 15 minutes, this is well within the capacity limits of common lab air supply lines. In terms of materials and cost, all components were readily available off the shelf or online from well-known vendors. No changes in image quality were apparent upon visible inspection or as phantoms or distortion in the image files themselves taken while the vibrators were functioning on subject within the scanner bore. The final design came in at a cost of about \$35 each with a lead-time of only about a half-day.

While the current design proved successful in the studies implemented here, the current design does have some limitations. For one, control of the vibration parameters themselves was somewhat limited. Altering the supply pressure could easily control vibration frequency. However, as the frequency was altered as a function of pressure the amplitude was also changed. The design does allow the mass to be swapped out fairly simply to account for this, however "on the fly" adjustments are not possible without interrupting

the experimental protocol. Other designs could incorporate control of the exhaust port as a means of controlling frequency [6].

The current design also experienced a lower limit, in terms of the vibration frequencies, that could be produced. Due to the mass and friction of the rotor plus offset mass, there is a minimum amount of air pressure required to maintain movement. As such, vibration frequencies below a certain threshold (~20 Hz) could not be reached by the current design. Since we were interested in much higher MSO disrupting frequencies, this did not pose any problems.

The design strategy and previous success does make possible exploration of additional designs, including those previously abandoned due to difficulty. Due to the rapid turnaround and low cost on such small and intricate parts in these types of devices, the advantages of RPM technology should be realized in biomechanics research.

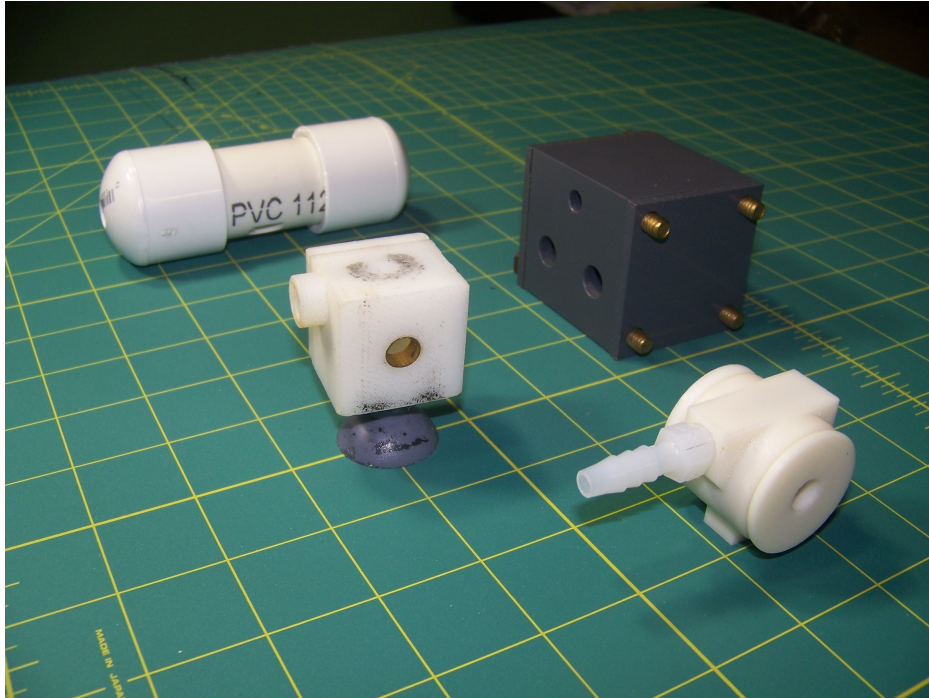


Figure 16: Pneumatic Vibrator Design Evolution

The evolution of the pneumatic vibrator is captured here. Background grid squares are 1" on each side. The back left design is the original "proof of concept" design and was created from simple PolyVinyl Chloride (PVC) tubing and end caps and a nylon rotor suspended on a brass rod inside. The second iteration (back right - dark grey) was created in the machine shop at the University of Kansas using traditional milling operation and PVC, it had a finned rotor design with a large offset brass mass. After a short period of time, the fin design began to show wear in the form of broken fins. The third design (front left) was the initial implementation of the rapid prototyping process and is primarily built from acrylonitrile butadiene styrene (ABS). This design was successfully implemented in the study in chapter three with bearing and mass material thought to be MRI compatible at the time. The current design (front right) was successfully implemented in the capstone study of chapter five and improved upon the previous design by having an equivalent footprint but much shorter height and faster lead time due to the reduced total amount of material in the design. This design also incorporated all MRI compatible materials.

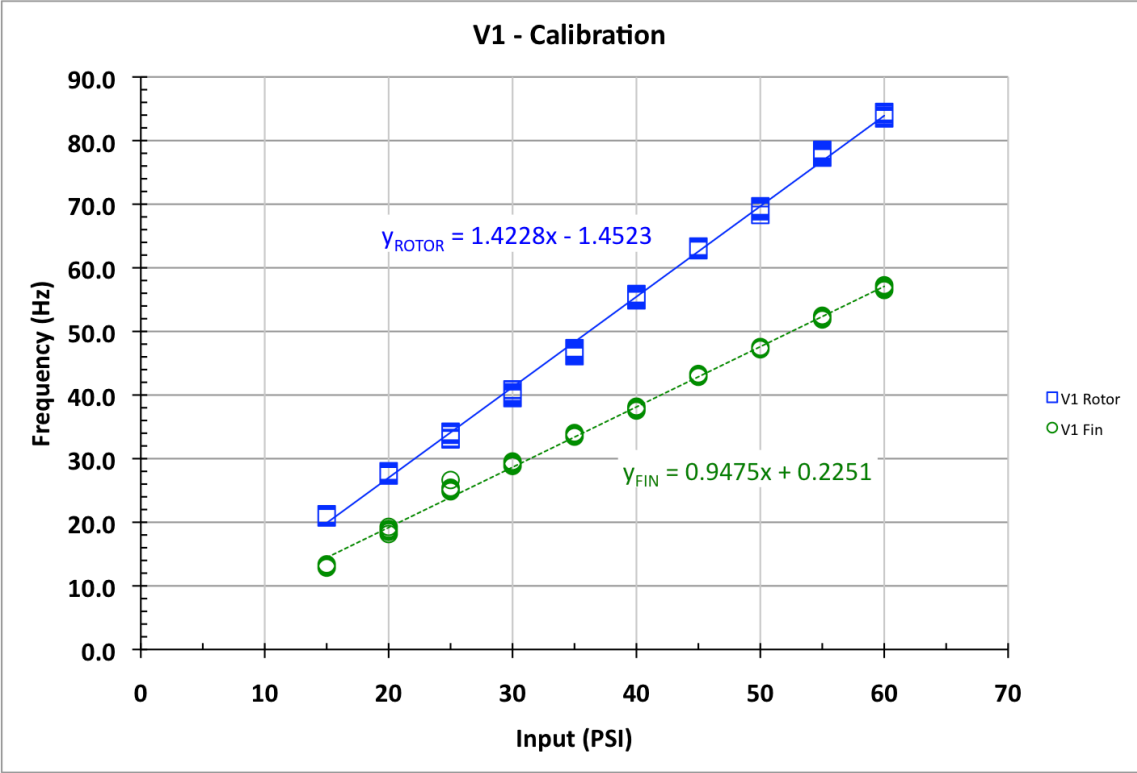


Figure 17: Comparison of Rotor Design - Frequency Performance

The output vibrator frequency measured along the vertical axis of the pneumatic vibrator V1 per input air pressure is displayed above. The "dental rotor" design is denoted by the open squares while the open circles denote the "finned" rotor. Per the prescribed stepping protocol the slope of the "dental" rotor design proved to be more efficient in converting the supplied air pressure into a mechanical vibration. Only the "finned" rotor design is included in for comparison, as it was the second most efficient design.

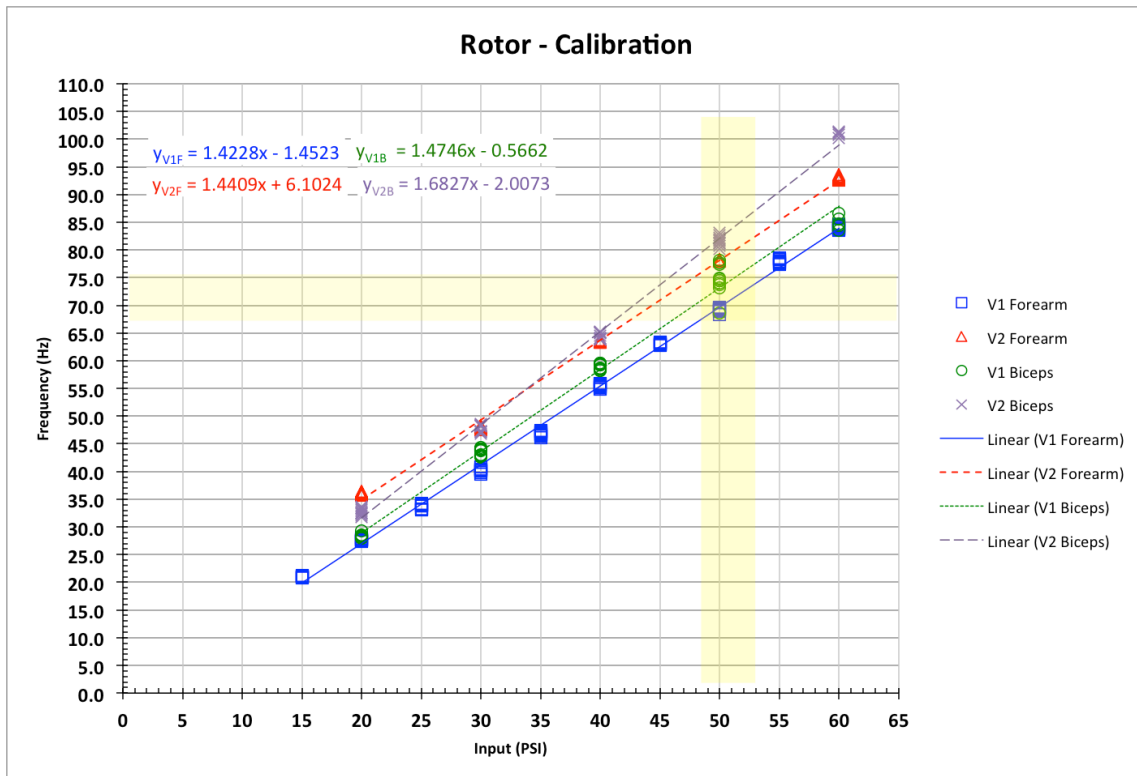


Figure 18: Performance Curves (Final Design)

The output vibrator frequency measured along the vertical axis of the pneumatic vibrators V1 and V2 per input air pressure are displayed above. Data were collected per the prescribed stepping protocol. In both cases slopes were higher when the vibrators were located over the biceps than on the forearms. The target frequency output was in the 70 Hz range (yellow highlighted area). This corresponded to locating V1 on the biceps and V2 on the supinator with an input air pressure of 50 psi.

References

- [1] R. W. Briggs, I. Dy-Liacco, M. P. Malcolm, *et al.*, A pneumatic vibrotactile stimulation device for fMRI. *Magn Reson Med*, 51: 640-3, 2004.
- [2] S. M. Golaszewski, F. Zschiegner, C. M. Siedentopf, *et al.*, A new pneumatic vibrator for functional magnetic resonance imaging of the human sensorimotor cortex. *Neurosci Lett*, 324: 125-8, 2002.
- [3] S. J. Graham, W. R. Staines, A. Nelson, *et al.*, New devices to deliver somatosensory stimuli during functional MRI. *Magn Reson Med*, 46: 436-42, 2001.
- [4] G. S. Harrington, C. T. Wright, J. H. Downs., A new vibrotactile stimulator for functional MRI. *Hum Brain Mapp*, 10: 140-5, 2000.
- [5] S. M. Golaszewski, C. M. Siedentopf, E. Baldauf, *et al.*, Functional magnetic resonance imaging of the human sensorimotor cortex using a novel vibrotactile stimulator *Neuroimage*, 17: 421-30, 2002.
- [6] M. Montant, P. Romaguère, J. P. Roll., A new vibrator to stimulate muscle proprioceptors in fMRI. *Hum Brain Mapp*, 30: 990-7, 2009.
- [7] M. Arashanapalli, S. E. Wilson., Paraspinal muscle vibration alters dynamic motion of the trunk. *J Biomech Eng*, 130:021001, 2008.
- [8] T. Kito, T. Hashimoto, T. Yoneda, *et al.*, Sensory processing during kinesthetic aftereffect following illusory hand movement elicited by tendon vibration. *Brain Res*, 1114: 75-84, 2006.
- [9] E. Naito, H. H. Ehrsson., Somatic sensation of hand-object interactive movement is associated with activity in the left inferior parietal cortex. *J Neurosci*, 26: 3783-90, 2006.
- [10] J. S. Soltys, S. E. Wilson., Directional sensitivity of velocity sense in the lumbar spine. *J Appl Biomech*, 24: 244-51, 2008.
- [11] S. M. Verschueren, S. P. Swinnen, P. J. Cordo, N. V. Dounskaia., Proprioceptive control of multijoint movement: unimanual circle drawing. *Exp Brain Res*, 127: 171-81, 1999.
- [12] Pocket guide air motors *Pocket Guide Air Motors*, 2003.
- [13] *Air Motors Handbook* (Gast Manufacturing Corporation, Benton Harbor, MI, 1986).
- [14] M. J. Pinches, *Power Pneumatics*, 1997.
- [15] J. P. Roll, J. P. Vedel., Kinesthetic role of muscle afferents in man, studied by tendon vibration and microneurography *Experimental Brain Research*, 47: 177-90, 1982.

Chapter 5 - Central Integration of Proprioceptive Information

Abstract

There exists a large body of research investigating the link between gross motor performance and vibration modulated spindle afferents. Of these investigations, the majority focuses on motor task performance during vibration, even though it has been demonstrated that altered performance may last for several minutes post vibration. Therefore individuals exposed to an occupational vibration may be at a higher risk of sustaining injury well past exposure.

By examining performance most investigations allow us to gage the total motor control loop. This approach, though useful, does not let us directly gage what is taking place during the intermediate steps in which spindle afferents are first perceived by the CNS, integrated, and used to generate a motor command. The widespread availability of neuro-imaging techniques, such as fMRI, has opened the opportunity to investigate these intermediate steps in the motor loop. More studies are utilizing these new modalities to investigate those intermediate steps. As of the time of this writing there exists relatively few studies that have attempted to measure the CNS response during a motor task and during vibration and none that have investigated post vibration effects.

For this study 10 healthy young subjects consented and performed a constant-velocity joystick-cursor pursuit task. All subjects in this study were self-identified as right-handed. Subjects were placed supine in a 3-Tesla fMRI scanner, and a projector-mirror system allowed them to view the computer screen in the bore. An fMRI compatible joystick was used for the pursuit task and moved by their dominant hand. The task was presented in a block paradigm with directions to match the movement of a red target cursor with a green, joystick controlled cursor, both with and without visual feedback. Collection time points included: before, during, immediately post, and 15-minutes-post a total continuous vibration duration of 15-minutes.

Significant changes observed in the average velocity of the pursuit task. During vibration, subjects tracked the cursor at a slower velocity than was employed at baseline. Immediately post vibration a faster than baseline movement was observed. We examined %BOLD cortical activity occurring during the observed velocity changes for locations that likely contributed to the speed modifications. As expected, changes in activity were observed in supporting motor and sensory areas, but also in locations normally associated with cognitive, visual, and auditory locations with an observed lateralization contralateral the tested arm. These findings suggest that the current understanding of proprioception and kinesthesia does need to take into account both the cognitive and motor aspects of the experimental task.

Introduction

The proprioceptive system creates an internalized map locating limbs and joints in relation to one another in both space and time. This internalized body map is the result of the brain processing the combined information from several different sensory elements (such as muscle spindle organs, cutaneous sensors, and golgi tendon organs) throughout the body [1, 2]. The central nervous system collects this information and then interprets it to create a perception of the limb's position and movement relative to the rest of the body [3]. The CNS to generate an appropriate response strategy can then use this feedback [4]. In biomechanics research, the body's sense of self-location and movement is termed proprioception [1]. In a simple example, the proprioceptive system allows one to successfully perform tasks like touching one's own nose with one's eyes closed.

The muscle spindle organ (MSO) provides feedback based on the changes in elongation of extrafusal muscle fibers. These elongations may be driven by the motor system itself (gamma motor loop) or externally (passive movement). These factors may include occupational conditions such as vibration, which has been documented by numerous studies to modulate both the static and dynamic signaling of the muscle spindle organs [5-7]. This altered proprioceptive feedback has also been implicated to result in increased errors during both position and velocity based performance tasks [8-10]. The MSO is particularly sensitive to applied vibrations in the range of 20-120 Hz, with a "sweet spot" for inducing a kinesthetic illusion between 60 and 80 Hz, which coincide with the greatest changes in performance error, and perception of kinesthetic illusions [11-13].

There is ample evidence that these performance errors persist beyond the period of vibration exposure. These persistent errors may be attributed to changes in the afferent signal, increased delays in muscle response, and changes in muscle excitability [9, 13, 14]. The experimental results of many groups have indicated induced errors have persisted for anywhere from a few minutes to a half-hour post vibration [8, 15-18].

This is somewhat complicated by observations via direct microneurographic recordings indicating that the spindle afferents recover relatively quickly, on the order of seconds, once removed from the influence of applied vibrations [7, 14]. Similarly, effects on motor excitability were also only observed as temporary [19, 20]. Taken together these findings would seem to suggest that the persistent errors may be a centrally developed phenomenon and not readily explained by studies investigating the end motor task performance [21]. A growing number of studies have taken advantage of recent advancements in medical imaging to investigate the perception of movement elicited by vibration during static tasks [12, 22-25].

Sensorimotor Centers of the CNS

Though it is not clearly understood why a persistent change in task performance after vibration exposure exists, an increasing number of studies are investigating how vibration alters cortical excitation and intracortical communications [19, 26]. The total system response to proprioceptive feedback, as observed through recordings of intracortical excitability were dependent not only on applied vibration itself but whether or not the perceived task was velocity or position based [27, 28]. Any study attempting to answer such questions, must then take into account the focal parameters of the task chosen as well as the motor implications.

We already understand that vibration alters muscle spindle afferents and several researchers have worked to create vibration devices compliant with the fMRI environment [5, 29, 30]. Testing of such devices has demonstrated cortical activations in both hemispheres of motor and sensory regions including: Primary Motor (M1), Primary Sensory (S1), Secondary Sensory (S2), Supplemental Motor Areas (SMA), Frontal Gyrus (GF), Temporal Gyrus (GS), and subcortical regions such as the Thalamus, Cerebellum, and Insula [30-32]. Repeatedly, imaging studies with subjects having reported kinesthetic illusions corrected for vibration have implied the perception of movement may actually be derived in motor areas rather than sensory areas, observing activity in SMA, Cingulate Motor Area (CMA), the Dorsal Premotor Cortex (PMd), and M1 [12, 22, 23, 33-36]. Christensen et al., recently reported that repeated transcranial

magnetic stimulation (TMS) of the PMd resulted in cortical activity culminating in a perceived movement where one did not exist [37]. Similarly, repeated exposures to vibration have led to persistent changes not only in the relative excitability of flexor and extensor muscle pairs but also the extent of motor cortex activated by TMS [38, 39].

While the previously mentioned studies provide suggestions for where proprioceptive feedback may be integrated, the reported results are primarily from inactive or finger tapping type tasks. Very few studies have attempted to look at proprioceptive centers during an active task. Turner et al., utilized a computer joystick based pursuit task to demonstrate activity in many of the same areas reported previously, but that M1, S1, SMA, Putamen, Cerebellum, and Basal Ganglia were most likely responsible for controlling task parameters such as movement extent and velocity [40, 41]. There are no known studies at this time looking at cortical activity during an active pursuit-type task using a vibration based MSO disruption paradigm neither during or post exposure.

Objectives and Hypotheses

The objective of this study was to determine where the CNS interprets peripherally derived and centrally driven proprioceptive information. More specifically we aimed to identify regions of the central nervous system that process and integrate velocity-based proprioceptive information during an active motor task. This was primarily an attempt to answer the question, "What cortical regions are active during a normal pursuit task and what changes in activity are observed during and post vibratory stimulus?" A secondary objective was to determine if an association in task performance and change in activity of sensory and/or perceptual area(s) of the brain exists.

We hypothesized that changes from baseline performance of a constant velocity pursuit task would be observed both during and immediately post vibration. Additionally, we hypothesized the changes in

motor performance would correspond with decreases in activations of known sensorimotor processing cortex locations, including M1, S1, and CMA.

Making the link between brain activity and motor performance would allow us to determine whether or not central habituation or another phenomenon may be responsible for performance-based errors associated with prolonged vibration exposure. This link would in turn allow for the development of appropriate guidelines or interventions to limit potential injuries and also aid in rehabilitation for pathologies related to compromised motor control.

Methods

Ten young and healthy subjects (5F, 5M, Aged 25.8 years +/- 4.1), all self-reported as right-handed were recruited for participation in this study. Each subject was required to provide written consent before participation as approved by the University of Kansas Human Subjects Committee and the University of Kansas Medical Center institutional review board (IRB). Additionally, each subject was required to pass a pre-screening to ensure his or her safety in the MRI environment. This screening disqualified subjects at risk of injury by being placed in a strong magnetic environment. Such disqualifying factors included but were not limited to: metal working as a profession, non-MRI compatible medical implants, and claustrophobia. A general health screening was also given to control for complicating conditions. Subjects were included in this study if after screening they reported no musculoskeletal conditions including but not limited to: tendonitis of the elbow, low back pain, etc. in the past 2 months or hand-arm-vibration syndrome (HAVS) acquired by prolonged exposure to vibration. These individuals were then randomly assigned into one of two groups that determined the order they experienced the test conditions.

The assessment trials were conducted in the 3-Tesla fMRI (Siemens; Integra) located at the Hoglund Brain Imaging Center at the University of Kansas Medical Center. Subjects were asked to arrive at least 30 minutes prior to their scheduled scanning time. Subjects lay supine on the scanner table with legs

slightly bent and supported. Custom pneumatically driven vibrators were fit over supinating muscles of the wrist (biceps and supinator). An fMRI compatible joystick (Model HHSC-JOY-1, Current Designs, Philadelphia, PA) was positioned and secured on the subjects' thigh in a manner to allow for clearance with the scanner bore and also allow ample movement to complete the task with minimal difficulty. The maximum angular range of the joystick was a total of 30 degrees (15 degrees each direction from center). The elbow was bent and supported throughout the entire experiment. A projector-and-mirror system was used to project the cursor information for the task from the computer screen to the subject in the MRI bore. The subject was then moved into the scanner.

Initial scans were performed to calibrate the MRI and identify the total brain volume and structure of each subject. Upon completion of the structural scans the functional scans were performed while the subjects were presented with the targeting-task and the stimulus conditions. The functional scans were performed with an echo time of 30 ms, a repetition time of 2000 ms, and a slice thickness of 4 mm (4.52 mm spacing).

A baseline level of performance was collected at each level of the pursuit task. The pursuit task levels were: A.) Feedback: Watching a target move along a straight-line path at a constant-velocity while simultaneously trying to match the target motion with a visible joystick controlled cursor, B.) No-Feedback: Watching a target move along a straight-line path at a constant-velocity while simultaneously trying to match the target motion with an invisible joystick controlled cursor, and C.) Rest: Watching a target move along a straight-line path at a constant-velocity. The tasks were presented in an ABC block diagram fashion [Figure 19]. Each individual block was 20 seconds in duration and the sequence was repeated three times for each condition. Both the target and joystick cursor positions were recorded using a LabVIEW virtual instrument running at 40 Hz. The baseline performance was the averaged performance of three pre-vibration collection trials.

After the baseline measurements, subjects in group 1 were presented with an approximately 70 Hz vibration applied to the supinating musculature of the forearm for 15 minutes duration. Data collection trials were conducted at the 5 and 10-minute marks of cumulative vibration exposure. Immediately following the end of the full 15-minute vibration exposure a third period of data collection was conducted. A final collection was conducted at the conclusion of a washout period 15 minutes post-vibration. Those in group 2 saw the washout and vibration orders changed [Figure 20].

For this experiment, the tolerance was set as a target circle of radius 10% joystick max (+/- 3 degrees). The peak-to-peak movement amplitude was defined as the joystick movement between changes in direction. For the data collection the maximum peak-to-peak movement of the target cursor was 60% of max for a total peak-to-peak movement of 18 degrees. The peak-to-peak movement was calculated as the distance between the maximum leftward and rightward movements for consecutive changes in direction of the Joystick-controlled cursor. The peak-to-peak target speed was set at 5 seconds per cycle resulting in a target velocity of 7.2 degrees per second.

The following statistics were calculated for each trial of each subject. Time-on-target was defined as the portion of the task blocks that the subject kept the joystick-controlled cursor within the tolerance of the target cursor. The peak-to-peak movement amplitude was defined as the total joystick movement between changes in direction of the subject cursor (joystick movement between consecutive max and min pairs). The average velocity was defined using multiple methods. First, the slope of the line between consecutive max/min pairs (corresponding to changes in direction) was calculated using a first order pVEL command in Matlab. These pVEL velocity values were then averaged for each pronation and supination movement to provide an average pVEL velocity (pVEL) for each block. The other velocity calculation was the average instantaneous velocity (iVEL), as calculated by the difference in joystick movement between consecutive samples, averaged per block. The average of these difference values were calculated for each

task block. The number of samples between consecutive max/min pairs (DT) was calculated to account for any shift in time that may occur.

A Huyhn-Feldt, repeated measures ANOVA was performed in SPSS to test for significant differences in the dependent variables with $\alpha = 0.05$. If a main effect was observed for a particular variable a simple contrast was computed as a post hoc analysis to determine significance between levels.

The fMRI files were analyzed using Brainvoyager (v2.2). Each functional trial was preprocessed with a slice scan correction, 3D motion correction, temporal filtering, and a spatial smoothing. The functional trials were then mapped to their respective subject through a coregistration process and transformed into standard talairach space for between subject comparisons. A general linear model, multi-subject, random-effects (RFX) analysis was used to examine the functional data. To test for significant changes in %BOLD activation an uncorrected p-value of 0.001 and a minimum cluster size of 3 was used as an initial screen. Post hoc regions were tested with an uncorrected p-value of 0.0001 and a minimum cluster size of 6 adjacent voxels.

Results

Joystick Kinematics

A similar pattern of joystick kinematics was observed in this study as in chapter three [Figure 21, Figure 22, & Figure 23]. Subject velocities decreased significantly while vibration was being applied and later increased immediately after the vibration was turned off before returning to baseline values. As we had observed previously, the magnitudes of the velocity deviations from baseline (DV and PV) were approximately the same (0.5 deg/sec) but in opposite directions and of a smaller magnitude than observed previously (approximately 1.2 deg/sec). One observed deviation from the previous results was that in both the iVEL and Pk-Pk measures, subjects undershot the target movement extents and speeds while the pVEL measure was a closer approximation of the target velocity.

pVEL

A main effect due to condition was observed in the pVEL measure ($p = 0.001$) as was a significant interaction of condition*feedback ($p=0.004$) [Table 6]. During vibration there was a significant decrease ($p=0.000$) of about 0.6 degrees/second when compared to baseline. Immediately post vibration there was a nearly identical increase ($p=0.016$) over the baseline velocity. No significant difference was observed post washout when compared to baseline ($p>0.05$). After a Bonferonni correction the during vibration condition remained significantly different from both the baseline ($p=0.000$) and post vibration ($p=0.006$) conditions.

A significant interaction was observed ($p = 0.000$) when comparing during vibration versus baseline and task level A versus B indicating a larger change in velocity with the removal of feedback during vibration than during baseline (Vibration more greatly affected the proprioceptive condition). During the fMRI joystick task, subjects in general were moving ahead of the target as indicated by the higher than target velocities, whereas in the previous study they generally were trailing the target.

iVEL

The instantaneous velocity data (iVEL) displayed main effects due to stimulus condition ($p = 0.000$) and feedback ($p=0.005$) [Table 7]. The iVEL was significantly slower during vibration ($p=0.003$) and faster iVEL post vibration ($p=0.001$) when compared to baseline. These differences mirrored those observed in the pVEL average. A pairwise comparison with an applied Bonferonni correction upheld these respective differences ($p=0.020$; $p = 0.005$). During vibration iVEL was also significantly slower than the post vibration ($p=0.000$) value. Additionally the post washout values were significantly different from during vibration ($p=0.045$) and the post vibration iVEL ($p=0.014$) values.

A significant interaction was also observed between the stimulus condition and feedback conditions ($p=0.006$). This interaction again demonstrated a greater slowing of the iVEL during the proprioceptive

challenging no feedback condition both when vibration was being applied (DV) and immediately after (PV).

Peak to Peak

While the average of all subjects consistently undershot the targeted movement extents, a significant main effect due to condition was observed in the peak-to-peak movement data ($p=0.012$) and feedback ($p=0.005$) when compared to baseline [Table 8]. A post hoc analysis of the peak-to-peak measure left only the observed difference between during vibration and baseline ($p=0.002$) as significant.

A significant interaction between feedback and condition was also observed ($p=0.049$) again demonstrating a much smaller extent of movement during vibration without visual feedback. When a Bonferonni correction was applied to the pairwise comparisons the observed difference between during vibration and baseline ($p = 0.011$) and during vibration and post vibration ($p = 0.036$) remained significant.

Brain Activations

BOLD imaging contrasts were setup in Brainvoyager reflecting the ANOVA comparisons of the joystick data. Contrasts were set to specifically examine the effects vibratory stimulus had from the pre-stimulus state (BL). Specifically we tested for differences that could be attributed to the during vibration (DV) state and differences in activations that could be attributed to the immediately post vibration (PV) state. An additional comparison was made contrasting the during and post vibration states to determine if differences existed.

The following procedure was used to label the contrasts. Two symbolic “predictors” indicating the visual feedback condition followed the stimulus condition abbreviation. The first indicator always represented the predictor case of visual feedback and the second predictor always represented the case of no visual

feedback. A plus (+) symbol was used to indicate relatively greater than control activations while a minus (-) symbol indicated lesser activations when compared to the control condition (Task C - Rest). The main effects were reflected in contrasts where the symbolic indicators were both positive for the first stimulus condition and both negative for the second stimulus condition. For example in the case of the contrast BL++ vs DV- -, positive "t" values would represent cluster locations where the activity during the pre-vibration condition was more influential, and negative "t" values would indicate locations where the activity during vibration predictor activations were more influential. Interactions between vibration condition and feedback were then be carried out by altering the predictor values to oppose each other on the appropriate vibration conditions (BL+- vs DV-+) and supplemented with an additional plot to indicate the direction of the response change.

Multiple activations were found in each contrast and region and are noted in entirety (including peak X, Y, and Z talairach coordinates) in Appendix F. Summarized tables are included here highlighting the main effects can be found in Tables 5.1-5.3. Each table reports the number of voxels indicated in each active cluster located by cerebral hemisphere, lobe, and gyrus. The assigned Brodmann area of the active cluster separates the data by columns. The total voxels by division are located in the last column of the tables. The T-statistic is reported for each activation after the gyrus. For interactions the table reports the unique cluster location with the gyrus location so that it may be used to reference the appropriate interaction on subsequent table.

Main Effects

BL++ vs DV--

During the contrast of Baseline (Pre-Vibration) versus During Vibration (Table 9 & Table 10), significant activations were observed in premotor (PMA), supplemental motor (SMA), somatosensory association (SSA), and prefrontal cortex (PreF) with additional activations of the insula. Total voxels active prior to

vibration exposure were distributed between the two hemispheres with a majority on the right (ipsilateral) side. During the vibration period the extent of voxels active decreased in both hemispheres with the majority of active voxels now on the left (contralateral side). Increased activity was observed contralateral in both PMA and PreF locations whereas PMA was previously observed to be bilateral. The anterior cingulate was also found to contribute more to the observed activation while vibration was present, but again only on the contralateral side. Previously limbic activity was found on the cingulate gyrus on both sides of the brain. In summary, activations appeared to shift from predominately ipsilateral to contralateral during the application of vibration.

BL++ vs PV--

When the Baseline (Pre-Vibration) versus Post Vibration (PV) contrast was conducted there were relatively few activations observed in both quantity and total voxels active. In both conditions of the contrast the great majority of active voxels were located on the ipsilateral hemisphere. During baseline the contrast yielded significant activity in PMA and PreF regions located on the middle frontal gyrus (Table 11 & Table 12). There was an additional contralateral activation in a multimodal association area (MMA) on the fusiform gyrus of the temporal lobe at the pre-vibration condition. Immediately after the removal of vibration, total active voxels increased on the right side due primarily to spatially large activation in the parahippocampal gyrus. A similarly large activation in a secondary somatosensory area (S2) on the inferior parietal lobule was also observed post vibration. Other sensory regions (SMA and SSA) were more active as well, though were contralateral the active arm. In general, while there was little deviation from control for the baseline condition, immediately after the removal of the vibration stimulus there did appear to be a change in several somatosensory locations.

DV++ vs PV--

In order to determine changes occurring between during and immediately post vibration conditions a contrast of DV and PV was included [Table 13 & Table 14]. Similarly to what was observed in the BL vs DV contrast, while vibration was present the great majority of total voxels active were located contralateral the controlled hand. Inferior and superior frontal gyrus displayed greater contribution to signal change DV. This was a somewhat surprising finding as the right inferior frontal gyrus has been implicated in motor inhibition, but not the left (as was observed here). Also, as had been previously observed during vibration, the anterior cingulate was again observed to be contribute more to the signal change during vibration with the cingulate gyrus more active PV. PMA activity at this time was limited to the superior frontal gyrus of the right side. When the examination turned to those areas more active PV, changes were observed on the left side in M1, S1, and SSA. The observations here primarily seem to support the shifts in lateralization observed earlier, while also suggesting that the largest changes in primary motor and secondary motor occur at the transition from vibration to no vibration.

Interactions

Tables 15-20 illustrate the interactions for visual feedback and vibration condition. In particular we have investigated the BL versus DV, BL vs PV, and DV vs PV interactions to determine whether the observed changes may have been more likely attributed to the applied vibration or the availability of visual information. Please note that the tables themselves cannot describe the actual change taking place at a particular location (unlike the statistics in the main effects) but rather allow us to identify those regions of greatest interest. It is therefore necessary to supplement the data in these particular tables with plots of the actual %BOLD change signal to understand how the interaction is being manifested.

Of these interactions, much information was gleaned from the contrast of BL-+ versus DV+-. As expected significant activations were found in premotor (areas 6&8), somatosensory areas (7&40), and the prefrontal cortex (9&10). Somatosensory locations were active contralateral to the task hand while prefrontal areas were active ipsilateral. Premotor activations were found in each hemisphere. Area 44 was

interesting due to its location on the precentral gyrus (typically M1) and supporting evidence that it is active inhibiting motor activity. In each of the non-somatosensory locations, the application of vibration appears to have decreased the overall change in cortical activations due to feedback. In many cases this was observed as a decrease in the total overall change from the control. The sensory locations changed little in terms of magnitude but were actually observed to reverse (increasing when they had previously decreased due to visual feedback).

When examining the pre-vibratory and post-vibratory contrasts significant activations were primarily found in prefrontal (10), auditory (22&23), and the cingulate gyrus (33). The premotor response was decreased and reversed with a decreasing between feedback levels PV. A similar response was observed in the cingulate gyrus. Visual areas showed response consistent with changes primarily due to the change in feedback as opposed to vibration. Area 22 showed a large increase PV that disappeared when feedback was removed. Area 23 actually showed a decrease due to the vibration condition that became greater when visual feedback was removed. Overall activations found in this contrast seem unrelated to events pertaining to performance of the task itself.

The final interaction contrasting the pre and post vibration conditions was equally confounding. A large extent of activity was detected in the insula on the right side that was essentially a reversal of activation pattern (becoming much less active). Prefrontal activity was also observed that also become much more active reversing its pattern of activation across conditions. A bilateral activation in a multimodal association area repeated this reversal pattern ipsilateral to the task hand but displayed a dampened increase in activity due to feedback after the vibration was removed. The visual locations and Broca's areas showed changes in activity more consistent with changes in feedback presentation than due to vibration.

Discussion

The results of the current study can be described in two distinct parts: the joystick kinematics and the cortical activations. While the results of the joystick data correlated well with the findings previously stated in Chapter 3, the interpretation of the cortical activations is somewhat more ambiguous. Regardless, there were some interesting conclusions that could be drawn from the data that may lead to meaningful changes in our understanding of proprioceptive control and how it is, and possibly should be, investigated.

Joystick Data

The joystick kinematics corresponded well with the findings described in chapter 3 despite the additional restrictions placed on the protocol by the physical limitations of the fMRI environment. The joystick velocity pattern was similar to that observed in the previous study with a slowing velocity observed during active vibration and an opposite and approximately equal increase in velocity observed immediately post vibration. This suggests the efficacy of the custom pneumatic vibrator in the ability to sufficiently modulate spindle afferents during the current protocol to succeed in challenging the proprioceptive system.

While the velocity changes between vibration conditions were similar to our previous study, the magnitudes of the changes in the current study were smaller. In particular the magnitude of the velocity changes was approximately 0.5 deg/sec as opposed to almost a full 1.0 deg/sec in the previous experiment. This could be attributed to additional sensory feedback from cutaneous sensors or slight movement of the joystick relative to its base. Whereas, we were previously able to tightly control both the elbow and joystick using a custom support frame, this was not possible in the fMRI. In order to fit both the subject and joystick in the bore to obtain an image it was necessary to support the joystick on the subjects' hips. Another possible source of error could be attributed, in part at least, to the differences between the joystick designs used in the two studies. The fMRI compatible joystick had both a smaller total range of motion (resulting in a slower target velocity) and a straight foam control stick (as opposed to a molded stick with hand support). We were also unable to control the orientation angle of the forearm and joystick

(as we had previously), which may have allowed some of the pronation/supination to be accomplished via wrist flexion. Many of these limitations could be addressed in future studies by utilizing a "paddle-wheel" designed computer controller, modified for the MRI environment, similar to the original Atari controller for the game "Pong". This would have both the small footprint to fit in the bore with the subject, and be easier to align with the subjects arm anatomy to control for additional movement.

While these additional considerations do not change our understanding of the joystick kinematics they may create some confounds when interpreting the cortical activations. Especially when considering that the joystick effects observed were not as well defined as in the previous experiment.

Cortical Activations

Our results demonstrated that a constant velocity pursuit-type task displays similarities, in terms of cortical activations, as common motor tasks and cognitive classical Stroop tasks [42]. During our pursuit task we observed changes in cortical activations bilaterally in both primary and secondary motor, sensory, and association areas. The findings would seem to implicate that proprioception involves a circuit that is much more complex than originally thought.

While the current BOLD image contrasts do not allow us to definitively state that inhibition was occurring in a particular motor or sensory locations (this would require a more intensive ROI analysis) there are some interesting observations that supported our hypothesis. Examining the contrasts displaying changes in cortical activation between the vibration and post vibration condition [Table 13 & Table 14] we found some supporting evidence. The first piece, when filtering to look at those locations more active PV, was the noted increase in activity of the precentral gyrus (M1), postcentral gyrus (S1) and superior parietal lobule (SSA) all of which are located ipsilateral (left brain) the tested hand/arm. A second, supporting piece of evidence, found in the contrast of pre-vibration and post vibration [Table 11 & Table 12] are the increased activations in the paracentral lobule (SMA), superior parietal lobule (SSA) both on

the left, and inferior parietal lobule (S2) on the right. Taken together these suggest that motor, and in particular, sensory locations contributed much more to the observed BOLD signal change immediately after the vibratory stimulus was removed as opposed to either the baseline or pre-vibration conditions, where such activations were not observed.

In order to strength then case that inhibition was occurring due to vibration we investigated the changes occurring during the interaction contrasts. In particular, we focused on the baseline versus during vibration contrasts and observed significant activations in the inferior parietal lobule (S2), superior parietal lobule (SSA), and the precentral gyrus (M1). The interactions for the corresponding clusters 39, 42, 34, and 4 respectively [Table 16] were generally observed to decrease in total % BOLD change between the baseline condition while vibration was being applied. Taken together with the previous findings of increased activity, this would seem to suggest inhibition of at least some motor and sensory locations consistent with the task. This decreased motor function could therefore have been responsible for the observed decrease in joystick pursuit velocity.

There is additional support for the increased brain activity observed in the post vibration contrasts being responsible for the increased joystick velocity. The interactions noting post vibratory activations do not include any of the previously mentioned regions, while this would seem to suggest an increase in activity when switching from the during vibration condition to the post vibration condition, these increases were not significantly higher than the simple observation control task (Task C). So while it is tempting to make such a claim that increased activity led to the increased velocity observed, the data in this case were inconclusive at best. However, in our original hypothesis we had stated that the observed changes during vibration would persist post vibration, which due to the observed changes between during and post vibration contrasts, is clearly not the case.

Another interesting observation included the observed changes in the limbic lobe, and in particular the cingulate gyrus. Activity was observed to consistently shift to the left side anterior cingulate gyrus while vibration was actively applied from the more posterior cingulate gyrus, with bilateral activations in both the baseline and post vibration conditions. When considering the cortical projections of these locations we noted evidence of corresponding changes in activity. When the cingulate gyrus is active (BL and PV conditions) there were observed increases both in the prefrontal cortex (Brodmann 9, 10, & 11) and parietal lobule consistent with the commonly defined projections. Locations that received input from the anterior cingulate gyrus were consistently more active during the vibration condition along with activations in the premotor cortex (Brodmann 6 & 8).

The Cingulate activity observed here was consistent with that often observed in motor inhibition studies implementing a Go/No-Go and Stop protocols [42, 43]. Bernal et al, recently described separate loops for both cortical and motor inhibition that included four common areas including: the inferior frontal gyrus, inferior parietal lobe, posterior temporal area, and the anterior cingulate gyrus [42]. These separate loops were described by the observed lateralized activation patterns of the previously noted locations, indicating motor inhibition consistent with right hemisphere activations and cognitive inhibition consistent with left activations. While we did observe activation locations consistent with this theory (inferior frontal gyrus and anterior cingulate gyrus during vibration), our activations were primarily in the left hemisphere leading us to infer subjects in the current study were utilizing a cognitive inhibition loop.

While this may seem to be incongruent with the current task, unquestionably having an obvious motor component, this can be rectified by revisiting our understanding of proprioception and postulating a more explicit understanding of proprioceptive control. The definitions of kinesthesia (movement) and proprioception (perception of movement) are often used interchangeably, but the current findings suggest this should not necessarily be the case as proprioception includes both a motor and cognitive component.

In looking at the current study, the pursuit task used was similar to that implemented in previous imaging studies [40, 41]. In those studies subjects were always provided visual feedback of performance (Task A current study). The result of this was a predominantly motor task in which the visual information was likely to be the dominant feedback to help learn the task. This was manifested ultimately, as the subjects being able to retain their baseline pursuit velocity, regardless of the vibration condition if visual feedback was available. So any error due to the modulated spindle afferent could be overcome. This was accomplished through a cortical circuit including the cingulate gyrus and the Dorso-Lateral Prefrontal Cortex (DLPFC).

In order to test the proprioceptive system the additional "No Feedback" condition (Task B) was incorporated. While previously subjects could rely on the visual information to override performance errors, that mechanism no longer existed without visual feedback. The result was a task that required subjects to remember their perceived velocity and use the remembered velocity to replicate their previous performance. While in the Go/No Go tasks, subjects understand and are aware that they are initiating a motor event, in the current study (Task B), subjects are unaware of errors in their performance and are theoretically continuing the pursuit task as if visual feedback were available. This is supported by subjects maintaining a similar performance during Task A regardless if feedback were available. Once vibration was applied however, average subject pursuit speeds slowed significantly from baseline (both in this study and in chapter 3) suggesting some form of inhibition. The performance in this particular case was then apparently under the influence of a different cortical circuit utilizing the anterior cingulate gyrus and premotor locations, while at the same time suppressing somatosensory locations. This could be a device through which different control strategies are chosen [44]. The increased speed post vibration becomes much more difficult to explain, though it is likely a combination of increased activity in somatosensory and motor locations and the return to the cingulate DLPFC loop of the baseline condition may contribute.

Additionally, we observed in many of our interactions activity in cortical regions distinctly known as auditory areas. Though it would seem completely unrelated to the task at hand, it is not without precedent that an auditory region would be active during applied vibration. Feldman and Latash had demonstrated in 1982 that vibration induced reflexes would reverse when subjects were presented with an unanticipated audible stimulus [45]. Exactly how this activation should play into the current observations of task performance and cortical activations is still unexplained. It is possible such a safety mechanism for early developing humans, who would have needed to respond quickly to surroundings when focus was primarily on a different task. It would thus make sense that auditory regions would play a part in inhibiting current motor activity so that attention could be diverted to a more appropriate response. This may be further supported by the proximity of the descending channels of auditory and motor response of the ventromedial motor pathways. This area has also been demonstrated to be active in other protocols utilizing vibration, but has thus far not been widely included in discussions as to why [29, 42, 46, 47].

Summary

The goal of this study was to utilize the imaging capabilities of functional MRI to expand on the current understanding of proprioceptive control. In particular we were interested in identifying cortical regions most likely responsible for both during and post vibration induced pursuit task velocity changes. While there was indeed evidence for suppressed activity during application of vibration in both motor and sensory locations, changes in the contrasts performed were predominately observed in the secondary sensory, premotor regions, and cognitive locations. While our observations agreed well with previously documented findings on CNS locations responsible for task inhibition, the regions observed currently were in the contralateral hemisphere as opposed to the right hemisphere, suggesting a controlling loop that was cognitive in origin.

This would seem to suggest that the proprioceptive loop actually exists between the brain hemispheres (generally thought to be divided to cognitive and motor locations). Control would then be established

based on the best available feedback source (visual, somatosensory, and auditory) and the focus of the task or possibly indicate differences in control strategy. Although the current extent of this investigation is not enough to state this with certainty, it is an interesting notion that could be investigated further by investigating deeper the current data set.

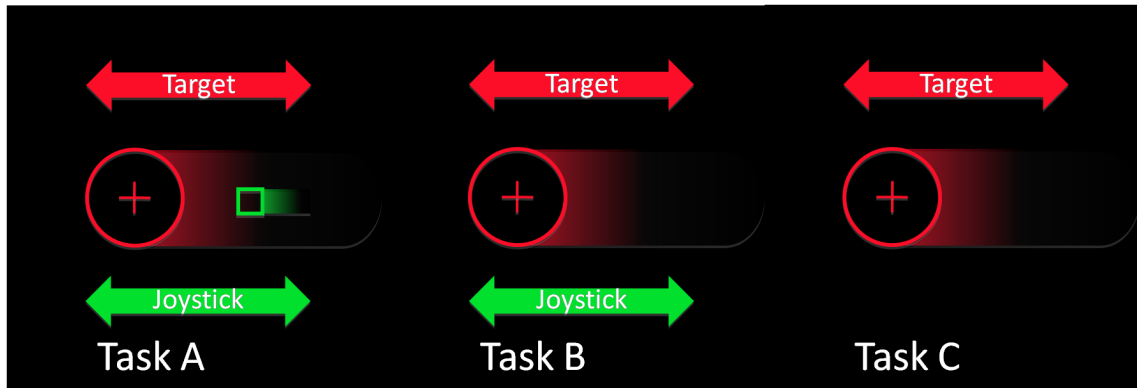


Figure 19: Pursuit Task Protocol - fMRI

The pursuit task was presented to the subjects in three separate instruction blocks always presented in the same order. During the first block (Task A) subjects manipulated a joystick attempting to keep a square green cursor within the defined radius of a constant velocity target cursor. During the second task block (Task B) subjects continued to use the joystick in attempting to keep the square green cursor within the constant velocity target radius, however the green joystick cursor was now no longer visible. During the final task block (Task C) subjects returned the joystick to the neutral starting position and simply watched the target radius. Task blocks were 20 seconds in duration and the entire protocol was repeated three times per data collection period. Target cursor and joystick cursor movements were limited to the medial-lateral direction only. Subjects were instructed to "Keep the joystick cursor within the target cursor by focusing on the movement velocity of the target cursor." The pursuit task protocol was written using LabVIEW (National Instruments) software and collected joystick cursor position at 40 Hz.

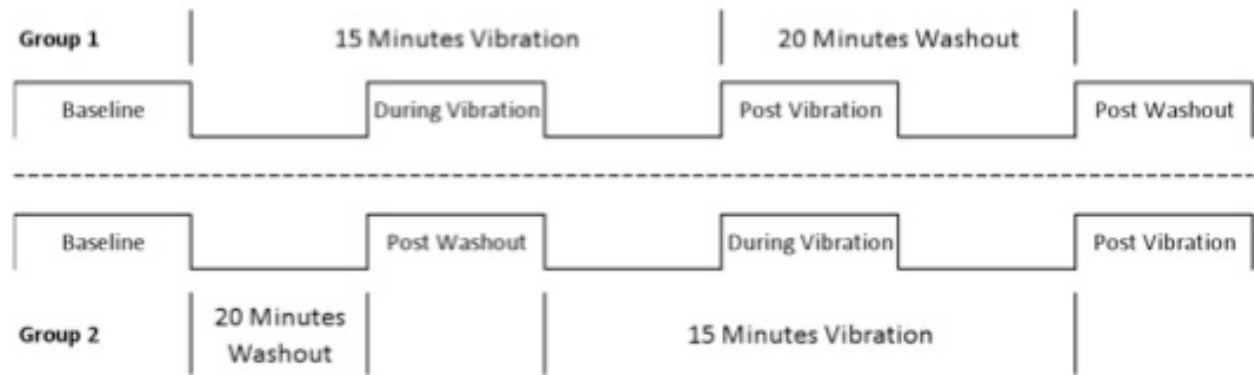


Figure 20: Experimental Timeline - fMRI

Subjects were randomly assigned to one of two groups determining the order of vibration exposure. An averaged pre-vibration performance level was calculated by averaging three separate runs of the collection protocol. Those in group 1 (top) were then continuously exposed to the vibration condition for 15 minutes. During this stimulus condition an averaged during vibration performance level was calculated by averaging two separate runs of the collection protocol. An immediately post vibration performance level was calculated by a single trial run starting at the end of the vibration period. A final post washout performance level was calculated by a single run of the collection protocol beginning exactly 20 minutes after the cessation of the applied vibration stimulus. Those subjects in group 2 were given the post-washout period evaluation 15 minutes after the baseline performance level was determined before continuing the timeline as before.

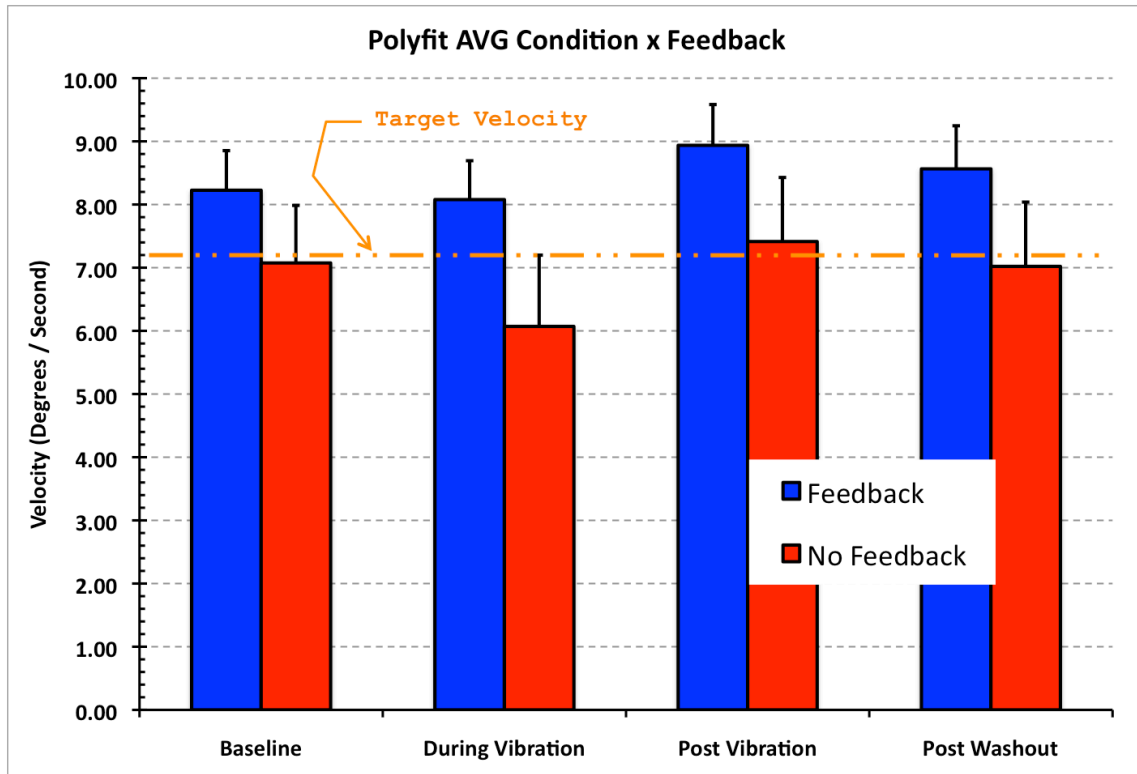


Figure 21: Results fMRI - Polyfit Velocity (pVEL)

The slopes of the linear curve fits in degrees per second across feedback and vibration conditions are represented here. The with feedback condition (Task A) is represented by the solid blue columns; the no feedback condition (Task B) is represented by the red hatched column. The orange dashed line depicts Target cursor velocity (7.2 deg/sec). Columns are represented with standard deviations. Subjects exhibited a statistically significant decrease in velocity during vibration with an equivalent magnitude increase in velocity immediately post vibration. An interaction was also observed indicating a greater influence of vibration during the no feedback condition (Task B).

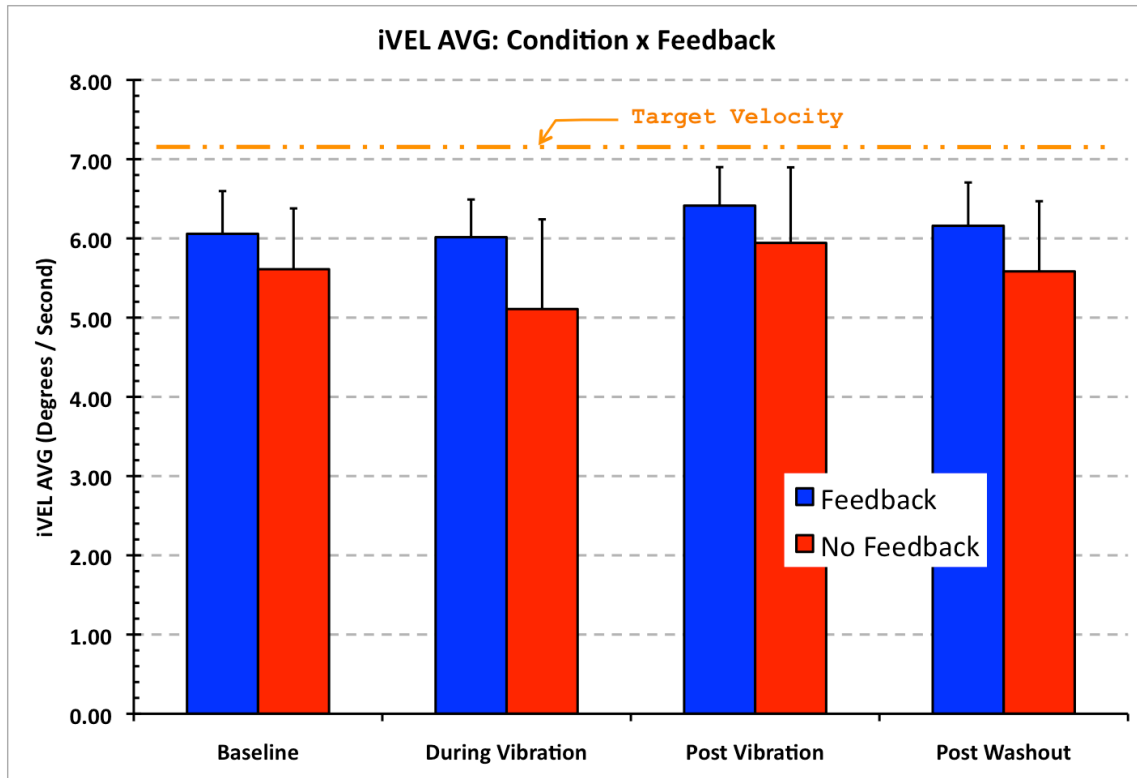


Figure 22: Results fMRI - Instantaneous Velocity (iVEL)

The average step-by-step velocities in degrees per second across feedback and vibration conditions are represented here. The with feedback condition (Task A) is represented by the solid blue columns, the no feedback condition (Task B) is represented by the red hatched column. Target cursor velocity (7.2 deg/sec) is represented by the orange dashed line. Columns are depicted with standard deviations. Subjects exhibited a statistically significant decrease in velocity during vibration with an equivalent magnitude increase in velocity immediately post vibration. An interaction was also observed indicating a greater influence of vibration during the no feedback condition (Task B).

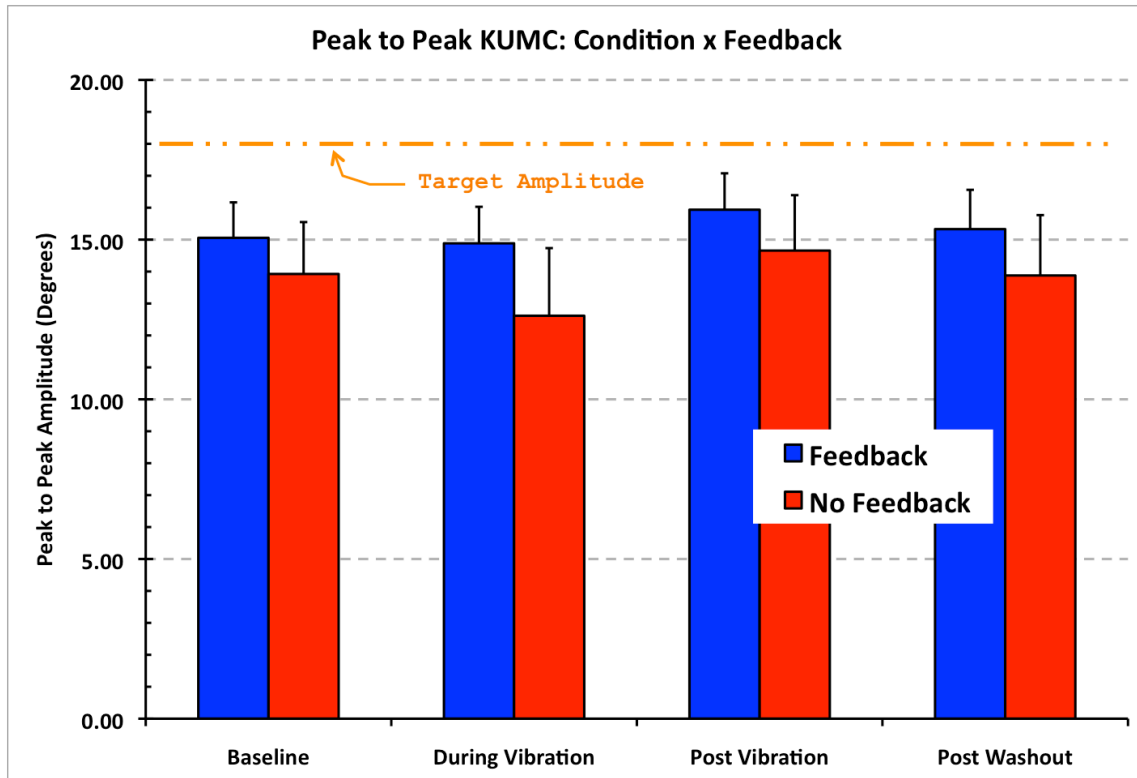


Figure 23: Results fMRI - Peak to Peak Movement (Pk Pk)

The average extent of subject joystick movement (in degrees) for both feedback and vibration conditions are represented here. The with feedback condition (Task A) is represented by the solid blue columns; the no feedback condition (Task B) is represented by the red hatched column. Target cursor movement extent (18 deg) is represented by the orange dashed line. Columns are represented with standard deviations. Subjects exhibited a statistically significant decrease in movement extent during vibration. An interaction was also observed indicating a greater influence of vibration during the no feedback condition (Task B).

Table 6: fMRI Pursuit pVEL ANOVA

Tests of Within-Subjects Effects
Measure:pVEL_AVG

Source	df	F	Sig.	Partial Eta Squared	Observed Power ^a
Condition	2.529	9.419	.001	.511	.982
Repeat	1.986	3.799	.042	.297	.612
Feedback	1.000	84.623	.000	.904	1.000
Condition * Repeat	6.000	2.219	.055	.198	.733
Condition * Feedback	2.832	5.983	.004	.399	.914
Repeat * Feedback	2.000	.771	.477	.079	.161
Condition * Repeat * Feedback	4.356	.408	.817	.043	.138

a. Computed using alpha = .05

Table 7: fMRI Pursuit iVEL ANOVA

Tests of Within-Subjects Effects
Measure:iVEL_AVG

Source	df	F	Sig.	Partial Eta Squared	Observed Power ^a
Condition	3.000	20.956	.000	.700	1.000
Repeat	1.542	2.529	.124	.219	.378
Feedback	1.000	13.858	.005	.606	.911
Condition * Repeat	6.000	1.981	.084	.180	.675
Condition * Feedback	3.000	5.229	.006	.367	.885
Repeat * Feedback	1.544	2.020	.175	.183	.311
Condition * Repeat * Feedback	5.102	.405	.846	.043	.146

a. Computed using alpha = .05

Table 8: fMRI Pursuit Pk-Pk ANOVA

Tests of Within-Subjects Effects
Measure:PK-PK

Source	df	F	Sig.	Partial Eta Squared	Observed Power ^a
Condition	1.657	6.545	.012	.421	.795
Repeat	1.252	1.334	.283	.129	.198
Feedback	1.000	13.220	.005	.595	.898
Condition * Repeat	5.132	1.042	.406	.104	.341
Condition * Feedback	2.232	3.411	.049	.275	.602
Repeat * Feedback	1.968	.757	.481	.078	.157
Condition * Repeat * Feedback	4.619	1.169	.340	.115	.358

a. Computed using alpha = .05

Table 9: Contrast BL ++ vs DV - -

BL++ vs DV--		BL											
Sum of # Voxels	Broadmann Number	6	7	8	9	13	18	22	24	31	40	47	Grand Total
Location													
Left Cerebrum		54	12			73			5	10			154
Frontal Lobe		54								10			64
Medial Frontal Gyrus		10											10
Paracentral Lobule		44								10			54
Limbic Lobe									5				5
Cingulate Gyrus									5				5
Parietal Lobe			12										12
Precuneus			12										12
Sub-lobar						73							73
Insula						73							73
Right Cerebrum		53	8	15	8	61	19	35	12		4	12	227
Frontal Lobe		53		15	8							12	88
Inferior Frontal Gyrus												12	12
Middle Frontal Gyrus		26		15	8								49
Superior Frontal Gyrus		27											27
Limbic Lobe									12				12
Cingulate Gyrus									12				12
Occipital Lobe							19						19
Lingual Gyrus							19						19
Parietal Lobe			8								4		12
Inferior Parietal Lobule											4		4
Precuneus			8										8
Sub-lobar						61							61
Insula						61							61
Temporal Lobe								35					35
Middle Temporal Gyrus								35					35
Grand Total		107	20	15	8	134	19	35	17	10	4	12	381

The table above lists locations within the cortex that were reported active in terms of %BOLD activation. The first column contains the naming information of the hemisphere, lobe, and gyrus of the activation. Locations identified in this table are more active during the BL condition. The first row (in shaded column) indicates Brodmann location assigned by the Talairach Daemon application. The cells within the table indicate the number of active voxels in each active location (cluster) with sums for gyrus, lobe, and hemisphere. Total active voxels are listed in the grand total column and row (reference only). The table above has been simplified to include only areas primarily understood to be motor (6&8), sensory (7&40), or cognitive (9,10,11) in nature.

Table 10: Contrast BL ++ vs DV --

BL++ vs DV--		DV									
Sum of # Voxels	Broadmann Number	8	10	11	17	19	21	24	32	Caudate Head	Grand Total
Location											
Left Cerebrum		3	4	3	4			16	5	14	49
Frontal Lobe		3	4	3							10
Medial Frontal Gyrus			4	3							7
Middle Frontal Gyrus		3									3
Limbic Lobe								16	5		21
Anterior Cingulate								16	5		21
Occipital Lobe				4							4
Inferior Occipital Gyrus				4							4
Sub-lobar										14	14
Caudate										14	14
Right Cerebrum						25	8			5	38
Limbic Lobe						25					25
Parahippocampal Gyrus						25					25
Sub-lobar										5	5
Caudate										5	5
Temporal Lobe							8				8
Middle Temporal Gyrus							8				8
Grand Total		3	4	3	4	25	8	16	5	19	87

The table above lists locations within the cortex that were reported active in terms of %BOLD activation. The first column contains the naming information of the hemisphere, lobe, and gyrus of the activation. Locations identified in this table are more active during the DV condition. The first row (in shaded column) indicates Brodmann location assigned by the Talairach Daemon application. The cells within the table indicate the number of active voxels in each active location (cluster) with sums for gyrus, lobe, and hemisphere. Total active voxels are listed in the grand total column and row (reference only). The table above has been simplified to include only areas primarily understood to be motor (6&8), sensory (7&40), or cognitive (9,10,11) in nature.

Table 11: Contrast BL ++ vs PV --

BL++ vs PV--		BL		
Sum of # Voxels	Broadmann Number			
Location	6	9	37	Grand Total
▼ Left Cerebrum			4	4
▼ Temporal Lobe			4	4
▶ Fusiform Gyrus			4	4
▼ Right Cerebrum	7	10		17
▼ Frontal Lobe	7	10		17
▶ Middle Frontal Gyrus	7	10		17
Grand Total	7	10	4	21

The table above lists locations within the cortex that were reported active in terms of %BOLD activation. The first column contains the naming information of the hemisphere, lobe, and gyrus of the activation. Locations identified in this table are more active during the BL condition. The first row (in shaded column) indicates Brodmann location assigned by the Talairach Daemon application. The cells within the table indicate the number of active voxels in each active location (cluster) with sums for gyrus, lobe, and hemisphere. Total active voxels are listed in the grand total column and row (reference only). The table above is the complete list for this particular contrast. Activations were primarily observed to be Premotor (6), sensory (7&40), cognitive (9), or associative (37) in nature. Ipsilateral activation was also observed in the visual and sub lobar areas (19).

Table 12: Contrast BL ++ vs PV --

BL++ vs PV--		PV				
Sum of # Voxels	Broadmann Number	6	7	19	40	Grand Total
Location						
▼ Left Cerebrum		4	3			7
▼ Frontal Lobe		4				4
▶ Paracentral Lobule		4				4
▼ Parietal Lobe			3			3
▶ Superior Parietal Lobule			3			3
▼ Right Cerebrum				40	17	57
▼ Limbic Lobe				37		37
▶ Parahippocampal Gyrus				37		37
▼ Occipital Lobe				3		3
▶ Middle Occipital Gyrus				3		3
▼ Parietal Lobe					17	17
▶ Inferior Parietal Lobule					17	17
Grand Total		4	3	40	17	64

The table above lists locations within the cortex that were reported active in terms of %BOLD activation. The first column contains the naming information of the hemisphere, lobe, and gyrus of the activation. Locations identified in this table are more active during the BL condition. The first row (in shaded column) indicates Brodmann location assigned by the Talairach Daemon application. The cells within the table indicate the number of active voxels in each active location (cluster) with sums for gyrus, lobe, and hemisphere. Total active voxels are listed in the grand total column and row (reference only).

Table 13: Contrast DV ++ vs PV --

DV

DV++ vs PV--

Sum of # Voxels	Broadmann Number	8	10	24	45	Grand Total
Left Cerebrum			8	7	28	43
Frontal Lobe			8		28	36
Inferior Frontal Gyrus					28	28
Superior Frontal Gyrus			8			8
Limbic Lobe				7		7
Anterior Cingulate				7		7
Right Cerebrum		5				5
Frontal Lobe		5				5
Superior Frontal Gyrus		5				5
Grand Total		5	8	7	28	48

The table above lists locations within the cortex that were reported active in terms of %BOLD activation. The first column contains the naming information of the hemisphere, lobe, and gyrus of the activation. Locations identified in this table are more active during the DV condition. The first row (in shaded column) indicates Brodmann location assigned by the Talairach Daemon application. The cells within the table indicate the number of active voxels in each active location (cluster) with sums for gyrus, lobe, and hemisphere. Total active voxels are listed in the grand total column and row (reference only). The table above is the complete list for this particular contrast. Activations observed were motor and premotor (4&8), sensory (3&7), and cognitive (10) in nature. Contralateral activation was also observed in sub lobar areas (24&31).

Table 14: Contrast DV ++ vs PV --

DV++ vs PV--		PV					
Sum of # Voxels	Broadmann Number	3	4	7	19	31	Grand Total
Location							
Left Cerebrum		4	12	12		5	33
Frontal Lobe			12				12
Precentral Gyrus			12				12
Limbic Lobe						5	5
Cingulate Gyrus						5	5
Parietal Lobe		4		12			16
Postcentral Gyrus		4					4
Superior Parietal Lobule				12			12
Right Cerebrum						11	11
Occipital Lobe						11	11
Middle Occipital Gyrus						11	11
Grand Total		4	12	12	11	5	44

The table above lists locations within the cortex that were reported active in terms of %BOLD activation. The first column contains the naming information of the hemisphere, lobe, and gyrus of the activation. Locations identified in this table are more active during the PV condition. The first row (in shaded column) indicates Brodmann location assigned by the Talairach Daemon application. The cells within the table indicate the number of active voxels in each active location (cluster) with sums for gyrus, lobe, and hemisphere. Total active voxels are listed in the grand total column and row (reference only).

Table 15: Interaction Contrast BL - + vs DV + -

BL-+ vs DV+- Location	Brodmann Number									Grand Total
	6	7	8	9	10	40	44	45		
Left Cerebrum	5	19				21			45	
Frontal Lobe	5								5	
Medial Frontal Gyrus	5								5	
27	5								5	
Parietal Lobe		19				21			40	
Inferior Parietal Lobule						21			21	
39						18			18	
42						3			3	
Precuneus		3							3	
36		3							3	
Superior Parietal Lobule		16							16	
34		16							16	
Right Cerebrum			11	3	7		31	42	94	
Frontal Lobe			11	3	7		31	42	94	
Inferior Frontal Gyrus								42	42	
3								42	42	
Middle Frontal Gyrus			11		7				18	
8			11						11	
15					7				7	
Precentral Gyrus							31		31	
4							31		31	
Superior Frontal Gyrus				3					3	
23				3					3	

The table above lists locations within the cortex that were reported active in terms of %BOLD activation. The first column contains the naming information including hemisphere, lobe, and gyrus of the activation. Nested under gyrus is the unique cluster identification number for the activation (used for reference in Table 16). The first row indicates the Brodmann Area location identified using the Talairach Daemon application according to the peak activation coordinates of the clusters. The cells within the table indicate the number of active voxels in each location with sums for gyrus, lobe, and hemisphere. Total active voxels are listed in the grand total column. The table above has been simplified to include only areas immediately understood as contributing to the motor loop. Observations included activity in PreMotor (6&8), Sensory (7&40), and Cognitive (9,10) locations including Broca's area (44&45).

Table 16: Interaction Direction BL - + vs DV + -

BL-+ vs DV+-		%BOLD Change from Baseline				Interaction	Relevant Functions	Broadmann
Cluster #	BL:F	BL:NF	DV:F	DV:NF				
3	-0.137	0.289	-0.027	0.020		Language: Rhythm; Motor: Grasping Mirror Neurons, Response Inhibition; Music: Melody; "Broca's Area"	45	
4	0.036	0.327	0.060	0.134		Language: Rhythm; Motor: Mirror Neurons, response inhibition; Melody	44	
8	0.169	0.625	0.014	0.159		Motor: Learning, imagery, control, executive, planning. Response to Proprioceptive stimulus; Visuospatial Attention	8	
15	-0.302	-0.105	-0.076	-0.070		Memory; Auditory (non-speech); Decision Making; Joint Attention	10	
23	-0.070	0.211	0.049	0.084		Memory; Motor: Executive Control; Error Processing	9	
27	0.050	0.362	0.133	0.273		Motor: Planning, Preparation, Imagery, Horizontal Saccades, Visual Attention, Executive Control	6	
34	-0.041	0.110	0.041	-0.101		Motor: Execution, Mirror Neurons, Saccades; Memory; Visuomotor Attention; Goals-Intensive Processing	7	
36	0.020	0.071	0.110	-0.029		Motor: Execution, Mirror Neurons, Saccades; Memory; Visuomotor Attention; Goals-Intensive Processing	7	
39	-0.066	0.084	0.067	-0.037		Motor: Executive Control, Visually Guided Movements, Visuomotor Transformation; Proprioceptive Integration	40	
42	-0.011	0.089	0.004	0.026		Motor: Executive Control, Visually Guided Movements, Visuomotor Transformation; Proprioceptive Integration	40	





This table summarizes the %BOLD changes over the control condition for the Baseline (BL) versus During Vibration (DV) condition. Baseline represents the pre-vibration condition. The identifying cluster number is listed in the first column. The immediately adjacent columns represent the possible combination of vibration and feedback for this contrast. The letter F indicates visual feedback present while the letters NF indicate No visual Feedback present. Numbers listed are % change in the activation per cluster from the control condition (Task C - Just watch). The interaction is visible in the small plot immediately to the right with the columns corresponding to the respective stimulus combination (presented in the same order). A brief description of observed functionality and the associated Broadmann area are also listed for reference.

Table 17: Interaction Contrast BL - + vs PV + -

BL-+ vs PV+-	Broadmann Number					
Location	10	21	22	33	Grand Total	
Left Cerebrum	8	7			15	
Frontal Lobe	8				8	
Middle Frontal Gyrus	8				8	
9	8				8	
Temporal Lobe		7			7	
Middle Temporal Gyrus		7			7	
13		7			7	
Right Cerebrum			17	7	24	
Limbic Lobe				7	7	
Anterior Cingulate				7	7	
4				7	7	
Temporal Lobe			17		17	
Superior Temporal Gyrus			17		17	
1			17		17	
Grand Total	8	7	17	7	39	

The table above lists locations within the cortex that were reported active in terms of %BOLD activation. The first column contains the naming information including hemisphere, lobe, and gyrus of the activation. Nested under gyrus is the unique cluster identification number for the activation (used for reference in Table 18). The first row indicates the Brodmann Area location identified using the Talairach Daemon application according to the peak activation coordinates of the clusters. The cells within the table indicate the number of active voxels in each location with sums for gyrus, lobe, and hemisphere. Total active voxels are listed in the grand total column. The table above is the complete list for this particular contrast. Activations were primarily observed to be Prefrontal (10) and auditory (21&22) locations. Ipsilateral activation was also observed in the anterior cingulate (33).

Table 18: Interaction Direction BL - + vs PV + -

BL-+ vs PV+-		%BOLD Change from Baseline				Interaction	Relevant Function	Broadmann
Cluster #	BL:F	BL:NF	PV:F	PV:NF				
1	0.287	0.956	1.247	0.896		Non-Verbal Sounds; Remembered Saccades; "Auditory Association Area"	22	
4	-0.112	-0.015	-0.080	-0.132		Motor: Inhibition, Planning, Imagery; Memory; Attention	33	
9	0.055	0.119	0.150	0.056		Memory: spatial, time-based; Verb generation, Joint Attention (sensory stim.)	10	
13	0.248	0.457	-0.360	-0.608		Observation of Motion (+B45); Complex Sounds (+B22); Deductive Reasoning	21	

This table summarizes the %BOLD changes over the control condition for the Baseline (BL) versus Post Vibration (PV) condition. Baseline represents the pre-vibration condition. The identifying cluster number is listed in the first column. The immediately adjacent columns represent the possible combination of vibration and feedback for this contrast. The letter F indicates visual feedback present while the letters NF indicate No visual Feedback present. Numbers listed are % change in the activation per cluster from the control condition (Task C - Just watch). The interaction is visible in the small plot immediately to the right with the columns corresponding to the respective stimulus combination (presented in the same order). A brief description of observed functionality and the associated Broadmann area are also listed for reference.

Table 19: Interaction Contrast DV - + vs PV+ -

Sum of NrOfVoxels	Broadmann Number	20	21	45	46	*	Grand Total
Location	13						
▼ Left Cerebrum		11	7				18
▼ Temporal Lobe		11	7				18
▼ Inferior Temporal Gyrus		11					11
5.48845		5					5
6.327591		6					6
▼ Middle Temporal Gyrus			7				7
6.568998			7				7
▼ Right Cerebrum	44		7	3	6	9	69
▼ Frontal Lobe				3	6		9
▼ Inferior Frontal Gyrus				3	6		9
-5.242929					6		6
-5.242802				3			3
▼ Sub-lobar	44					9	53
▼ Insula	44						44
8.555195	44						44
▼ Thalamus						9	9
5.909487						9	9
▼ Temporal Lobe			7				7
▼ Middle Temporal Gyrus			7				7
-5.920239			7				7
Grand Total	44	11	14	3	6	9	87

The table above lists locations within the cortex that were reported active in terms of %BOLD activation. The first column contains the naming information including hemisphere, lobe, and gyrus of the activation. Nested under gyrus is the unique cluster identification number for the activation (used for reference in Table 20). The first row indicates the Brodmann Area location identified using the Talairach Daemon application according to the peak activation coordinates of the clusters. The cells within the table indicate the number of active voxels in each location with sums for gyrus, lobe, and hemisphere. Total active voxels are listed in the grand total column. The table above is the complete list for this particular contrast. Activations were primarily observed to be Prefrontal (10&46) and auditory (21) locations.

Table 20: Interaction Direction DV - + vs PV + -

DV-+ vs PV+-		%BOLD Change from Baseline				Interaction	Relevant Functions	Brodmann
Cluster #	DV:F	DV:NF	PV:F	PV:NF				
1	-0.246	-0.404	-0.463	0.443		Observation of Motion (+B45); Complex Sounds (+B22); Language: Rhythm	21	
2	-0.104	-0.220	-0.060	0.451		Language: Rhythm; Motor: Grasping Mirror Neurons, Response Inhibition; Music: Melody; "Broca's Area"	45	
6	0.116	-0.139	-0.314	0.263		Memory: Encoding; Motor: Executive Control, Mirror Neurons, Horizontal Saccades	46	
8	0.034	0.101	0.081	-0.088		Vibration; Motor: planning, limb integration, vestibular; Visual Attention/Anticipation	13	
25	-0.122	0.156	-0.136	-0.344		Visual Fixation; Language	20	
27	-0.192	-0.118	0.441	0.200		Visual Fixation; Language	20	
28	-0.116	0.604	-0.156	-0.095		Observation of Motion (+B45); Complex Sounds (+B22); Deductive Reasoning	21	

This table summarizes the %BOLD changes over the control condition for the During Vibration (DV) versus Post Vibration (PV) condition. Baseline represents the pre-vibration condition. The identifying cluster number is listed in the first column. The immediately adjacent columns represent the possible combination of vibration and feedback for this contrast. The letter F indicates visual feedback present while the letters NF indicate No visual Feedback present. Numbers listed are % change in the activation per cluster from the control condition (Task C - Just watch). The interaction is visible in the small plot immediately to the right with the columns corresponding to the respective stimulus combination (presented in the same order). A brief description of observed functionality and the associated Brodmann area are also listed for reference.

References

- [1] D. F. Collins, K. M. Refshauge, G. Todd, S. C. Gandevia., Cutaneous receptors contribute to kinesthesia at the index finger, elbow, and knee. *Journal of Neurophysiology*, 94: 1699-706, 2005.
- [2] U. Windhorst. Muscle proprioceptive feedback and spinal networks. *Brain Res Bull*, 73: 155-202, 2007.
- [3] G. K. Kerr, C. J. Worringham., Velocity perception and proprioception *Sensorimotor Control of Movement and Posture*, 508: 79-86, 2002.
- [4] L. A. Jones. Motor illusions: what do they reveal about proprioception? *Psychol Bull*, 103: 72-86, 1988.
- [5] M. Montant, P. Romaguère, J. P. Roll., A new vibrator to stimulate muscle proprioceptors in fMRI. *Hum Brain Mapp*, 30: 990-7, 2009.
- [6] U. Proske. The mammalian muscle spindle *News in Physiological Sciences*, 12: 37-42, 1997.
- [7] E. Ribot-Ciscar, C. Rossi-Durand, J. P. Roll., Muscle spindle activity following muscle tendon vibration in man. *Neurosci Lett*, 258: 147-50, 1998.
- [8] M. Arashanapalli, S. E. Wilson., Paraspinal muscle vibration alters dynamic motion of the trunk. *J Biomech Eng*, 130:021001, 2008.
- [9] L. Li, F. Lamis, S. E. Wilson., Whole-body vibration alters proprioception in the trunk *International Journal of Industrial Ergonomics*, 38: 792-800, 2008.
- [10] J. S. Soltys, S. E. Wilson., Directional sensitivity of velocity sense in the lumbar spine. *J Appl Biomech*, 24: 244-51, 2008.
- [11] J. B. Fallon, V. G. Macefield., Vibration sensitivity of human muscle spindles and Golgi tendon organs. *Muscle Nerve*, 36: 21-9, 2007.
- [12] E. Naito. Sensing limb movements in the motor cortex: how humans sense limb movement. *Neuroscientist*, 10: 73-82, 2004.
- [13] J. P. Roll, J. P. Vedel., Kinesthetic role of muscle afferents in man, studied by tendon vibration and microneurography *Experimental Brain Research*, 47: 177-90, 1982.
- [14] T. Kito, T. Hashimoto, T. Yoneda, *et al.*, Sensory processing during kinesthetic aftereffect following illusory hand movement elicited by tendon vibration. *Brain Res*, 1114: 75-84, 2006.
- [15] Y. Ishihara, M. Izumizaki, T. Atsumi, I. Homma., Aftereffects of mechanical vibration and muscle contraction on limb position-sense. *Muscle Nerve*, 30: 486-92, 2004.
- [16] D. K. Rogers, A. P. Bendrups, M. M. D. Lewis., Disturbed proprioception following a period of muscle vibration in humans *Neuroscience letters*, 57: 147-52, 1985.
- [17] T. Seizova-Cajic, J. L. Smith, J. L. Taylor, S. C. Gandevia., Proprioceptive movement illusions due to prolonged stimulation: reversals and aftereffects. *PLoS One*, 2:e1037, 2007.
- [18] M. M. Wierzbicka, J. C. Gilhodes, J. P. Roll., Vibration-induced postural posteffects. *J Neurophysiol*, 79: 143-50, 1998.

- [19] A. Forner-Cordero, M. Steyvers, O. Levin, *et al.*, Changes in corticomotor excitability following prolonged muscle tendon vibration. *Behav Brain Res*, 190: 41-9, 2008.
- [20] A. Kossev, S. Siggelkow, H. Kapels, *et al.*, Crossed effects of muscle vibration on motor-evoked potentials. *Clin Neurophysiol*, 112: 453-6, 2001.
- [21] R. M. Enoka. Central Modulation of Motor Unit Activity. *Medicine & Science in Sports & Exercise*, 37:2111, 2005.
- [22] P. Romaiguère, J. L. Anton, M. Roth, *et al.*, Motor and parietal cortical areas both underlie kinaesthesia. *Brain Res Cogn Brain Res*, 16: 74-82, 2003.
- [23] E. Naito, P. E. Roland, H. H. Ehrsson., I feel my hand moving: a new role of the primary motor cortex in somatic perception of limb movement. *Neuron*, 36: 979-88, 2002.
- [24] E. Naito, T. Nakashima, T. Kito, *et al.*, Human limb-specific and non-limb-specific brain representations during kinesthetic illusory movements of the upper and lower extremities. *Eur J Neurosci*, 25: 3476-87, 2007.
- [25] N. Hagura, T. Takei, S. Hirose, *et al.*, Activity in the posterior parietal cortex mediates visual dominance over kinesthesia. *J Neurosci*, 27: 7047-53, 2007.
- [26] K. N. Mileva, J. L. Bowtell, A. R. Kossev., Effects of low-frequency whole-body vibration on motor-evoked potentials in healthy men. *Exp Physiol*, 94: 103-16, 2009.
- [27] K. Rosenkranz, A. Pesenti, W. Paulus, F. Tergau., Focal reduction of intracortical inhibition in the motor cortex by selective proprioceptive stimulation *Experimental Brain Research*, 149: 9-16, 2003.
- [28] K. Rosenkranz, J. C. Rothwell., Differential effect of muscle vibration on intracortical inhibitory circuits in humans. *Journal of Physiology*, 551: 649-60, 2003.
- [29] R. W. Briggs, I. Dy-Liacco, M. P. Malcolm, *et al.*, A pneumatic vibrotactile stimulation device for fMRI. *Magn Reson Med*, 51: 640-3, 2004.
- [30] S. M. Golaszewski, F. Zschiegner, C. M. Siedentopf, *et al.*, A new pneumatic vibrator for functional magnetic resonance imaging of the human sensorimotor cortex. *Neurosci Lett*, 324: 125-8, 2002.
- [31] P. T. Fox, H. Burton, M. E. Raichle., Mapping human somatosensory cortex with positron emission tomography *Journal of neurosurgery*, 67: 34-43, 1987.
- [32] S. M. Golaszewski, C. M. Siedentopf, E. Baldauf, *et al.*, Functional magnetic resonance imaging of the human sensorimotor cortex using a novel vibrotactile stimulator *Neuroimage*, 17: 421-30, 2002.
- [33] E. Naito, H. H. Ehrsson, S. Geyer, *et al.*, Illusory arm movements activate cortical motor areas: a positron emission tomography study. *J Neurosci*, 19: 6134-44, 1999.
- [34] E. Naito, P. E. Roland, C. Grefkes, *et al.*, Dominance of the right hemisphere and role of area 2 in human kinesthesia. *J Neurophysiol*, 93: 1020-34, 2005.
- [35] E. Naito, R. Matsumoto, N. Hagura, *et al.*, Importance of precentral motor regions in human kinesthesia: a single case study. *Neurocase*, 17: 133-47, 2011.

- [36] K. Toma, M. Honda, T. Hanakawa, *et al.*, Activities of the primary and supplementary motor areas increase in preparation and execution of voluntary muscle relaxation: an event-related fMRI study. *J Neurosci*, 19: 3527-34, 1999.
- [37] M. S. Christensen, J. Lundbye-Jensen, M. J. Grey, *et al.*, Illusory sensation of movement induced by repetitive transcranial magnetic stimulation. *PLoS One*, 5:e13301, 2010.
- [38] B. Marconi, G. M. Filippi, G. Koch, *et al.*, Long-term effects on motor cortical excitability induced by repeated muscle vibration during contraction in healthy subjects. *J Neurol Sci*, 275: 51-9, 2008.
- [39] P. Romaiguère, S. Calvin, J. P. Roll, Transcranial magnetic stimulation of the sensorimotor cortex alters kinaesthesia. *Neuroreport*, 16: 693-7, 2005.
- [40] R. S. Turner, S. T. Grafton, J. R. Votaw, *et al.*, Motor subcircuits mediating the control of movement velocity: a PET study. *J Neurophysiol*, 80: 2162-76, 1998.
- [41] R. S. Turner, M. Desmurget, J. Grethe, *et al.*, Motor subcircuits mediating the control of movement extent and speed. *J Neurophysiol*, 90: 3958-66, 2003.
- [42] B. Bernal, N. Altman., Neural networks of motor and cognitive inhibition are dissociated between brain hemispheres: an fMRI study. *Int J Neurosci*, 119: 1848-80, 2009.
- [43] J. Fan, J. I. Flombaum, B. D. McCandliss, *et al.*, Cognitive and brain consequences of conflict. *Neuroimage*, 18: 42-57, 2003.
- [44] S. T. Grafton, P. Schmitt, J. Van Horn, J. Diedrichsen., Neural substrates of visuomotor learning based on improved feedback control and prediction. *Neuroimage*, 39: 1383-95, 2008.
- [45] A. G. Feldman, M. L. Latash., Inversions of vibration-induced senso-motor events caused by supraspinal influences in man. *Neurosci Lett*, 31: 147-51, 1982.
- [46] S. Bense, T. Stephan, T. A. Yousry, *et al.*, Multisensory cortical signal increases and decreases during vestibular galvanic stimulation (fMRI). *J Neurophysiol*, 85: 886-99, 2001.
- [47] C. M. Siedentopf, K. Heubach, A. Ischebeck, *et al.*, Variability of BOLD response evoked by foot vibrotactile stimulation: influence of vibration amplitude and stimulus waveform. *Neuroimage*, 41: 504-10, 2008.

Chapter 6 - Summary

While there were several interesting findings in the studies included, these should be considered a starting point for future work. In this chapter we briefly review the results of the previous chapters, discuss the limitations of each, and provide suggestions for future work based on the current conclusions.

Review of the Included Studies

In chapter two the goal was to determine if an average velocity measure would be sensitive to a known proprioceptive disrupting vibratory stimulus. A static balance paradigm was chosen and average seated sway speed was calculated from the measured ground reaction forces. We observed an increase in the mean sway speed associated with the application of muscle vibration. The increased seated sway velocity was found to exist regardless of whether the seat was stable or unstable and whether or not visual feedback was available. Unaccounted for in this particular analysis were the effects of the vestibular system.

The work of chapter three extended upon the results of the sway study to determine if an average velocity measure in conjunction with a pursuit task would be sensitive to a known proprioceptive disrupting vibratory stimulus. Our results indicated that this was indeed the case and further, in partial support of our initial hypothesis, average velocity measures indicated changes in proprioceptive feedback that persisted beyond the period of applied vibration. Specifically, we had observed a decrease in pursuit velocity while vibration was being applied to the supinating musculature of the forearm, and that the average pursuit velocity then increased (above baseline) immediately after vibration was removed. Though we had predicted the presence of a persistent change in velocity post vibration, we simply had the direction wrong. Post vibration, the velocity errors were shown to reverse (from slower than target movements to faster than target movements). Similar to windup errors in a proportional plus integral controller, the "corrective errors" observed post-vibration were similar in magnitude to those observed during vibration. While the findings of the current study aren't designed to support a particular theory of motor control, the

use of such a paradigm as described could provide useful insight in determining likely feedback models in use by the CNS.

In chapter four the basic concept to develop a vibratory stimulus device for use in strong magnetic fields was visited. We have demonstrated with the work in this chapter that it was indeed possible to create a reliable inertial vibratory device for low cost utilizing rapid prototyping techniques and readily available materials. The prototypes built and tested were all measured to provide vibration frequencies in the necessary range commonly associated with modulated muscle spindle organ afferents. Multiple iterations of this design were successfully used to provide MSO disruption, demonstrated by the joystick results in both chapters three and five. While the basic rotor design increased frequency in a linear fashion with increased air pressure, this would become impractical for long exposures at higher frequencies (necessitating a large air supply). Future iterations could be made to optimize the design and achieve similar output frequencies at lower supply pressures.

In the final study, the attempt was made to utilize the velocity based pursuit task in conjunction with functional magnetic resonance imaging to investigate which cortical activation changes corresponded to changes in pursuit task performance. Similar to the previous pursuit task study, changes in average pursuit velocity were observed, slowing during vibration and a persistent increase post vibration. Activations in motor and sensory areas were observed for the overall pursuit task, corresponding with a typical motor task. Some support for central inhibition during vibration was found to exist, but results to explain the post vibration increase were inconclusive. Contrasts of %BOLD signal change indicated however an increase in activation extent contralateral the tested arm. Additional activations were observed in the temporal and frontal lobes, corresponding with auditory and memory processing centers. Previous studies utilizing a Stroop, Go/No Go, or static kinesthetic illusions have typically reported activations indicating right lateralization consistent with motor inhibition, where we had observed primarily left activations suggesting cognitive inhibition. While the ramifications of these activations are not immediately clear, the

suggestion may be that proprioception is indeed a higher order process and possibly acts as an intermediary loop communicating between the motor and cognitive inhibitory loops.

Limitations of the Current Research and Suggestions

The current suite of studies does not on their own answer the question of specifically which cortical and/or subcortical locations are primarily responsible for proprioception. They do suggest that the inhibition observed in vibration disrupted pursuit tasks rely on both cognitive and motor centers. The findings lay groundwork for future advancements in our understanding of human motor control. In order to build on the existing findings the following suggestions are made.

The seated sway measure could become useful in the investigation of low back pain. The current study however was limited to localized vibration rather than the whole body vibration encountered in many workplaces. Future studies should be undertaken to determine if this type of task would be sensitive to vibrations of frequency and amplitude experienced in industry. Further studies should also consider whether or not this velocity based sway measure remains changed beyond the period of vibration.

The joystick pursuit task in chapter three provided a bounty of information. While the paradigm proved extremely useful in demonstrating persistent changes in proprioceptive performance due to vibration, a few changes could provide additional information. While the current study has shown recovery of velocity after the washout period, the actual time course of recovery is not known. Future work would be necessary to indicate if subjects had truly recovered all aspects of performance and how length of exposure is related to rate of recovery. Additionally, the current task was a continuous tracking task and it is of interest to see if a similar response were elicited using an event related design. Such a paradigm would help determine which aspects (distance or time) of the velocity signal are actually altered by vibration. Currently subjects were observed to reverse direction when the target changed direction, regardless of their own movement extent providing an unintentional cue on movement extent.

Development of unique pursuit tasks with different movement extents could clarify how these changes would be manifested absent all visual cues.

In chapter four the basic concept to develop a vibratory stimulus device for use in strong magnetic fields was visited. We have demonstrated with the work in this chapter that it is indeed possible to create a reliable inertial vibratory device for low cost utilizing rapid prototyping techniques and readily available materials for finishing. The prototypes built and tested were all measured to reliably provide vibration frequencies in the necessary range most commonly associated with muscle spindle organ afferent disruption. Further, these devices were demonstrated to successfully alter pursuit task velocity in both chapters three and five. While the basic rotor design increased frequency in a linear fashion with increased air pressure, this can become impractical for long exposures at higher frequencies (necessitating a large air supply). Future iterations can be made to improve the current design and also explore other designs to optimize the economy of the frequency to psi relationship.

A conservative approach was used for the capstone imaging study in chapter five. The protocol utilized a block design for the presentation of visual stimulus and investigated only %BOLD activation levels via image contrasts in Brainvoyager. While we successfully induced the velocity pursuit changes mentioned previously, the design presentation could be modified to an event-related or even a mixed-type design. Such a change would add to the strength of the findings of the cortical activations and allow for discrete aspects of the velocity movement themselves to be investigated using a traditional systems engineering approach (overshoot, error, settling time). We also currently acknowledge that the process incorporated in the present study does not strictly adhere to the methodologies of previous motor control studies. However, if such a methodology were used many of the interesting insights (such as the auditory activations) may have been overlooked. We do propose it is necessary to investigate further the cortical interactions of the different conditions by more rigidly performing a traditional region of interest (ROI) analysis and further investigating the network connections observed.

In regard to the observed velocity changes not being as large as in the previous pursuit study several aspects of the physical setup should be addressed. The physical limitations of the bore in accordance with the variability in subject size did not allow for the same consistency in standardizing the arm position and supporting of the joystick controller. This could have easily led to additional movements of the elbow, shoulder, and wrist joints making the task less of a pure rotation type task. We suggest the possible solutions of limiting the size of the subjects to be scanned or preferably utilizing a modified computer controller design (knob style "paddle controller") in future iterations. We also recommend continued revision of the vibrator to economize both the size of the device and the air supply necessary for operation.

Conclusions

The results of the current work suggest velocity based measures provide a useful paradigm to investigate proprioceptive performance during a pursuit task. This was demonstrated by vibration-induced changes in pursuit task velocity both during and after the period of vibration exposure. These changes in pursuit task performance were possibly due to changes in cortical locations that have been associated with cognitive inhibition and were dependent on association areas integrating feedback from multiple sensory sources. It is possible then that proprioception exists as a network of cortical connections controlling lateral communications between for cognitive and motor networks.

Appendices

Appendix A: Common Abbreviations

CNS	Central Nervous System
PNS	Peripheral Nervous System
MSO	Muscle Spindle Organ
LBP	Low Back Pain
MSS	Mean Sway Speed
AP	Anterior-Posterior
ML	Medial-Lateral
COP	Center Of Pressure
PFL	Proprioceptive Feedback Loop
TMS	Transcranial Magnetic Stimulation
iVEL	Instant Velocity
pVEL	Polyfit Velocity
PK-PK	Peak to Peak Movement
DT	Difference Time
BOLD	Blood Oxygenation Level Dependent
fMRI	Functional Magnetic Resonance Imaging
M1	Primary Motor Area
S1	Somatosensory Area
M2	Secondary Motor Area
S2	Secondary Somatosensory Area
CMA	Cingulate Motor Area
SMA	Supplemental Motor Area
PreF	Prefrontal Cortex

Appendix B: Forms

Sway Consent Form

Approved by the Human Subjects Committee University of Kansas, Lawrence Campus (HSCL). Approval expires one year from 8/8/2006.

Seated Sway with Galvanic Stimulation

INTRODUCTION

The Department of Mechanical Engineering at the University of Kansas supports the practice of protection for human subjects participating in research. The following information is provided for you to decide whether you wish to participate in the present study. You may refuse to sign this form and not participate in this study. You should be aware that even if you agree to participate, you are free to withdraw at any time without penalty. If you do withdraw from this study, it will not affect your relationship with this unit, the services it may provide to you, or the University of Kansas.

PURPOSE OF THE STUDY

We are interested in evaluating the proprioceptive mechanisms (the ability to sense posture and velocity) of the human spine, specifically in the lumbar region. With a more comprehensive understanding of the sensors in place and how they work, conditions for the prescription and prevention of low back pain may be identifiable.

PROCEDURES

If you choose to participate, we will first give you a health questionnaire to make sure you do not have any heart problems that might make walking difficult.

We may choose to use an electrogoniometer and/or electromagnetic markers taped to your back, to record your movements. These devices are commonly used in biomechanics research.

You will be asked to sit in a special chair that measures how your weight shifts in space over time. We will ask you to sit in this chair with your arms folded across your chest for a period of approximately 5 minutes. You will be asked to repeat this 6 times, three with your eyes open and three with your eyes closed. Rest periods will be provided.

During one-third of the trials we will apply a very low current electrical stimulus behind your ear. This electrical stimulus is very low and is usually not felt. However, it will alter your sense of balance. For an additional one-third of the trials we will place a vibratory device against your back. The vibration you experience will be comparable to what you would feel using a store bought massager.

Your participation is strictly voluntary and you can stop at anytime. We assure that your name will not be associated in any way with the research findings. This protocol will take approximately two hours to complete.

RISKS

The potential risks are nominal and include possible skin irritation from the adhesives used in the tape. In addition the galvanic stimulation may make one lose their balance. However, we will

only use the stimulation while you are seated. There is little chance of injury other than incidents that accompany any physical activity such as exercise.

If you would like additional information concerning this research before or after it is complete, please feel free to contact Dr. Sara Wilson by phone (785-864-2103) or mail (3138, Learned Hall, sewilson@ku.edu). If you have any concerns or questions about your rights as a research participant you may contact the University of Kansas' Human Subjects Committee – Lawrence (HSC-L) at (785) 864-7429, Youngberg Hall or by email to David Hann at dhann@ku.edu.

BENEFITS

With this research we hope to better understand how people stabilize their spine motion. There is no direct benefit for the subject with this study.

PAYMENT TO PARTICIPANTS

Subjects will receive a compensation of \$10 per hour (rounded up to the nearest half hour) for participation in the study. In order to receive payment we will need to get your social security number and visa status. This information may be shared with IRS if amounts of payment for studies at KU exceed \$600.

INFORMATION TO BE COLLECTED

To perform this study, researchers will collect information about you. This information will be obtained from a questionnaire that will assess if you have heart problems that might make too much walking inadvisable. Also, information will be collected from the study activities that are listed in the Procedures section of this consent form. This includes information about your age, height, and your weight.

Your name will not be associated in any way with the information collected about you or with the research findings from this study. The researcher(s) will use a study number instead of your name.

Some persons or groups that receive your information may not be required to comply with the Health Insurance Portability and Accountability Act's privacy regulations, and your information may lose this federal protection if those persons or groups disclose it.

The researchers will not share information about you with anyone not specified above unless required by law or unless you give written permission.

Permission granted on this date to use and disclose your information remains in effect indefinitely. By signing this form you give permission for the use and disclosure of your information for purposes of this study at any time in the future.

INSTITUTIONAL DISCLAIMER STATEMENT

In the event of injury, the Kansas Tort Claims Act provides for compensation if it can be demonstrated that the injury was caused by the negligent or wrongful act or omission of a state employee acting within the scope of his/her employment.

REFUSAL TO SIGN CONSENT AND AUTHORIZATION

You are not required to sign this Consent and Authorization form and you may refuse to do so without affecting your right to any services you are receiving or may receive from the University of Kansas or to participate in any programs or events of the University of Kansas. However, if you refuse to sign, you cannot participate in this study.

CANCELLING THIS CONSENT AND AUTHORIZATION

You may withdraw your consent to participate in this study at any time. You also have the right to cancel your permission to use and disclose information collected about you, in writing, at any time, by sending your written request to: Dr. Sara Wilson, Mechanical Engineering, University of Kansas, Lawrence, KS 66045. If you cancel permission to use your information, the researchers will stop collecting additional information about you. However, the research team may use and disclose information that was gathered before they received your cancellation, as described above.

PARTICIPANT CERTIFICATION:

I have read this Consent and Authorization form. I have had the opportunity to ask, and I have received answers to, any questions I had regarding the study and the use and disclosure of information about me for the study. I understand that if I have any additional questions about my rights as a research participant, I may call (785) 864-7429 or write the Human Subjects Committee Lawrence Campus (HSCL), University of Kansas, 2385 Irving Hill Road, Lawrence, Kansas 66045-7563, email dhann@ku.edu.

I agree to take part in this study as a research participant. I further agree to the uses and disclosures of my information as described above. By my signature I affirm that I am at least 18 years old and that I have received a copy of this Consent and Authorization form.

Type/Print Participant's Name

Date

Social Security Number

Visa Status

Participant's Signature

Researcher Contact Information

Sara E. Wilson
Principal Investigator
Mechanical Engineering
3013 Learned Hall, University of Kansas
Lawrence, KS 66045. Phone: (785) 864-2103

Joystick Pursuit Consent Form

THE EFFECTS OF LOCAL VIBRATION ON LIMB TARGETING ABILITY

INTRODUCTION

The Department of Mechanical Engineering at the University of Kansas supports the practice of protection for human subjects participating in research. The following information is provided for you to decide whether you wish to participate in the present study. You may refuse to sign this form and not participate in this study. You should be aware that even if you agree to participate, you are free to withdraw at any time without penalty. If you do withdraw from this study, it will not affect your relationship with this unit, the services it may provide to you, or the University of Kansas.

PURPOSE OF THE STUDY

We are interested in evaluating the proprioceptive mechanisms (the ability to sense position and velocity) of the arm. Specifically we are interested in what combination of factors changes task performance. This information can then be used to increase our understanding of the role of the central nervous system in the proprioceptive feedback system.

PROCEDURES

If you choose to participate, we will first give you a health questionnaire to make sure you do not have any musculoskeletal or general health conditions that would make this study difficult for you.

We may choose to use an electrogoniometer and/or electromagnetic markers taped to your arm, to record your movements. These devices are commonly used in biomechanics research.

You will be asked to sit in front of a computer monitor. With your dominant hand you will use a joystick or similar device to control a specific cursor on the screen. You will have three tasks. In one task, you will simply watch a target cursor move along a specific path on the screen. In another task, you will try to replicate the target cursors movements with your joystick-controlled cursor while your cursor is visible. Lastly, you will try to replicate the movements of the target cursor with your joystick-controlled cursor while your cursor is invisible. The tasks will be presented in multiple blocks of 30 seconds each.

These tasks will be performed under different stimulus conditions including: pre, during, and post vibration exposure. The vibration you experience will be comparable to what you would feel using a store bought massager, and not last longer than 30 minutes total.

Your participation is strictly voluntary and you can stop at anytime. We assure that your name will not be associated in any way with the research findings. Your visit will not exceed 3 hours in duration.

RISKS

The potential risks are nominal and include possible skin irritation from the adhesives used in the tape. Vibration may make your arm feel temporarily numb (similar to if you had been using a vibrating hand tool). However this feeling should go away after a short period.

If you would like additional information concerning this research before or after it is complete, please feel free to contact Dr. Sara Wilson by phone (785-864-2103) or mail (3138, Learned Hall, sewilson@ku.edu). If you have any concerns or questions about your rights as a research participant you may contact the University of Kansas' Human Subjects Committee – Lawrence (HSC-L) at (785) 864-7429, Youngberg Hall or by email to David Hann at dhann@ku.edu.

BENEFITS

With this research we hope to better understand the role of the central nervous system in interpreting proprioceptive feedback. There is no direct benefit for the subject with this study.

PAYMENT TO PARTICIPANTS

Subjects will receive a compensation of \$10 per hour (rounded up to the nearest half hour) for participation in the study. In order to receive payment we will need to get your social security number and visa status. This information may be shared with IRS if amounts of payment for studies at KU exceed \$600.

INFORMATION TO BE COLLECTED

To perform this study, researchers will collect information about you. This information will be obtained from a questionnaire that will assess if you have health or heart problems that might make too much walking or the activity previously described inadvisable. Also, information will be collected from the study activities that are listed in the Procedures section of this consent form. This includes information about your age, height, and your weight.

Your name will not be associated in any way with the information collected about you or with the research findings from this study. The researcher(s) will use a study number instead of your name.

Some persons or groups that receive your information may not be required to comply with the Health Insurance Portability and Accountability Act's privacy regulations, and your information may lose this federal protection if those persons or groups disclose it.

The researchers will not share information about you with anyone not specified above unless required by law or unless you give written permission.

Permission granted on this date to use and disclose your information remains in effect indefinitely. By signing this form you give permission for the use and disclosure of your information for purposes of this study at any time in the future.

INSTITUTIONAL DISCLAIMER STATEMENT

In the event of injury, the Kansas Tort Claims Act provides for compensation if it can be demonstrated that the injury was caused by the negligent or wrongful act or omission of a state employee acting within the scope of his/her employment.

REFUSAL TO SIGN CONSENT AND AUTHORIZATION

You are not required to sign this Consent and Authorization form and you may refuse to do so without affecting your right to any services you are receiving or may receive from the University

of Kansas or to participate in any programs or events of the University of Kansas. However, if you refuse to sign, you cannot participate in this study.

CANCELLING THIS CONSENT AND AUTHORIZATION

You may withdraw your consent to participate in this study at any time. You also have the right to cancel your permission to use and disclose information collected about you, in writing, at any time, by sending your written request to: Dr. Sara Wilson, Mechanical Engineering, University of Kansas, Lawrence, KS 66045. If you cancel permission to use your information, the researchers will stop collecting additional information about you. However, the research team may use and disclose information that was gathered before they received your cancellation, as described above.

PARTICIPANT CERTIFICATION:

I have read this Consent and Authorization form. I have had the opportunity to ask, and I have received answers to, any questions I had regarding the study and the use and disclosure of information about me for the study. I understand that if I have any additional questions about my rights as a research participant, I may call (785) 864-7429 or write the Human Subjects Committee Lawrence Campus (HSCL), University of Kansas, 2385 Irving Hill Road, Lawrence, Kansas 66045-7563, email dhann@ku.edu.

I agree to take part in this study as a research participant. I further agree to the uses and disclosures of my information as described above. By my signature I affirm that I am at least 18 years old and that I have received a copy of this Consent and Authorization form.

Type/Print Participant's Name

Date

Social Security Number

Visa Status

Participant's Signature

Researcher Contact Information

Sara E. Wilson
Principal Investigator
Mechanical Engineering
3013 Learned Hall, University of Kansas
Lawrence, KS 66045. Phone: (785) 864-2103

fMRI Pursuit Consent Form

CONSENT FORM

The Role of the Central Nervous System in the Integration of Proprioceptive Information

INTRODUCTION

You are being invited to participate in a study to examine the relationship between your performance in a motor-control cursor-targeting task, both with and without applied local vibration, and the activity in your brain. This research study will be conducted at the University of Kansas Medical Center with Laura E. Martin, Ph.D. as the principal investigator and Sara E. Wilson as Co-PI. Approximately 12 subjects will be enrolled at KUMC.

You do not have to participate in this research study. It is important that before you make a decision to participate, you read the rest of this form. You should ask as many questions as needed to understand what will happen to you if you participate in this study.

PURPOSE

The purpose of this study is to investigate how brain activity during performance of a known task changes after exposure to arm vibration. The procedures involved in the study are standard experimental techniques. Today's study will investigate how both your brain activity and your ability to manipulate a computer cursor change with and without arm vibration.

PROCEDURES

If you are eligible and decide to participate in this study, your participation will last up to 2 hours on a single visit to the Hoglund Brain Imaging Center at KUMC. Your participation will be comprised of one Magnetic Resonance Imaging (MRI) session during which you will be asked to perform a number of motor control tests.

The study involves collection and analysis of data obtained from a set of brain imaging methods including Magnetic Resonance Imaging (MRI). MRI examines how water molecules in the brain behave in the presence of a magnetic field. MRI provides a detailed picture of what the brain looks like, and it can also provide information on blood flow, metabolism, and function of the brain. This method is considered to be non-invasive and is commonly used in the routine evaluation of brain structure and function.

Female participants will have a urine pregnancy test to confirm they are not pregnant.

During testing, you will lay on a table that "slides" into the scanner. Your head will be positioned within the scanning coil. This coil comes close to the face and partly restricts head movements. During the scanning session, you will be asked to wear goggles that will allow you to view a computer screen. Depending on the test condition you will see a green cursor whose movement you control with your joystick and/or a red cursor controlled by the computer, moving at a constant speed from side-to-side. Using a

HSC Submission Date:

HSC #: 11074
Approval Date: 8/25/10 to 8/24/11
Assurance #: FWA00003411

joystick to control a visible second (green) cursor, you will try to match the motion of the target (red) cursor. The second joystick-controlled cursor will then become invisible and you will try to continue matching the target cursor motion from your "muscle-memory". This will be repeated both with and without vibration applied to your right arm. The vibration will be delivered by a small, non-magnetic, air-powered device attached to your arm by a strap. The vibration you will feel will be similar to what you would experience using a store bought massager. The MRI evaluation takes less than one hour to complete.

RISKS

During the MRI, you will be by yourself in the scan room, although a technologist or an investigator can stay with you at your request. MRI per se has no known associated health risks, but it is important that you complete the metal screening form accurately prior to evaluation. If you have a pacemaker, blood vessel clips, or other internal metal, you may not be allowed to participate in this study. If you have a pacemaker or vascular clip and accidentally enter the MRI suite, a life-threatening situation can develop. Some subjects experience mild claustrophobia during MRI. To minimize this, you will be wearing goggles that allow you to see a computer screen during the scan. Also, the MRI unit makes loud noises during the examination. To minimize any possible discomfort from these, you will be given earplugs.

Although no adverse effects for MRI have been demonstrated, because MRI imparts a small amount of energy to the body, imaging should not be done with pregnant women. For this reason, all female subjects will have pregnancy ruled out via urine pregnancy test.

There may be other risks that have not yet been identified, and unexpected side effects that have not been previously observed may occur.

NEW FINDINGS STATEMENT

You will be informed if any significant new findings develop during the course of the study that may affect your willingness to participate in this study.

BENEFITS

You will not benefit directly from participating in this study. It is hoped that additional information gained in this research study may provide new insights into how the brain functions and may be useful in the treatment and/or prevention of musculo-skeletal injuries.

ALTERNATIVES

Participation in this study is voluntary. Deciding not to participate will have no effect on the care or services you receive at University of Kansas Medical Center.

HSC #: 11074 Approval Date: 8/25/10 to 8/24/11 Assurance #: FWA00003411

COSTS

There will be no cost to you for any procedures you receive during this study.

PAYMENT TO SUBJECTS

You will be paid fifty dollars (\$50) for participating in this study.

Your name, address, social security number, and the title of this study will be given to the KU Center for Research. Payments are taxable income.

IN THE EVENT OF INJURY

In the event you experience a serious side effect during this study, you should immediately contact Dr. Martin at 913-588-7279. If it is after 5:00 p.m., a holiday or a weekend, you should call the emergency room.

If you have a bodily injury as a result of participating in this study, care will be provided for you at the usual charge. Claims will be submitted to your health insurance policy, your government program, or other third party, but you will be billed for the costs of that care to the extent insurance does not cover them. You do not give up any of your legal rights by signing this form.

INSTITUTIONAL DISCLAIMER STATEMENT

If you think you have been harmed as a result of participating in research at the University of Kansas Medical Center (KUMC), you should contact the Director, Human Research Protection Program, Mail Stop #1032, University of Kansas Medical Center, 3901 Rainbow Blvd., Kansas City, KS66160. Under certain conditions, Kansas state law or the Kansas Tort Claims Act may allow for payment to persons who are injured in research at KUMC.

CONFIDENTIALITY AND PRIVACY AUTHORIZATION

Efforts will be made to keep your personal information confidential. Researchers cannot guarantee absolute confidentiality. If the results of this study are published or presented in public, information that identifies you will be removed.

The privacy of your health information is protected by a federal law known as the Health Insurance Portability and Accountability Act (HIPAA). By signing this consent form, you are giving permission ("authorization") for KUMC to use and share your health information for the purposes of this research study. If you decide not to sign the form, you cannot be in the study.

To do this research, we need to collect health information that identifies you. We will collect information from activities described in the Procedures section of this form.

Your study-related health information will be used at KU Medical Center by Dr. Martin,

HSC #: 11074 Approval Date: 8/25/10 to 8/24/11 Assurance #: FWA00003411

members of the research team, the KU Center for Research, the KUMC Human Subjects Committee and other committees and offices that review and monitor research studies. Study records might be reviewed by government officials who oversee research, if a regulatory review takes place.

By signing this form, you are giving Dr. Martin and the research team permission to share information about you with persons or groups outside KUMC. Your information will be shared with researchers on the KU-Lawrence campus, and U.S. agencies that oversee human research (if a study audit is performed). These groups or agencies may make copies of study records for audit purposes. The purpose for using and sharing your information is to make sure the study is done properly. Some of the persons or groups who receive your health information may not be required by law to protect it. Once your information has been shared outside of KUMC, it might be disclosed by others and no longer protected by the federal privacy laws or this authorization.

Permission granted on this date to use and disclose your health information remains in effect indefinitely. By signing this form you give permission for the use and disclosure of your information for purposes of the study at any time in the future. Your permission to use and share your health information will not expire unless you cancel it.

QUESTIONS

You have read the information in this form. Dr. Martin or her associates have answered your question(s) to your satisfaction. You know if you have any more questions, concerns, or complaints after signing this, you may contact Dr. Martin or one of her associates at (913) 588-7279. If you have any questions about your rights as a research subject, you may call (913) 588-1240 or write the Human Subjects Committee, Mail Stop #1032, University of Kansas Medical Center, 3901 Rainbow Blvd., Kansas City, KS 66160.

SUBJECT RIGHTS AND WITHDRAWAL FROM THE STUDY

Your participation in this study is voluntary and that the choice not to participate or to quit at any time can be made without penalty or loss of benefits. Not participating or quitting will have no effect upon the medical care or treatment you receive now or in the future at the University of Kansas Medical center. The entire study may be discontinued for any reason without your consent by the investigator conducting the study.

You have a right to change your mind about allowing the research team to have access to your health information. If you want to cancel permission to use your health information, you should send a written request to Dr. Martin. The mailing address is Laura E. Martin, Ph.D., Hoglund Brain Imaging Center, University of Kansas Medical Center, 3901 Rainbow Boulevard, Kansas City, KS 66160. If you cancel permission to use your health information, you will be withdrawn from the study. The research team will stop collecting any additional information about you. The research team may use and share information that was gathered before they received your cancellation.

HSC #: 11574
Approval Date: 8/25/10 to 8/24/11
Assurance #: FWA00003411

Consent Form Addendum

fMRI Studies of Manual and Spoken Word Recognition

In addition to the main study, you are also being asked to participate in an optional separate study involving the creation of a research database. You can participate in the main study without needing to agree to participate in this optional database.

You will not directly benefit from participating in the database.

If you agree to participate in the database, information collected during today's testing, including the images of your brain, will be copied and stored in the research database. This information will be saved indefinitely. It will be used now by Dr. Martin and members of the research team. It may be used in the future by researchers both at KUMC and outside KUMC to help answer questions about memory, thinking, and aging. It will not be used for any other research purposes.

If your information is shared with other researchers, it will be sent using a code number, your date of birth, and the date the information was collected. It will not include your name or identify you in any other way. By limiting the information, we will protect your privacy and lessen the risk of your identity being re-disclosed to outside individuals. If study records are inspected, only authorized persons will have access to your information.

Even if you agree to participate in the database now, you have a right to change your mind later. You may cancel your permission to use your information in the future by sending a request to Dr. Laura Martin, University of Kansas Medical Center, 3901 Rainbow Boulevard, Mail Stop 1052, Kansas City, KS 66160. The research team may use and share information that was gathered before they received your cancellation.

Allowing us to store your information is completely voluntary. If you decide not to sign this consent addendum, then we will not store your information in the research database. If you have any questions about the research, you may call Dr. Martin at (913)588-7279.

Permission to be included in the MRI Database

_____ I agree to allow my data from this study to be stored indefinitely in the KU Structural MRI database for future research use.

_____ I do not agree to allow my data from this study to be stored indefinitely in the KU Structural MRI database for future research use, but it may be used for purposes of this study only.

In the future, researchers at KUMC will be conducting additional studies from data included in the MRI database, which may require additional information. Please check the

HSC #: 11574
Approval Date: 8/25/10 to 8/24/11
Assurance #: FWA00003411

appropriate line to indicate whether or not you are willing to have us contact you when such future studies come up:

_____ Yes, I am willing to be contacted about future studies for which I might be eligible.

_____ No, I do not want to be contacted about future studies for which I might be eligible.

A separate consent would be obtained at the time of your participation in any additional studies.

I will be given a signed copy of this consent form to keep for my records.

Type/Print Subject's Name

Signature of Subject

Time

Date

Type/Print Name of Person Obtaining Consent

Signature of Person Obtaining Consent

Date

HSC #: Approval Date: _____ to _____ Assurance #: FWA00003411

Appendix C: Additional Figures

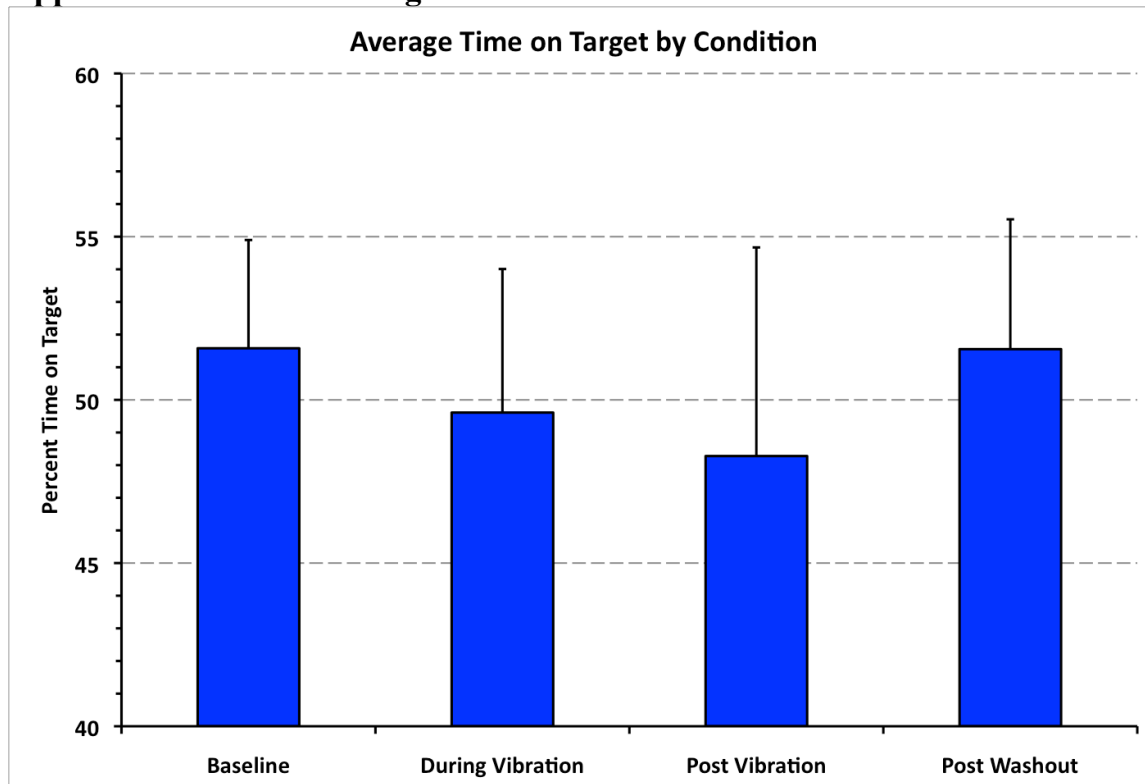


Figure 24: Joystick Pursuit Time On Target (TOT)

Average time on target per condition (all feedback levels combined) during the joystick pursuit task study in chapter 3.

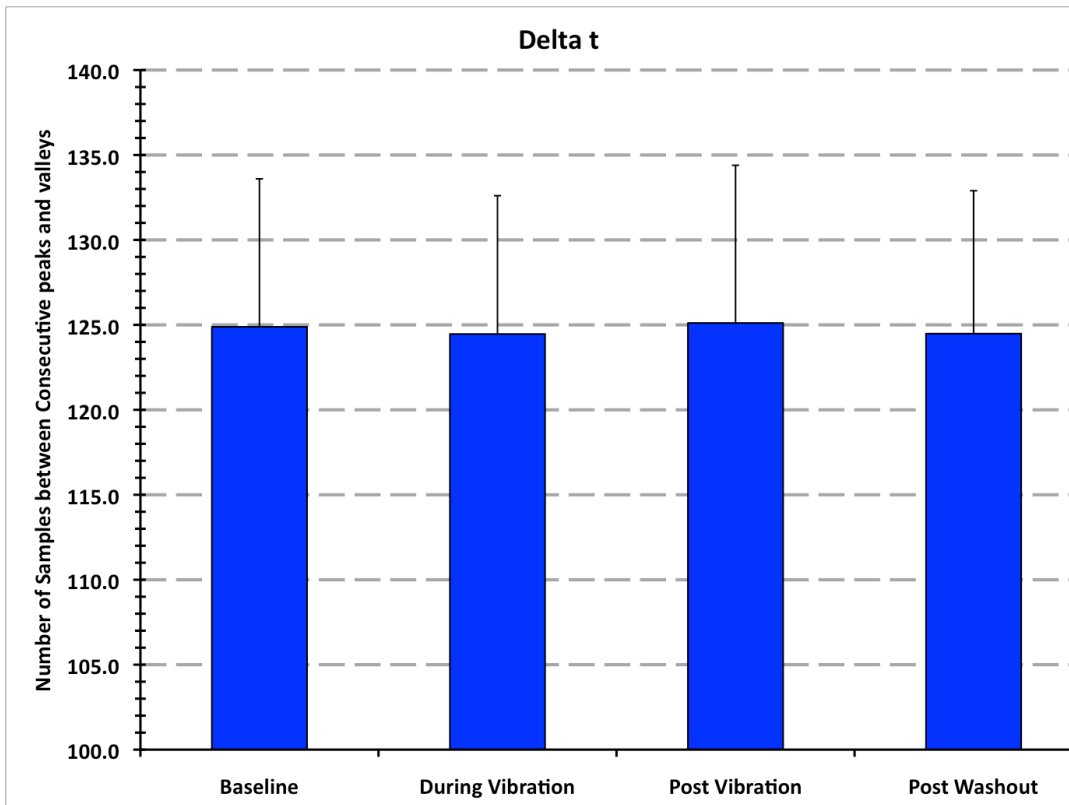


Figure 25: Joystick Pursuit Time Between Peaks (DT)

Average number of samples between peaks during the joystick pursuit task.

Table 21: Joystick Pursuit ANOVA (DT)

Tests of Within-Subjects Effects
Measure: DT

Source	df	F	Sig.	Partial Eta Squared	Observed Power ^a
Condition	2.110	.195	.835	.024	.076
Direction	1.000	3.243	.109	.288	.355
Feedback	1.000	3.371	.104	.296	.366
Condition * Direction	2.906	.407	.743	.048	.118
Condition * Feedback	2.262	1.317	.295	.141	.260
Direction * Feedback	1.000	.006	.938	.001	.051
Condition * Direction * Feedback	2.722	.267	.830	.032	.091

a. Computed using alpha = .05

Table 22 Joystick Pursuit iVEL – ANOVA Post Hoc

Tests of Within-Subjects Contrasts

Measure: iVEL

Source	Condition	Repeat	Feedback	df	F	Sig.	Partial Eta Squared	Observed Power ^a
Condition	DV vs. BL			1	79.948	.000	.930	1.000
	PV vs. BL			1	5.476	.058	.477	.502
	PW vs. BL			1	.190	.678	.031	.066
Repeat	1 vs. 3			1	1.728	.237	.224	.199
	2 vs. 3			1	4.796	.071	.444	.452
Feedback			F vs. NF	1	.775	.413	.114	.116
Condition * Repeat	DV vs. BL	1 vs. 3		1	6.337	.045	.514	.559
		2 vs. 3		1	.375	.563	.059	.082
	PV vs. BL	1 vs. 3		1	.853	.391	.125	.123
		2 vs. 3		1	.039	.850	.006	.053
	PW vs. BL	1 vs. 3		1	.510	.502	.078	.093
		2 vs. 3		1	.017	.899	.003	.051
Condition * Feedback	DV vs. BL		F vs. NF	1	27.066	.002	.819	.990
	PV vs. BL		F vs. NF	1	2.245	.185	.272	.245
	PW vs. BL		F vs. NF	1	.491	.510	.076	.092
Repeat * Feedback	1 vs. 3		F vs. NF	1	.138	.723	.023	.062
	2 vs. 3		F vs. NF	1	1.031	.349	.147	.138
Condition * Repeat * Feedback	DV vs. BL	1 vs. 3		1	2.962	.136	.330	.306
		2 vs. 3		1	.005	.948	.001	.050
	PV vs. BL	1 vs. 3		1	.116	.745	.019	.060
		2 vs. 3		1	.345	.578	.054	.079
	PW vs. BL	1 vs. 3		1	.402	.550	.063	.084
		2 vs. 3		1	.990	.358	.142	.135

a. Computed using alpha = .05

Table 23: Joystick Pursuit iVEL Bonferroni

Pairwise Comparisons

Measure: iVEL

(I) Condition	(J) Condition	Mean Difference (I-J)	Std. Error	Sig. ^a	95% Confidence	
					Lower Bound	Upper Bound
Baseline	DV	1.213*	.136	.001	.689	1.738
	PV	-0.932	.398	.347	-2.470	.606
	PW	-.123	.282	1.000	-1.213	.967
During Vibration	BL	-1.213*	.136	.001	-1.738	-.689
	PV	-2.145*	.338	.004	-3.450	-.840
	PW	-1.336*	.212	.004	-2.154	-.518
Post Vibration	BL	0.932	.398	.347	-.606	2.470
	DV	2.145*	.338	.004	.840	3.450
	PW	0.809	.229	.074	-.076	1.694
Post Washout	BL	.123	.282	1.000	-.967	1.213
	DV	1.336*	.212	.004	.518	2.154
	PV	-0.809	.229	.074	-1.694	.076

Based on estimated marginal means

*. The mean difference is significant at the .05 level.

a. Adjustment for multiple comparisons: Bonferroni.

Table 24: Joystick Pursuit pVEL - ANOVA Post Hoc

Tests of Within-Subjects
Contrasts
pVEL

Source	Condition	Repeat	Feedback	df	F	Sig.	Partial Eta Squared	Observed Power ^a
Condition	DV vs. BL			1	115.679	.000	.951	1.000
	PV vs. BL			1	7.130	.037	.543	.608
	PW vs. BL			1	.310	.598	.049	.076
Repeat		1 vs. 3		1	.146	.715	.024	.062
		2 vs. 3		1	3.681	.103	.380	.365
Feedback			F vs. NF	1	.012	.916	.002	.051
Rotation				1	.899	.380	.130	.127
Condition * Repeat	DV vs. BL	1 vs. 3		1	11.895	.014	.665	.818
		2 vs. 3		1	.009	.926	.002	.051
	PV vs. BL	1 vs. 3		1	.088	.776	.015	.057
		2 vs. 3		1	.818	.401	.120	.120
	PW vs. BL	1 vs. 3		1	.510	.502	.078	.093
		2 vs. 3		1	.785	.410	.116	.117
Condition * Feedback	DV vs. BL		F vs. NF	1	47.874	.000	.889	1.000
	PV vs. BL		F vs. NF	1	3.025	.133	.335	.311
	PW vs. BL		F vs. NF	1	.250	.635	.040	.071
Repeat * Feedback		1 vs. 3	F vs. NF	1	.959	.365	.138	.132
		2 vs. 3	F vs. NF	1	3.933	.095	.396	.386
Condition * Repeat * Feedback	DV vs. BL	1 vs. 3	F vs. NF	1	4.116	.089	.407	.400
		2 vs. 3	F vs. NF	1	.010	.924	.002	.051
	PV vs. BL	1 vs. 3	F vs. NF	1	.003	.957	.001	.050
		2 vs. 3	F vs. NF	1	1.124	.330	.158	.146
	PW vs. BL	1 vs. 3	F vs. NF	1	.007	.937	.001	.051
		2 vs. 3	F vs. NF	1	1.984	.209	.249	.222

a. Computed using alpha = .05

Table 25: Joystick Pursuit pVEL Bonferroni

Pairwise Comparisons

Measure: pVEL

(I) Condition	(J) Condition	Mean Difference (I-J)	Std. Error	Sig. ^a	95% Confidence	
					Lower Bound	Upper Bound
Baseline	DV	1.485*	.138	.000	.952	2.019
	PV	-1.080	.405	.222	-2.643	.483
	PW	-.136	.244	1.000	-1.077	.806
During Vibration	BL	-1.485*	.138	.000	-2.019	-.952
	PV	-2.565*	.388	.003	-4.065	-1.066
	PW	-1.621*	.190	.001	-2.357	-.885
Post Vibration	BL	1.080	.405	.222	-.483	2.643
	DV	2.565*	.388	.003	1.066	4.065
	PW	0.944	.276	.085	-.122	2.011
Post Washout	BL	.136	.244	1.000	-.806	1.077
	DV	1.621*	.190	.001	.885	2.357
	PV	-0.944	.276	.085	-2.011	.122

Based on estimated marginal means

*. The mean difference is significant at the .05 level.

a. Adjustment for multiple comparisons: Bonferroni.

Table 26: Joystick Pursuit Pk-Pk - ANOVA Post Hoc

Tests of Within-Subjects Contrasts

Pk-Pk

Source	Condition	Repeat	Feedback	df	F	Sig.	Partial Eta Squared	Observed Power ^a
Condition	DV vs. BL			1	56.360	.000	.904	1.000
	PV vs. BL			1	4.888	.069	.449	.459
	PW vs. BL			1	.228	.650	.037	.069
Repeat		1 vs. 3		1	.357	.572	.056	.080
		2 vs. 3		1	7.163	.037	.544	.610
Feedback			F vs. NF	1	.899	.380	.130	.127
Rotation				1	.153	.710	.025	.063
Condition * Repeat	DV vs. BL	1 vs. 3		1	.000	.990	.000	.050
		2 vs. 3		1	.823	.399	.121	.120
	PV vs. BL	1 vs. 3		1	.650	.451	.098	.105
		2 vs. 3		1	.002	.964	.000	.050
	PW vs. BL	1 vs. 3		1	.843	.394	.123	.122
		2 vs. 3		1	.485	.512	.075	.091
Condition * Feedback	DV vs. BL		F vs. NF	1	35.056	.001	.854	.998
	PV vs. BL		F vs. NF	1	2.941	.137	.329	.304
	PW vs. BL		F vs. NF	1	.762	.416	.113	.115
Repeat * Feedback		1 vs. 3	F vs. NF	1	.295	.607	.047	.075
		2 vs. 3	F vs. NF	1	1.642	.247	.215	.192
Condition * Repeat * Feedback	DV vs. BL	1 vs. 3	F vs. NF	1	.032	.863	.005	.053
		2 vs. 3	F vs. NF	1	.276	.618	.044	.073
	PV vs. BL	1 vs. 3	F vs. NF	1	.001	.982	.000	.050
		2 vs. 3	F vs. NF	1	.007	.937	.001	.051
	PW vs. BL	1 vs. 3	F vs. NF	1	.179	.687	.029	.065
		2 vs. 3	F vs. NF	1	.121	.740	.020	.060

a. Computed using alpha = .05

Table 27: Joystick Pursuit Pk-Pk Bonferroni

Pairwise Comparisons

Measure: Pk-Pk

(I) Condition	(J) Condition	Mean Difference (I-J)	Std. Error	Sig. ^a	95% Confidence	
					Lower Bound	Upper Bound
Baseline	DV	3.016*	.402	.002	1.464	4.568
	PV	-2.184	.988	.414	-6.001	1.632
	PW	-.336	.704	1.000	-3.055	2.383
During Vibration	BL	-3.016*	.402	.002	-4.568	-1.464
	PV	-5.200*	.762	.003	-8.145	-2.256
	PW	-3.352*	.465	.002	-5.149	-1.555
Post Vibration	BL	2.184	.988	.414	-1.632	6.001
	DV	5.200*	.762	.003	2.256	8.145
	PW	1.848	.535	.082	-.220	3.916
Post Washout	BL	.336	.704	1.000	-2.383	3.055
	DV	3.352*	.465	.002	1.555	5.149
	PV	-1.848	.535	.082	-3.916	.220

Based on estimated marginal means

*. The mean difference is significant at the .05 level.

a. Adjustment for multiple comparisons: Bonferroni.

Table 28: fMRI Pursuit pVEL - ANOVA Post Hoc

Tests of Within-Subjects Contrasts

Measure: Polyfit_AVG

Source	Condition	Repeat	Feedback	Type III Sum of Squares	df	F	Sig.	Partial Eta Squared	Observed Power ^a
Condition	DV vs. BL			3.318	1	53.871	.000	.857	1.000
	PV vs. BL			2.755	1	8.833	.016	.495	.753
	PW vs. BL			.203	1	.335	.577	.036	.081
Repeat		2 vs. 1		.000	1	.002	.968	.000	.050
		3 vs. 1		.275	1	3.897	.080	.302	.422
Feedback			F vs. NF	24.228	1	84.623	.000	.904	1.000
Condition * Repeat	DV vs. BL	2 vs. 1		.153	1	.348	.570	.037	.083
		3 vs. 1		.094	1	.310	.591	.033	.079
	PV vs. BL	2 vs. 1		1.548	1	4.432	.065	.330	.468
		3 vs. 1		.456	1	1.399	.267	.135	.185
	PW vs. BL	2 vs. 1		2.030	1	8.169	.019	.476	.721
		3 vs. 1		.407	1	1.333	.278	.129	.179
Condition * Feedback	DV vs. BL		F vs. NF	7.350	1	54.680	.000	.859	1.000
	PV vs. BL		F vs. NF	1.385	1	3.998	.077	.308	.431
	PW vs. BL		F vs. NF	1.547	1	3.791	.083	.296	.413
Repeat * Feedback		2 vs. 1	F vs. NF	.146	1	1.662	.229	.156	.211
		3 vs. 1	F vs. NF	.017	1	.129	.728	.014	.062
Condition * Repeat * Feedback	DV vs. BL	2 vs. 1	F vs. NF	.267	1	.182	.679	.020	.067
		3 vs. 1	F vs. NF	.305	1	.314	.589	.034	.079
	PV vs. BL	2 vs. 1	F vs. NF	.552	1	.537	.482	.056	.101
		3 vs. 1	F vs. NF	.096	1	.077	.788	.008	.057
	PW vs. BL	2 vs. 1	F vs. NF	1.142	1	2.134	.178	.192	.258
		3 vs. 1	F vs. NF	.032	1	.030	.866	.003	.053

a. Computed using alpha = .05

Table 29: fMRI Pursuit pVEL Bonferroni

Pairwise Comparisons

Measure:pVEL_AVG

(I) Condition	(J) Condition	Mean Difference (I-J)	Std. Error	Sig. ^a	95% Confidence	
					Lower Bound	Upper Bound
Baseline	DV	.576*	.078	.000	.312	.840
	PV	-0.525	.177	.094	-1.119	.069
	PW	-.142	.246	1.000	-.970	.685
During Vibration	BL	-.576*	.078	.000	-.840	-.312
	PV	-1.101*	.230	.006	-1.874	-.328
	PW	-0.718	.247	.104	-1.549	.112
Post Vibration	BL	0.525	.177	.094	-.069	1.119
	DV	1.101*	.230	.006	.328	1.874
	PW	0.383	.233	.806	-.400	1.165
Post Washout	BL	.142	.246	1.000	-.685	.970
	DV	0.718	.247	.104	-.112	1.549
	PV	-0.383	.233	.806	-1.165	.400

Based on estimated marginal means

*. The mean difference is significant at the .05 level.

a. Adjustment for multiple comparisons: Bonferroni.

Table 30: fMRI iVEL - ANOVA Post Hoc

Tests of Within-Subjects Contrasts

Measure: iVEL

Source	Condition	Repeat	Feedback	df	F	Sig.	Partial Eta Squared	Observed Power ^a
Condition	DV vs. BL			1	79.948	.000	.930	1.000
	PV vs. BL			1	5.476	.058	.477	.502
	PW vs. BL			1	.190	.678	.031	.066
Repeat		1 vs. 3		1	1.728	.237	.224	.199
		2 vs. 3		1	4.796	.071	.444	.452
Feedback			F vs. NF	1	.775	.413	.114	.116
Condition * Repeat	DV vs. BL	1 vs. 3		1	6.337	.045	.514	.559
		2 vs. 3		1	.375	.563	.059	.082
	PV vs. BL	1 vs. 3		1	.853	.391	.125	.123
		2 vs. 3		1	.039	.850	.006	.053
	PW vs. BL	1 vs. 3		1	.510	.502	.078	.093
		2 vs. 3		1	.017	.899	.003	.051
Condition * Feedback	DV vs. BL		F vs. NF	1	27.066	.002	.819	.990
	PV vs. BL		F vs. NF	1	2.245	.185	.272	.245
	PW vs. BL		F vs. NF	1	.491	.510	.076	.092
Repeat * Feedback		1 vs. 3	F vs. NF	1	.138	.723	.023	.062
		2 vs. 3	F vs. NF	1	1.031	.349	.147	.138
Condition * Repeat * Feedback	DV vs. BL	1 vs. 3	F vs. NF	1	2.962	.136	.330	.306
		2 vs. 3	F vs. NF	1	.005	.948	.001	.050
	PV vs. BL	1 vs. 3	F vs. NF	1	.116	.745	.019	.060
		2 vs. 3	F vs. NF	1	.345	.578	.054	.079
	PW vs. BL	1 vs. 3	F vs. NF	1	.402	.550	.063	.084
		2 vs. 3	F vs. NF	1	.990	.358	.142	.135

a. Computed using alpha = .05

Table 31: fMRI Pursuit iVEL Bonferroni

Pairwise Comparisons

Measure:iVEL_AVG

(I) Condition	(J) Condition	Mean Difference (I-J)	Std. Error	Sig. ^a	95% Confidence	
					Lower Bound	Upper Bound
Baseline	DV	.273 [*]	.069	.020	.041	.505
	PV	-.343 [*]	.069	.005	-.575	-.111
	PW	-.037	.073	1.000	-.281	.207
During Vibration	BL	-.273 [*]	.069	.020	-.505	-.041
	PV	-.616 [*]	.090	.000	-.920	-.312
	PW	-.310 [*]	.091	.045	-.615	-.006
Post Vibration	BL	.343 [*]	.069	.005	.111	.575
	DV	.616 [*]	.090	.000	.312	.920
	PW	.306 [*]	.073	.014	.061	.550
Post Washout	BL	.037	.073	1.000	-.207	.281
	DV	.310 [*]	.091	.045	.006	.615
	PV	-.306 [*]	.073	.014	-.550	-.061

Based on estimated marginal means

*. The mean difference is significant at the .05 level.

a. Adjustment for multiple comparisons: Bonferroni.

Table 32: fMRI Pk-Pk - ANOVA Post Hoc

Tests of Within-Subjects Contrasts

Pk-Pk

Source	Condition	Repeat	Feedback	df	F	Sig.	Partial Eta Squared	Observed Power ^a
Condition	DV vs. BL			1	56.360	.000	.904	1.000
	PV vs. BL			1	4.888	.069	.449	.459
	PW vs. BL			1	.228	.650	.037	.069
Repeat		1 vs. 3		1	.357	.572	.056	.080
		2 vs. 3		1	7.163	.037	.544	.610
Feedback			F vs. NF	1	.899	.380	.130	.127
Rotation				1	.153	.710	.025	.063
Condition * Repeat	DV vs. BL	1 vs. 3		1	.000	.990	.000	.050
		2 vs. 3		1	.823	.399	.121	.120
	PV vs. BL	1 vs. 3		1	.650	.451	.098	.105
		2 vs. 3		1	.002	.964	.000	.050
	PW vs. BL	1 vs. 3		1	.843	.394	.123	.122
		2 vs. 3		1	.485	.512	.075	.091
Condition * Feedback	DV vs. BL		F vs. NF	1	35.056	.001	.854	.998
	PV vs. BL		F vs. NF	1	2.941	.137	.329	.304
	PW vs. BL		F vs. NF	1	.762	.416	.113	.115
Repeat * Feedback		1 vs. 3	F vs. NF	1	.295	.607	.047	.075
		2 vs. 3	F vs. NF	1	1.642	.247	.215	.192
Condition * Repeat * Feedback	DV vs. BL	1 vs. 3	F vs. NF	1	.032	.863	.005	.053
		2 vs. 3	F vs. NF	1	.276	.618	.044	.073
	PV vs. BL	1 vs. 3	F vs. NF	1	.001	.982	.000	.050
		2 vs. 3	F vs. NF	1	.007	.937	.001	.051
	PW vs. BL	1 vs. 3	F vs. NF	1	.179	.687	.029	.065
		2 vs. 3	F vs. NF	1	.121	.740	.020	.060

a. Computed using alpha = .05

Table 33: Talairach Peak Coordinates BL+ + vs DV - -

X coor	Y coor	Z coor	Gyrus	Brodmann	# Voxels	t	p
57	-46	1	Middle Temporal Gyrus	22	35	6.7165	0.000087
57	23	-11	Inferior Frontal Gyrus	47	12	6.3935	0.000126
57	20	37	Middle Frontal Gyrus	9	8	5.5729	0.000346
54	-16	-11	Middle Temporal Gyrus	21	8	-6.7424	0.000084
45	26	43	Middle Frontal Gyrus	8	10	6.1798	0.000163
42	11	10	Insula	13	58	7.3366	0.000044
42	29	40	Middle Frontal Gyrus	8	5	5.4229	0.00042
42	-13	1	Insula	13	3	4.9034	0.000844
36	-43	40	Inferior Parietal Lobule	40	4	6.0572	0.000189
36	-46	-2	Parahippocampal Gyrus	19	22	-6.7601	0.000083
33	2	61	Middle Frontal Gyrus	6	26	5.8312	0.00025
33	-43	-5	Parahippocampal Gyrus	19	3	-4.9026	0.000845
24	-73	49	Precuneus	7	8	6.1991	0.000159
21	-7	64	Superior Frontal Gyrus	6	7	6.3359	0.000135
15	-67	1	Lingual Gyrus	18	19	8.1855	0.000018
12	2	49	Cingulate Gyrus	24	5	6.3088	0.00014
9	20	4	Caudate	Caudate Head	5	-5.5394	0.000361
6	8	49	Superior Frontal Gyrus	6	20	8.1776	0.000019
6	11	31	Cingulate Gyrus	24	7	5.1455	0.000607
0	-52	61	Precuneus	7	12	6.5776	0.000102
0	32	-11	Medial Frontal Gyrus	11	3	-5.1574	0.000597
0	11	28	Cingulate Gyrus	24	5	4.957	0.000784
-3	-19	49	Medial Frontal Gyrus	6	10	6.4593	0.000117
-6	-22	46	Paracentral Lobule	31	10	5.37	0.00045
-9	29	1	Anterior Cingulate	24	16	-6.9619	0.000066
-9	17	-2	Caudate	Caudate Head	14	-6.0928	0.000181
-12	-28	49	Paracentral Lobule	6	44	9.444	0.000006
-9	32	-2	Anterior Cingulate	32	5	-5.5653	0.000349
-12	47	1	Medial Frontal Gyrus	10	4	-5.4352	0.000414
-18	32	40	Middle Frontal Gyrus	8	3	-5.4387	0.000412
-18	-91	-8	Inferior Occipital Gyrus	17	4	-5.5854	0.000341
-33	8	13	Insula	13	65	6.9503	0.000067
-39	-1	7	Insula	13	5	6.3061	0.00014
-42	-22	19	Insula	13	3	4.9847	0.000755

BL++ vs DV--

Table 34: Talairach Peak Coordinates BL+ +vs PV - -

X coor	Y coor	Z coor	Gyrus	Broadmann	# Voxels	t	p
60	11	34	Middle Frontal Gyrus	9	4	5.8464	0.000245
54	23	37	Middle Frontal Gyrus	9	6	5.7574	0.000274
42	-64	-26	Tuber	*	17	-6.4686	0.000116
42	-34	34	Inferior Parietal Lobule	40	5	-5.8196	0.000253
39	-49	-26	Culmen	*	3	-4.9568	0.000784
33	-46	-5	Parahippocampal Gyrus	19	32	-6.555	0.000105
33	-79	4	Middle Occipital Gyrus	19	7	-6.3638	0.000131
33	-55	-5	Parahippocampal Gyrus	19	4	-5.8408	0.000247
30	5	64	Middle Frontal Gyrus	6	3	5.2275	0.000544
6	-79	-20	Declive	*	4	-5.0267	0.000713
-6	-28	67	Paracentral Lobule	6	6	-5.8342	0.000249
-30	-49	43	Superior Parietal Lobule	7	5	-5.2751	0.00051
-36	-49	-14	Fusiform Gyrus	37	27	9.5816	0.000005

Table 35: Talairach Peak Coordinates DV+ + vs PV - -

X coor	Y coor	Z coor	Gyrus	Broadmann	# Voxels	t	p
36	-79	7	Middle Occipital Gyrus	19	11	-6.7753	0.000081
12	50	43	Superior Frontal Gyrus	8	5	6.4221	0.000122
0	62	28	Superior Frontal Gyrus	10	8	7.7915	0.000027
-6	38	7	Anterior Cingulate	24	7	5.6499	0.000314
-18	-25	58	Precentral Gyrus	4	12	-5.9464	0.000216
-18	-37	58	Postcentral Gyrus	3	4	-5.7454	0.000278
-18	-22	40	Cingulate Gyrus	31	5	-6.0231	0.000197
-30	-52	49	Superior Parietal Lobule	7	6	-5.3781	0.000446
-30	-52	43	Superior Parietal Lobule	7	6	-5.8563	0.000242
-48	35	1	Inferior Frontal Gyrus	45	28	6.898	0.000071

Table 36: Talairach Peak Coordinates BL-+ vs DV +-

X coor	Y coor	Z coor	Gyrus	Broadmann	# Voxels	t	p
48	20	7	Inferior Frontal Gyrus	45	42	7.903	0.000024
48	2	10	Precentral Gyrus	44	31	8.4175	0.000015
48	-10	-8	Superior Temporal Gyrus	22	13	7.3468	0.000043
45	26	4	Inferior Frontal Gyrus	13	18	5.5013	0.00038
42	-22	-20	Parahippocampal Gyrus	36	4	-5.2403	0.000535
36	35	43	Middle Frontal Gyrus	8	11	7.0147	0.000062
30	-73	19	Precuneus	31	7	-5.6534	0.000312
21	56	16	Middle Frontal Gyrus	10	7	6.8826	0.000072
21	-31	-41	Cerebellar Tonsil	*	9	-6.3998	0.000125
12	-76	-38	Inferior Semi-Lunar Lobule	*	14	6.6553	0.000093
9	56	34	Superior Frontal Gyrus	9	3	5.3889	0.000439
-6	-10	64	Medial Frontal Gyrus	6	5	5.3414	0.000468
-15	-31	-26	Culmen	*	6	-5.9672	0.000211
-15	-43	34	Precuneus	31	6	-5.9074	0.000227
-27	-61	52	Superior Parietal Lobule	7	16	5.858	0.000241
-27	-55	28	Middle Temporal Gyrus	39	27	-6.0784	0.000184
-27	-46	43	Precuneus	7	3	5.1243	0.000624
-30	-28	28	Sub-Gyral	*	7	-6.4346	0.00012
-30	-16	16	Clastrum	*	10	6.2052	0.000158
-33	-49	43	Inferior Parietal Lobule	40	18	6.5558	0.000104
-33	-19	16	Insula	13	7	5.4541	0.000404
-39	5	-2	Insula	13	10	6.0144	0.000199
-42	-34	37	Inferior Parietal Lobule	40	3	5.9223	0.000223

Table 37: Talairach Peak Coordinates BL-+ vs PV+-

X coor	Y coor	Z coor	Gyrus	Broadmann	Range (mm)	Cluster	# Voxels	t	p
66	-4	10	Superior Temporal Gyrus	22	1	1	17	6.0701	0.000186
9	11	25	Anterior Cingulate	33	2	4	7	6.292	0.000142
-30	44	13	Middle Frontal Gyrus	10	4	9	8	6.4971	0.000112
-39	-67	-26	Tuber	*	0	11	10	6.0302	0.000195
-48	5	-29	Middle Temporal Gyrus	21	1	13	7	7.2277	0.000049

Table 38: Talairach Peak Coordinates DV-+ vs PV+-

X	Y	Z	Gyrus	Brodmann	NrOfVoxels	t	p
63	-31	-14	Middle Temporal Gyrus	21	7	-5.920239	0.000223
57	20	19	Inferior Frontal Gyrus	45	3	-5.242802	0.000533
54	-19	13	Transverse Temporal Gyrus	41	1	5.391445	0.000438
54	35	-5	Inferior Frontal Gyrus	47	2	5.780358	0.000266
48	38	19	Middle Frontal Gyrus	46	1	-5.098475	0.000646
48	41	-2	Inferior Frontal Gyrus	46	6	-5.242929	0.000533
42	11	13	Insula	13	1	-4.887004	0.000863
36	-25	25	Insula	13	44	8.555195	0.000013
36	-61	19	Middle Temporal Gyrus	19	1	4.893155	0.000856
24	47	19	Superior Frontal Gyrus	10	1	5.018703	0.00072
15	-64	55	Superior Parietal Lobule	7	1	-4.916622	0.000828
9	-28	55	Paracentral Lobule	6	1	-4.935301	0.000807
9	-55	13	Posterior Cingulate	23	1	4.812586	0.000957
9	-34	-38	Cerebellar Tonsil	*	1	4.815473	0.000953
6	-34	4	Thalamus	*	9	5.909487	0.000226
6	44	1	Anterior Cingulate	32	2	5.223493	0.000547
-6	-46	40	Cingulate Gyrus	31	1	5.024759	0.000714
-9	44	25	Medial Frontal Gyrus	9	2	5.127019	0.000622
-18	-61	7	Posterior Cingulate	30	2	5.000208	0.000739
-27	14	19	Sub-Gyral	*	1	-4.809757	0.000961
-27	-76	-23	Uvula	*	1	5.025722	0.000714
-30	8	19	Insula	13	1	-5.045439	0.000695
-39	-31	1	Sub-Gyral	*	2	-5.402347	0.000432
-39	-64	-26	Tuber	*	4	5.294099	0.000498
-48	-28	-11	Inferior Temporal Gyrus	20	5	5.48845	0.000386
-48	35	10	Inferior Frontal Gyrus	46	1	4.839158	0.000922
-54	-28	-23	Inferior Temporal Gyrus	20	6	6.327591	0.000136
-63	-31	-8	Middle Temporal Gyrus	21	7	6.568998	0.000103